A.A. Marelis
4018265

Geothermal Energy screening study

A comparison between Ghana and Saba

TU Delft

Geothermal Energy screening study

A comparison between Ghana and Saba

By

A.A. Marelis

in fulfilment of the requirements for the

Research Minor Programme
in Applied Physics

at the Delft University of Technology,
to be defended publicly on Friday April 28, 2017 at 14:00 PM.

Supervisor:	Dr. M.E. Donselaar	TU Delft
	M. Wiemer	PanTerra Geoconsultants B.V.

TU Delft

Abstract

The potential for the application of geothermal energy in electricity generation has been reviewed for the countries of Ghana (West Africa) and Saba (Caribbean). This review is part of an internship project with the objective to establish a basic stepwise methodology (or work flow) for an initial screening level assessment of geothermal energy potential. This study also provides the research subject material for the Research Minor of Applied Earth Sciences at the Delft University of Technology.

Ghana shows varying potential for geothermal energy exploitation with power capacities ranging from 2.9 to 15.6 MWe for a single geothermal power plant. The overall geothermal potential displayed by potential high enthalpy resources in Ghana is considered moderate- to weak. Saba shows a potential with an estimated power capacity of 16.8 MW_e, and the concept is proven by the Bouillante geothermal field on Guadeloupe. Uncertainties related to estimates made for Ghana and risks related to geothermal development on Saba can be reduced by data acquisition and geological studies.

The subsurface of Ghana is characterized by African PreCambrian basement terrane in the West, a Neoproterozoic mobile thrust belt in the East, and a thick sedimentary basin fill ranging from Late PreCambrian to Paleozoic in the center. Thermal gradients are generally low (15-25 ^{o}C/km) and calculated gradients for Ghana range from 10 to 38 ^{o}C/km. Subsurface temperatures in Ghana are therefore estimated to range from 36 to 179 ^{o}C at depths from 1 to 4 km. Temperatures were estimated incorporating different scenarios of which the probability has been assessed using Monte Carlo simulations to determine the overall probability distribution of the geothermal gradient.

The island of Saba is part of an island arc resulting from a subduction zone and is characterized by an active volcanic setting. The presence of thermal fluids in the subsurface is clearly indicated by several thermal features (hot springs) occurring on the island. Potential resource temperatures are expected to range from 190 to 250 ^{o}C. Such high enthalpy resources are expected to be located at depths less than 1 km.

Acknowledgements

I would like to thank Rick Donselaar for giving me the opportunity of an internship position at PanTerra Geoconsultants B.V. on behalf of the Research Minor at the Delft University of Technology.
PanTerra Geoconsultants B.V. has a vast experience in geothermal energy exploitation in The Netherlands, but is looking to expand their geothermal practices internationally. To broaden their expertise, they have started to investigate opportunities in countries other than The Netherlands.

I would like to give a special thanks to Maarten Wiemer and Paul van der Vegt for their help and confidence regarding the performed research into the Geothermal Energy potential of Ghana and Saba. I have enjoyed my time at PanTerra very much and I have learned a lot, from working in a corporate environment to geothermal energy as a concept itself. Working on geothermal energy has allowed me to realize what a fascinating subject it is and convinced me to pursue this subject in my Master's programme at the university.

Contents

1. Introduction

Geothermal energy is a form of energy obtained from within the Earth, originating in its core (geothermal energy, n.d.). *Geothermal* originates from the Greek words 'γη' (ge) and 'θερμός' (thermos) which mean 'Earth' and 'heat' respectively. Geothermal energy is produced by extracting the Earth's internal heat and is often referred to as 'heat-mining' (Tester et al., 2006).

The average geothermal gradient for the Netherlands is 31^{o}C/km at 10 ^{o}C (average) surface temperature. An example is provided by the Middenmeer geothermal field, which is located in the province of Noord Holland, in the Netherlands. The reservoir of the Middenmeer geothermal field is the Slochteren formation (Rotliegend), a sandstone layer that was eroded upon the Texel-Ijsselmeer High. The reservoir consists of Aeolian sandstone deposits, is present at a depth of 2 km, is about 200 m thick in the area and has a temperature of approximately 85 ^{o}C (a gradient of 38 ^{o}C/km applies). The thermal energy extracted from the reservoir is solely used for the heating of greenhouses on an agricultural complex.

This study aims to investigate geothermal energy for generating electricity (rather than for heating) in countries that are currently generating electricity by burning fossil fuels. Ghana (Africa) and Saba (Caribbean) provide examples to assess the potential for high enthalpy geothermal energy, as high temperatures are required for such an application to be economically successful.
A key aim of this study is to create a general stepwise methodology (or work flow) for an initial assessment of geothermal energy potential by identifying high enthalpy geothermal resources on the basis of geological setting and subsurface temperature, by classifying the potential geothermal systems and by estimating the (minimum) installed power capacity of potential high enthalpy resources.

1.1 Brief geothermal history

Volcanoes, hot springs and other thermal (surface) features have always led people to believe that the Earth's interior was hot. When the first underground mines where excavated to depths of a few hundred meters, a relation of increasing temperature with depth was deduced from simple physical sensations (Dickson & Fanelli, 2003). The first measurements of subsurface temperatures were performed around 1740 using a thermometer in a mine near Belfort, France (Bullard, 1965, as cited in Dickson & Fanelli, 2003, p. 2). Since 1870, modern scientific methods have been used to study the earth's thermal regime. A full understanding of the Earth's heat balance and thermal history was reached in the twentieth century with the discovery of radiogenic heat contribution. All modern thermal models must take the heat generated by the decay of radioactive elements (uranium, thorium and potassium) into account.

In the early part of the nineteenth century energy was already being extracted in Italy from hot waters emerging naturally or from shallow boreholes by utilizing the heat that was being released in the evaporation process of extracting boric acid from these thermal waters. Not long after, exploitation of naturally occurring steam for its mechanical energy began. Utilization of low-pressure steam to heat industrial and residential buildings and greenhouses started between 1910 and 1940 in the area of Tuscany in Italy (Dickson and Fanelli, 2003). Iceland started using geothermal energy for domestic heating in 1928.

First attempts at generating electricity from geothermal steam were made in Italy in 1904 and their success indicated the industrial value of geothermal energy and marked the beginning of a new form of energy exploitation that has developed significantly from then on (Dickson & Fanelli, 2003). Since then, several countries such as Japan (1919), Iceland (1928), the United States (1921) and New Zealand (1958) have started using geothermal energy.

In March 2016, the world geothermal energy market reached a minimum of 13.3 GW (gigawatts) of geothermal power operating in 24 countries (Matek, 2016). Since the end of 2015, there has been a total addition in potential capacity of 12.5 GW in 82 countries spread across 700 to 750 projects. Figure 1 shows a prediction of 18.3 GW by 2021. "It is composed of announced completion dates of plants already under construction. This growth in new capacity will most likely come from European, East African, and South Pacific markets as these regions lead geothermal power's growth by substantial capacity additions in the next five years" (Matek, 2016, p. 8-9).

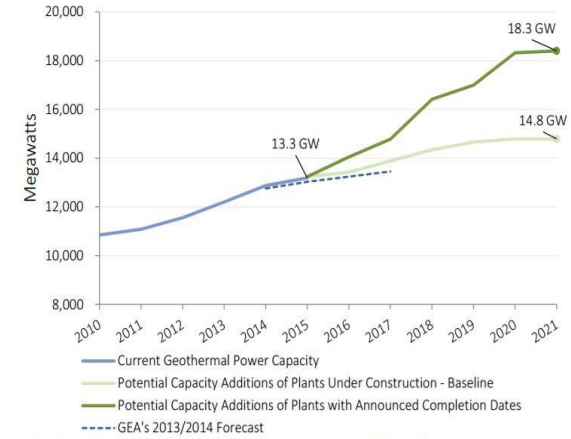

Note: PCA (Planned Capacity Additions), pilot plants and utility scale geothermal plants built in the first half of the 20th century and then decommissioned are not included in the above time series.

Figure 2: International Geothermal Power Capacity [MW]. From Matek, 2016.

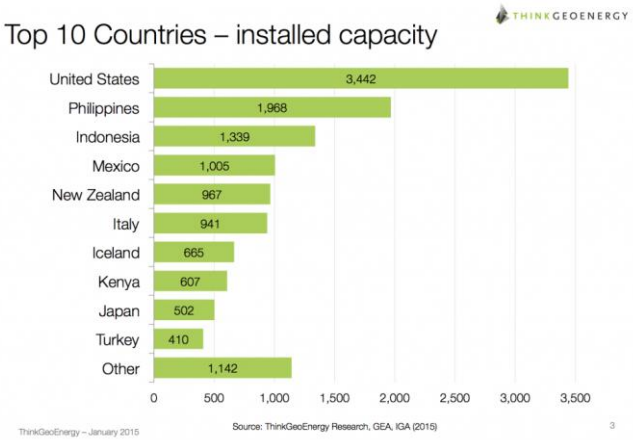

Figure 1: Top 10 countries based on installed geothermal power capacity as of January 2015. From http://www.thinkgeoenergy.com/newest-list-of-the-top-10-countries-in-geothermal-power/

The top 10 countries (worldwide, as of January 2015) in geothermal power are listed in Figure 2, with their ranking based on installed capacity. In terms of reliability on geothermal power for electricity production, Iceland is the leading country, with 29 percent of the total electricity production coming from geothermal power (Electricity Generation, n.d.). El Salvador (Central America) comes second, where 24 percent of its electricity production is generated by geothermal power (Hymans, n.d.). In addition, more than 15 percent of the electricity production in Kenya, the Philippines and Costa Rica comes from geothermal power.

1.2 Nature of geothermal systems

A geothermal system (Figure 3) can be described schematically as “convecting water in the upper crust of the Earth, which, in a confined space, transfers heat from a heat source to a heat sink, usually the free surface” (Hochstein, 1990, as cited in Dickson & Fanelli, 2003, p. 8). It consists of three main elements: 1) a heat source, 2) a reservoir and 3) a working fluid (Dickson & Fanelli, 2003; Tester et al., 2006).

The heat source is the only element of a geothermal system that must be occurring naturally (Dickson & Fanelli, 2003). Both other elements can either be natural or artificial. A working fluid can be re-injected into the reservoir to prolong reservoir life, permeability can be created or increased by hydraulic fracturing. This also means that when a geothermal fluid is not naturally occurring, it can be injected into the (artificial) reservoir. In this case, one could even choose the type of the geothermal fluid, opting for something other than water.

There are two types of geothermal systems. The currently most exploited is the hydrothermal (or volcanic-fuelled) system which derives heat directly from the Earth’s convective mantle (Dhansay et al., 2014). This system is associated with regions of higher than normal heat flow and is often referred to as a “conventional” geothermal system. These systems can occur in widely diverse geologic settings, sometimes without clear surface manifestations of the underlying resource. Hydrothermal systems contain all three elements of a geothermal system naturally and may therefore be somewhat limited in their location (Tester et al., 2006).
The second, currently less often exploited, is the Enhanced Geothermal System (or EGS) which exploits latent heat encapsulated in crustal rocks. This heat originates from the average heat flow through the Earth’s crust and/or from radioactive phenomena in the crust. Heat is transferred by conduction. This thermal energy is present everywhere, but usually stored at greater depth. With the exception of the heat source, all EGS lack at least one of the remaining elements of a geothermal system, or both (Tester et al., 2006; Dhansay et al., 2014). Enhanced Geothermal Systems are generally associated with hot, dry and impermeable rocks, while hydrothermal (or conventional) systems mainly exploit resources where heat, water and permeable rocks are naturally present.

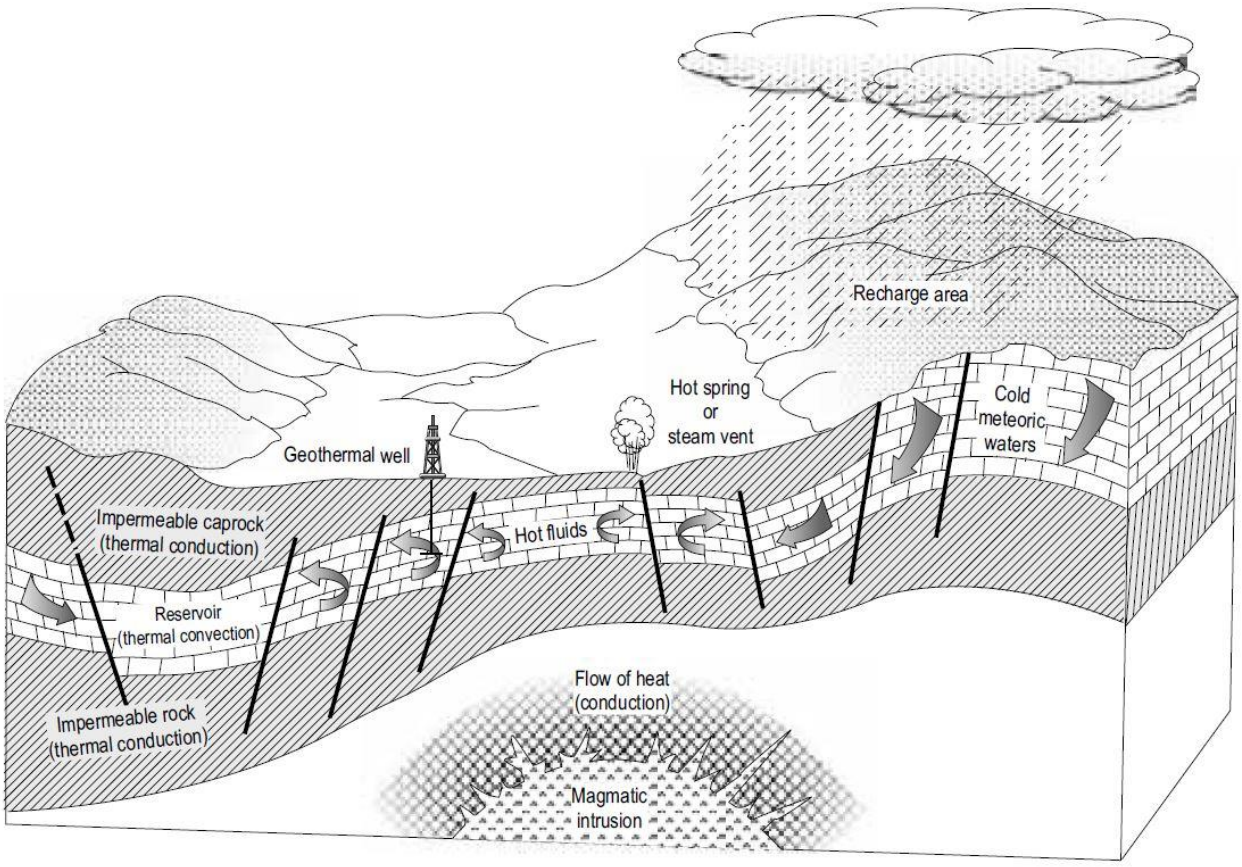

Figure 3: Schematic representation of an ideal geothermal system. Heat is supplied at the base of the system. Heated waters rise to permeable reservoirs as colder water originating from natural recharge sink towards the heat source. Thermal waters can be extracted from the reservoir using geothermal wells and then used in varying applications. From Dickson & Fanelli, 2003.

1.2.1 Heat source

When the average heat flow of continents (65 mW/m^2) and oceans (101 mW/m^2) is weighted by area, the global average heat flow through the Earth's crust is approximately 87 mW/m^2 (Pollack et al., 1993, as cited in Dickson & Fanelli, 2003, p. 6). For most of the continental crust, there are "two primary processes that influence heat flow: 1) upward convection and conduction of heat originating from the Earth's mantle and core, and 2) heat generated by the decay of radioactive elements in the crust, generally isotopes of uranium, thorium and potassium" (Tester et al., 2006, p. 1:9). Examples of heat sources are high-temperature magmatic intrusions that are situated at shallow depths and the average heat flow through the continental, and oceanic, crust of the Earth (increases with depth) (Dickson & Fanelli, 2003).

Regions of higher than average heat flow are generally associated with tectonic plate boundaries, such as active margins with an extensional or 'rifting' nature, and areas of geologically recent igneous activity and/or volcanic events, such as volcanic island arcs resulting from active subduction zones (Tester et al., 2006; Dickson & Fanelli, 2003). A good example is made by Iceland, which is considered to be one of the most tectonically active places on Earth (The Resource, n.d.). The extensional nature of the active margin (Mid-Atlantic ridge) and the unusually great volcanic activity on the island give rise to subsurface temperatures of 250 ^{o}C within 1000 m depth. However, upper crustal rocks that have large concentrations of radioactive elements can lead to a significant increase in local or regional heat flow (Tester et al., 2006). For example, in the White Mountains in New Hampshire, the extreme natural radioactivity of the granite increases heat flow to local highs of 100 mW/m^2 (Birch et al., 1968, as cited in Tester et al., 2006, p. 2:13,14).

Together with the thermal conductivity of crustal rocks, the heat flow can be expressed as a geothermal gradient which gives an indication of the increase in temperature with depth in the Earth's crust. The geothermal gradient is thus dependent on geologic, tectonic and radioactive phenomena. The global average geothermal gradient is about 2.5 to 3 ^{o}C/100m or 25 to 30 ^{o}C/km (Dickson & Fanelli, 2003).

1.2.2 Reservoir

Thermal energy (heat) is extracted from a reservoir, defined as a volume of hot permeable rocks, by coupled transport processes, i.e. convective (fluid convection) and conductive heat transfer in porous and/or fractured rock (Dickson & Fanelli, 2003; Tester et al., 2006). The most important reservoir property is permeability, which can be occurring naturally or can be provided by faults or a dense fracture network. The reservoir is generally overlain by impermeable cap-rocks. Ideally the reservoir is connected to a surficial recharge area in order to prevent depletion of the reservoir. When natural recharge is insufficient the extracted geothermal fluid, after its utilization, could be injected back into the reservoir, integrating natural with artificial recharge (Dickson & Fanelli, 2003; Tester et al., 2006).

1.2.3 Working fluid

The working fluid, or geothermal fluid, is water (Dickson & Fanelli, 2003). Depending on temperature and pressure conditions in the reservoir, water can occur in the liquid or vapour phase, or both. For example, the geothermal fluid can also occur as a saturated, liquid-vapour mixture or as a superheated steam vapour phase (Tester et al., 2006). The geothermal fluid acts as a carrier to transfer the heat from subsurface heat sources to the surface (Figure 4) (Dickson & Fanelli, 2003).

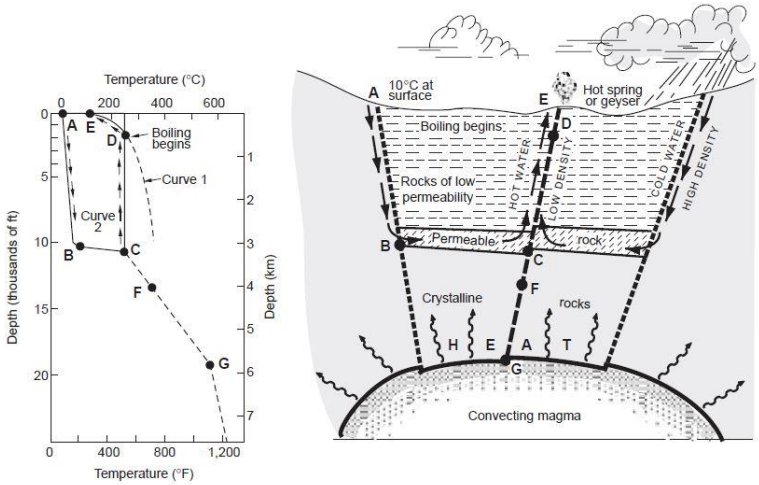

Figure 4: Model of geothermal fluid circulation. Curve 1 is the reference curve for the boiling point of pure water. Curve 2 shows the temperature profile along a typical circulation route from recharge (A) to discharge (E). From Dickson & Fanelli, 2003.

1.3 Definition and classification of geothermal resources

The concept of a geothermal resource is defined on the basis of a geothermal system and the most common classifications of geothermal systems are described in the context of the three components of such systems.

1.3.1 Definition

A geothermal system that can be developed for beneficial uses, such as electricity generation, is considered to be a geothermal resource (resource, n.d.). A geothermal resource is defined by the enthalpy of the geothermal system (Dickson & Fanelli, 2003). Enthalpy is used to express the heat content or thermal energy stored in a system and is more or less proportional to temperature. Geologic and tectonic phenomena play a major role in determining the location (depth and position) and quality (fluid chemistry and temperature) of a particular resource.

1.3.2 Classification

The most common criterion for classifying geothermal resources is thus based on enthalpy (Dickson & Fanelli, 2003). Geothermal resources are classified as low, medium and high enthalpy resources.
Table 1 shows classifications proposed by different authors. Due to the absence of a formal classification, this study will report temperature ranges for a classification of low to high enthalpy resource case by case.

Source: (a) Muffler and Cataldi (1978). (b) Hochstein (1990). (c) Benderitter and Cormy (1990). (d) Nicholson (1993). (e) Axelsson and Gunnlaugsson (2000).

	(a)	(b)	(c)	(d)	(e)
Low enthalpy resources	<90	<125	<100	<=150	<=190
Intermediate enthalpy resources	90-150	125-225	100-200	-	-
High enthalpy resources	>150	>225	>200	>150	>190

Table 1: Classification based on temperature (enthalpy), proposed by different authors. Temperatures are in degrees Celsius. Modified from Dickson & Fanelli, 2003.

A distinction can be made on the phase of the geothermal fluid: there are water- or liquid-dominated systems and vapor-dominated (or dry steam) geothermal systems (White, 1973, as cited in Dickson & Fanelli, 2003, p. 11).

- Water-dominated systems. Water is the continuous, pressure controlling fluid phase. Temperatures range from <125 ^{0}C to >225 ^{0}C. They can produce hot water, water/steam mixtures, wet steam and in some cases dry steam, depending on temperature and pressure conditions.
- Vapour-dominated systems. Vapour is the continuous, pressure controlling phase, but liquid water and vapour can coexist in the reservoir. These systems are classified as high temperature systems. They normally produce dry-to-superheated steam.

Another division made between geothermal systems is based on the reservoir equilibrium state (Nicholson, 1993, as cited in Dickson & Fanelli, 2003, p. 12). Equilibrium in a geothermal reservoir is dependent on the circulation of the geothermal fluid in the reservoir and the mechanism of heat transfer between rocks and fluids.

- Dynamic systems. The reservoir is continually recharged by water that is heated and then discharged from the reservoir either to the surface or into underground permeable formations. Heat is transferred through the system by convection and circulation of the fluid.
- Static systems (storage systems). There is minor to no recharge to the reservoir and heat is transferred only by conduction. An example of a static system is a reservoir that consists of permeable sedimentary rocks containing pressurized hot water that remained trapped at the moment of deposition of the sediments.

A separate distinction can be made regarding the energy extracted from geothermal resources (Dickson & Fanelli, 2003). The geothermal energy can be classified as renewable (property of resource) or as sustainable (utilization of resource). Renewable depends on the rate of energy recharge which happens by advection of thermal water on the same time scale as production from the resource. Sustainable is in regards to generation and consumption and is therefore dependent on the original quantity.

1.4 Utilization of geothermal resources

There are many different applications for geothermal resources (Dickson & Fanelli, 2003). High enthalpy resources are mainly used for electricity generation, while low enthalpy resources have a very wide range of applications. With the introduction of binary cycle power plants, which require a minimum temperature of 90 ^{o}C, low enthalpy resources can also be used for generating electricity. The diagram in Figure 5 shows different utilization possibilities according to resource temperatures and is derived from the classical Lindal diagram (Lindal, 1973, as cited in Dickson & Fanelli, 2003, p. 14).

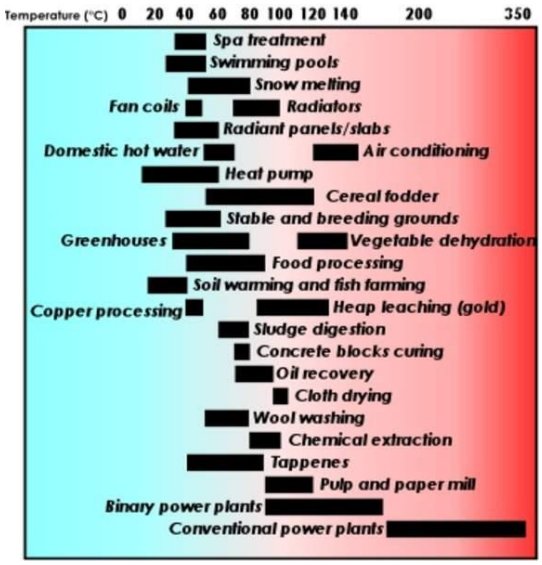

Figure 5: Modified Lindal diagram. Retrieved from https://www.geothermal-energy.org/what_is_geothermal_energy.html#c324

2. Methodology

In order to assess the geothermal potential of a certain country or area, a clear methodology is needed that is repeatable and applicable to different geological settings. Such a methodology should cover the basic geothermal exploration and development procedures. An overview of these procedures is given by the ' Best Practice Guide for Geothermal Exploration' (GeothermEx, Inc. & Harvey consultants, ltd., 2012) and the ESMAP's 'Geothermal Handbook' (Gehringer & Loksha, 2012). This section elaborates on the application of the validated methodologies in this study.

The aim of any geothermal potential assessment study is on minimizing, and otherwise mitigating, the technical risks and uncertainties related to a geothermal resource. The principal resource risks for geothermal energy exploitation include: 1) temperature (or enthalpy), 2) depth of the resource, and 3) output and sustainability of flow from producing wells, i.e. the thermal energy that can be extracted from the resource over a certain period of time.

Figure 6 illustrates the step-wise methodology proposed and adapted in this geothermal energy screening study. It incorporates the 'preliminary survey' and 'exploration' phases. Ghana and Saba will be discussed separately in light of these two phases in chapters 0 and 0. Results that can be obtained from the exploration phase are presented in chapter 0. This chapter also describes development analogues which can provide data that has not been acquired during (or does not result from) the exploration phase.

Based on the available data and obtained results from the exploration phase and the development analogues: (1) potential geothermal systems are classified and potential resources are identified, and a conceptual model of the geothermal resource is proposed in chapter 0, and (2) the potential of the identified geothermal resources is estimated by quantifying the installed power capacity in chapter 0.

The geothermal potential of both countries, Ghana and Saba, is compared in terms of geological setting, subsurface temperature, classification and installed power capacity.

Possible methods or strategies for reducing uncertainties involved in the initial estimates and decreasing risks related to geothermal potential will be recommended, by means of preferable data selection and aspects for further investigation.

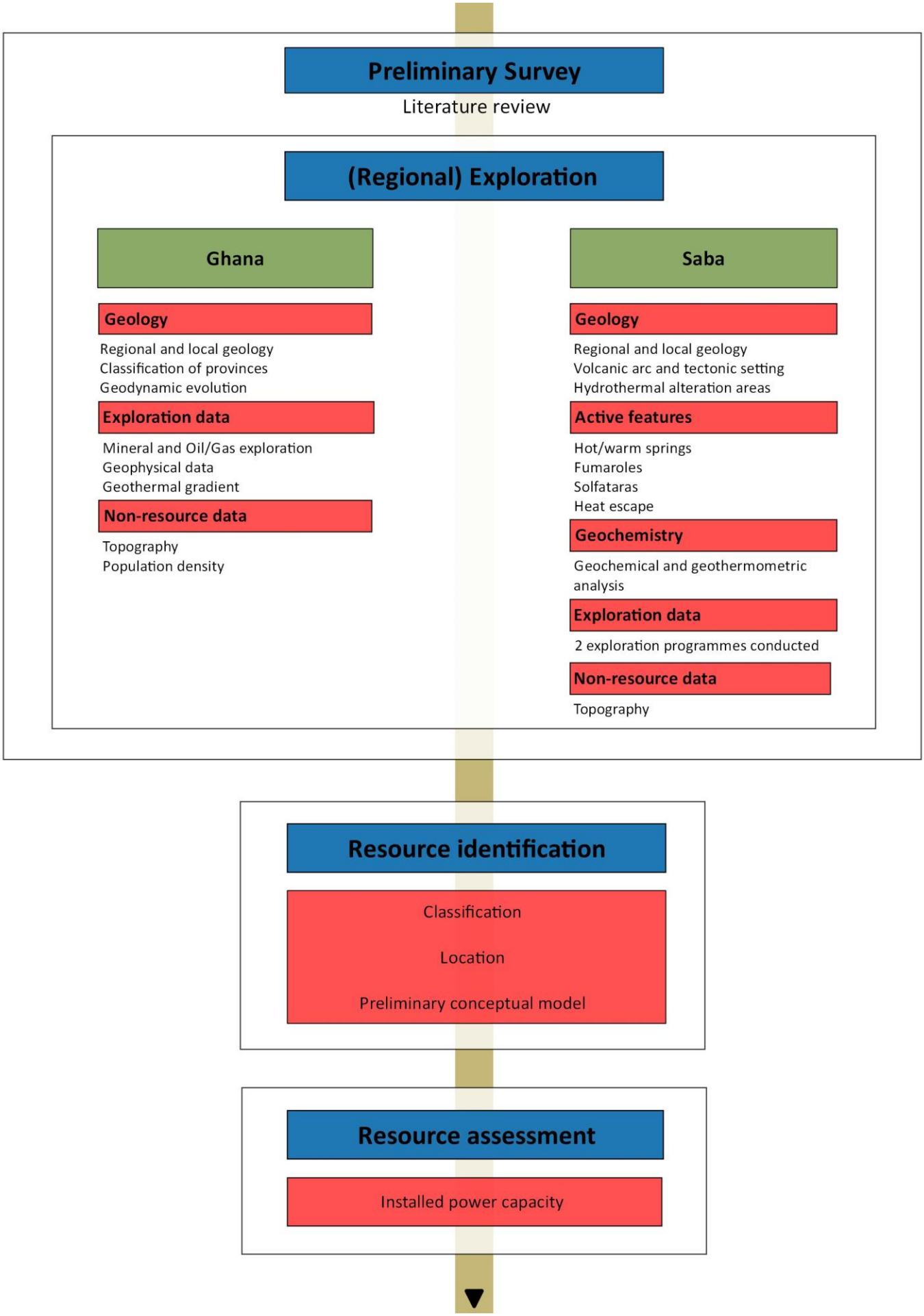

Figure 6: Geothermal potential screening flow chart as used in this study, incorporating 'preliminary survey' and 'exploration' phases as described in the 'Best Practice Guide for Geothermal Exploration' (GeothermEx, Inc. & Harvey consultants, Ltd., 2012) and the ESMAP's 'Geothermal Handbook' (Gehringer & Loksha, 2012). Created with QGis, 2016.

2.1 Preliminary survey and exploration

The preliminary survey is performed by a literature review of key aspects from the exploration phase. It incorporates geological-, thermal- (active features and geochemistry), exploration-, and other non-resource data. Surveying can be focussed on a regional and/or nationwide scale. The nationwide literature review performed in this study is based on openly accessible data, including academic publications, databases/reports from mineral and oil/gas exploration, databases/reports from geophysical survey departments and other relevant studies and organizations.

Additional information on accessibility (infrastructure and topography), regulations, land use and environmental factors (surface water and groundwater for example) forms an important aspect of the survey phase. However, this study focusses on estimating geothermal potential (technical feasibility) and therefore attention to non-resource data is limited. Only topography and population density are discussed as they can have a major influence on selecting a suitable location for geothermal energy exploitation.

A compilation of available data is made and evaluated for each country separately, identifying what is present and what is lacking. Data may include thermal feature distributions, heat flow contour maps and estimated vertical and horizontal temperature distributions at specific depths. Results are presented in tables and on maps of the project area. This process is facilitated by a free and open source geographic information system known as QGis (version 2.14.0) (QGis, 2016). All figures created with QGis are presented in the WGS84 coordinate system.

2.1.1 Geothermal gradient

A geothermal gradient (also known as a temperature gradient) is a representation of the increasing temperature with depth relationship described above. It is usually derived from actual well based temperature logs and/or bottom hole temperatures available from well data. An approximate geothermal gradient can be calculated from measured heat flow and thermal conductivity values. Using a calculated geothermal gradient, subsurface temperatures can be estimated at various depths. The radioactive component of heat flow (radioactive heat production) is not taken into account in the temperature estimations at this point.

Heat flow can be calculated using equation 1, when thermal conductivity and geothermal gradient are known. Equation 1 can be rewritten to equation 2 in order to calculate the geothermal gradient dT/dz in ^{o}C/km when the heat flow is known.

$$Q = -k \cdot \left(\frac{dT}{dz}\right) \tag{1}$$

$$\frac{dT}{dz} = -\frac{Q}{k} \tag{2}$$

With T being the temperature in degrees Celsius, the depth z in kilometres, heat flow Q in mW/m^2 and the thermal conductivity k in W/mK. Equation 2, as it is given, suggests that the geothermal gradient is negative. This is correct since heat flows down a temperature gradient. Depth is thus considered a negative distance and, for example, a depth of 2 km should be regarded as z = -2 km.

Equation 2 can be integrated to calculate the temperature at a given depth, resulting in equation 3, in which T_0 is the average annual surface temperature.

$$T = \frac{Q}{k} \cdot z + T_0 \tag{3}$$

The geothermal gradient can be extrapolated horizontally based on a generalization of heat flow data according to region and geological age (Terrestrial heat flow, n.d.). This generalization assumes constant thermal conductivity values throughout the region considered. Because thermal conductivity is a physical property of rock, it is dependent on lithology. Therefore, gradients are extrapolated horizontally according to

the outcrop distribution of dominant formations within the region considered. The gradient is also extrapolated vertically, based on a single layer model, when temperatures at depth are calculated. The estimated subsurface temperature distributions, resulting of horizontal and vertical extrapolation of the geothermal gradient, are mapped on a nationwide scale and at depths of 1, 2, 3 and 4 km to create resource maps (at depth) as a means of indicating geothermal potential.

In order to incorporate the error margins of the heat flow and thermal conductivity values, four different case scenarios are calculated for the resource maps, a low-, base-, high- and best case scenario. The values for heat flow and thermal conductivity as reported are considered in the base case scenario. The error margins are captured in the low- and high case scenario's, by adding or subtracting the margin from the reported value, thus creating possible low- and high values of heat flow and thermal conductivity. Reports of an upper limit of heat flow are incorporated in the best case scenario.

The low case scenario is defined by the lowest possible geothermal gradient that applies to a certain region. The gradient is calculated using the low value of heat flow and high value of thermal conductivity. The base case scenario is defined by an average geothermal gradient calculated using the reported values of heat flow and thermal conductivity. The high value of heat flow and low value of thermal conductivity result in a high estimate of the geothermal gradient and defines the high case scenario. As mentioned above, reports of upper limits of heat flow are considered in the best case scenario. Combined with the low values for thermal conductivity, this scenario is defined by the best possible geothermal gradient and thus sets an upper limit for the temperature-depth relation.

2.2 Resource identification

Available data acquired from the literature review of the exploration phase, in combination with data provided by the selected development analogues, is used to identify areas of potential high enthalpy resources. A classification of the expected geothermal system(s) and potential resource(s) is made, according to the classification parameters described in chapter 0. The preferable locations of such resources and their power plants are discussed in terms of non-resource data such as topography and population density. To assist in estimating the parameters for geothermal resource assessment, a preliminary conceptual model is proposed.

2.3 Resource assessment

Mendrinos et al. (2008) have proposed a method for geothermal resource assessment by expressing its potential in MW_e (MegaWatts electricity) of installed power over a certain time period. Main parameters of the geothermal resource, such as volume, temperatures and physical properties of rocks and fluids, can be estimated.
This method is used to estimate the potential of the geothermal resources defined in chapter 7 by quantifying the available energy (installed power) over a period of 30 years. A division is made between the amount of heat that is stored in the resource (equation 4) and the amount of heat that can be extracted from the resource (equation 5). Using equation 6, the extracted heat (expressed as thermal power) is converted to electrical (or mechanical) power and is defined over time.

$$E_{st} = [(1-\varphi)\cdot\rho_r\cdot C_r + \varphi\cdot\rho_w\cdot C_w]\cdot V\cdot(T-T_b) \quad (4)$$

$$E_r = E_{st}\cdot R \quad (5)$$

$$N_e = \frac{E_r\cdot n}{f\cdot t} \quad (6)$$

Where:

E_{st}	Stored heat [kJ]	T	Rock natural state temperature [^{o}C]
E_r	Recoverable heat [kJ]	T_b	Base temperature [^{o}C]
φ	Porosity [%]	R	Recovery factor
ρ_r	Rock density [kg/m3]	N_e	Installed power [MW_e]
ρ_w	Water density [kg/m3]	n	Conversion efficiency
C_r	Rock heat capacity [kJ/kg^{o}C]	f	Load factor
C_w	Water heat capacity [kJ/kg^{o}C]	t	Commercial life span of the plant [msec]
V	Rock Volume [m3]		

2.4 Monte Carlo simulation

The Monte Carlo simulation method uses randomness to solve problems that are or might be deterministic in principle. It is used to deal with complex problems that describe the distribution of known parameters by incorporating probability distributions. In the Monte Carlo simulations performed in this study, a triangular distribution has been applied to known parameters. A triangular distribution is suitable when a best guess value for a certain parameter can be specified along with high and low extremes. The Monte Carlo simulation is performed with a total of 10.000 runs. The result is a cumulative probability distribution that quantitatively incorporates the uncertainties involved in all parameters used (Gharaibeh, 2008).

The Monte Carlo simulation is used in this study to create an overall probability distribution of the geothermal gradient. The triangular probability distributions for the parameters involved in the analysis are defined as in equation 2. The results of the simulations are used to assess the probability of the defined deterministic case scenarios described above.

3. Ghana Preliminary and exploration

Ghana will be discussed in the context of the preliminary survey and exploration phases. A literature review of the following subjects is performed: 1) Regional and local geology, with special attention to the large amount of intrusives as these might pose important contributors to geothermal potential, 2) Thermal features, 3) Exploration data, with special attention to the geothermal gradient and 4) non-resource data.

3.1 Regional and local geology

The geology of West Africa can be subdivided into two main terrains (Wright et al., 1985). The first consists of “highly deformed metamorphic rocks and granitic intrusions” (Wright et al., 1985, p. 1), is mostly of Precambrian age and forms the basement terrane (Figure 7) (Wright et al., 1985). The second terrane is characterised by “nearly flat-lying sedimentary strata, which occupy broad basins and are sharply unconformable on the often steeply inclined metamorphic rocks” (Wright et al., 1985, p. 1), and is mostly of Late Precambrian to Paleozoic age (Wright et al., 1985).

A subdivision in the group consisting of metamorphic and granitic rocks is made based on their last period of crustal reactivation. The first group are the cratons, or shields, which consist of orogenic belts that have experienced their last deformation or metamorphism during the Eburnean orogeny (2000 +/- 200 Ma) and have been tectonically stable since (Tairou et al., 2012; Wright et al., 1985). The second group are the younger mobile belts that experienced their last crustal reactivation during the Pan-African orogeny (600 +/- 50 Ma). Both orogenies involved deformation and metamorphism, basement reactivation and emplacement of (mostly granitic) intrusives (Wright et al., 1985).

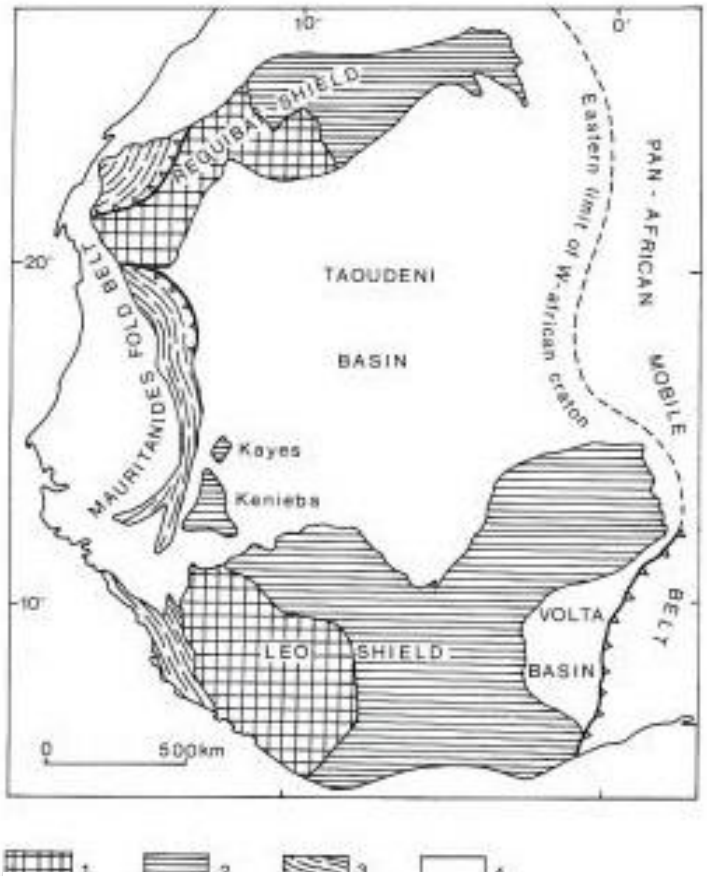

Figure 7: Simplified geological map of West Africa . 1 = Archean basement; 2 = Eburnean basement; 3 = Pan-African western mobile belt; 4 = Sedimentary cover. From Wright et al., 1985.

Ghana lies on the south eastern margin of the West African Craton. Four major geological provinces can be distinguished in Ghana based on age, type and composition of the rocks in each province (Figure 8). Metamorphic rocks and granitic intrusions of Paleoproterozoic age occur in the western half of the country (hereafter denoted as the Western Province), sedimentary rocks of Late Precambrian to Paleozoic age form the central part of the country (hereafter denoted as the Central Province) and the east and southeast of the country (hereafter denoted as the Eastern Province) is made up by supracrustal rocks of Neoproterozoic age (Schlüter, 2006, p. 110) and are part of the Pan-African mobile belt terrane, better known as the Dahomeyide mobile belt (Affaton et al., 1991). In the south of Ghana, along the coast, (hereafter denoted as Coastal Basins) Mesozoic sediments occur in several small basins (Schlüter, 2006).

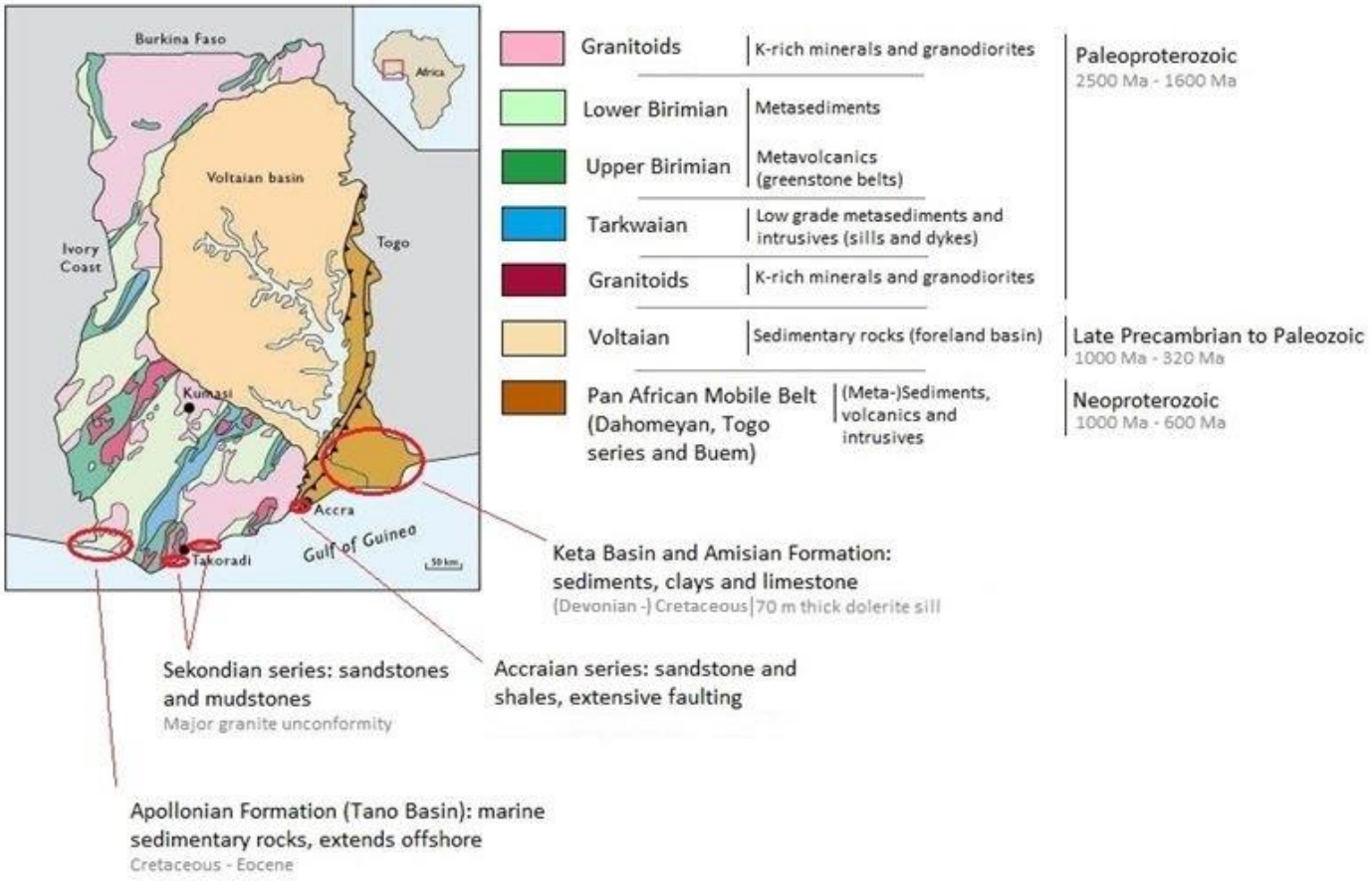

Figure 8: Geological map of Ghana. The composition and age of the dominant formations are indicated. Modified from Yendaw, 2005.

3.1.1 Western Province

The Western Province (Figure 9) occupies almost half of Ghana and it belongs to the shield area of the West African Craton (Yendaw, 2005). The Paleoproterozoic rocks of the Western Province consist of the Birimian Supergroup and the Tarkwaian Group (Schlüter, 2006). The Birimian Supergroup (light and dark green belts on the map in Figure 9) was deposited on a Precambrian basement (Wright et al., 1985; Yendaw, 2005) and now form extensive supracrustal belts, consisting of different sedimentary and volcanic strata (Wright et al., 1985). During the Eburnean event, the Birimian was deformed, metamorphosed and folded, resulting in a metasedimentary and metavolcanic rock composition (Wright et al., 1985; Yendaw, 2005). In Ghana, there is a subdivision into Lower- and Upper-Birimian (Wright et al., 1985). The Lower Birimian consists mainly of metasediments and the metavolcanics of the Upper Birimian are present as five evenly spaced volcanic belts (dark green belts, Figure 9), separated by the metasedimentary basins of the Lower Birimian (light green belts, Figure 9), and are all trending in a northeast-southwest direction forming synclinorial structures in a pre-existing basement. (Wright et al., 1985; Yendaw, 2005; Schlüter, 2006). “Based on several research works the Birimian has been dated between the Lower and Upper Proterozoic era, i.e. Middle Precambrian” (Yendaw, 2005, p. 12). “The total thickness of the Birimian in Ghana may be of the order of 10 to 15 km” (Wright et al., 1985, p. 40).

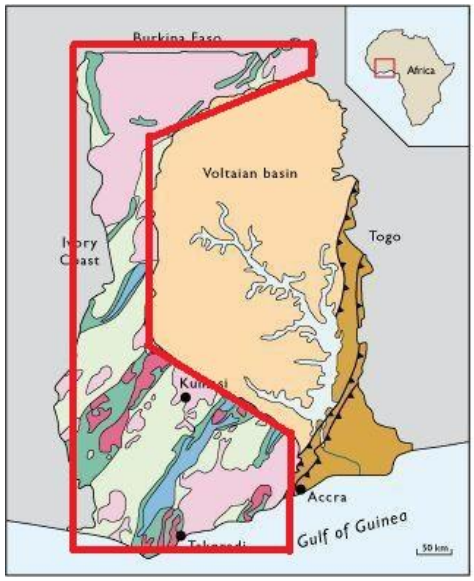

Figure 9: The Western geological Province indicated by the red bounding box. Modified from Yendaw, 2005.

The Tarkwaian Group consists of sedimentary rocks, which are mainly of shallow-water continental origin, that were deposited in intracratonic basins bordered by metavolcanic belts of the Birimian

Supergroup and were emplaced as a molassic sequence derived from erosion of Birimian rocks (Wright et al., 1985; Schlüter, 2006; Yendaw, 2005). The sediments of the Tarkwaian Group have undergone significantly less metamorphism and are concentrated in the Tarkwa area, where they outcrop in a Birimian metavolcanic belt, and in the Bui Syncline in the western part of the country (Yendaw, 2005). The Tarkwaian Group is a derivative of the Birimian Supergroup and therefore of about the same age (Yendaw, 2005).

3.1.2 Central Province

The Central Province (Figure 10) is better known as the Voltaian Basin. It consists of a thick series of largely clastic sedimentary rocks that rest with a major basal unconformity on the Eburnean basement comprised by the Birimian Supergroup and Tarkwaian Group of the Western Province (Yendaw, 2005; Wright et al., 1985; Mensah, 2015; Affaton et al., 1991). The sediments of the Voltaian Basin have experienced minimal deformation and metamorphism (Wright et al., 1985) and cover a time span of Neoproterozoic to Early Palaeozoic, with younger sediments ranging from Ordovician to Devonian or even younger (Mensah, 2015; Wright et al., 1985).

The sediments have been deposited in a composite setting ranging from an intracontinental basin, to a passive margin and ultimately a fore land basin terrane related to the Pan-African orogeny (Affaton et al., 1991; Yendaw, 2005). The basin fills contain both marine and terrestrial (fluviatile and lacustrine) sediments and contain traces of repeated trans- and re-gressions as well as remnants of two glaciations, one in the Infracambrian and the other in the Upper Ordovician (Wright et al., 1985).

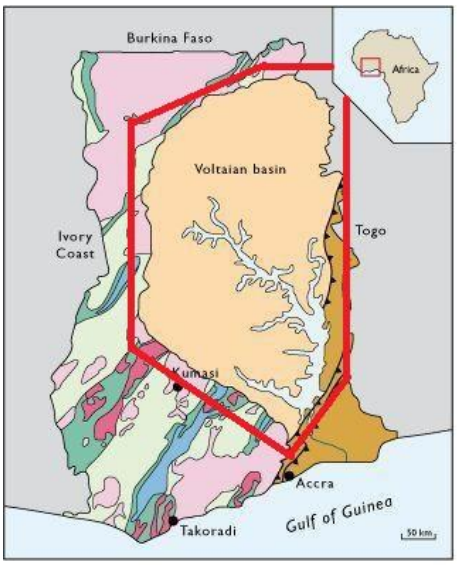

Figure 10: The Central geological Province indicated by the red bounding box. Modified from Yendaw, 2005.

In the east, the Voltaian Basin is overthrusted in some part by the Dahomeyide mobile belt (Eastern Province), resulting in folding and (progressive) thickening of the eastern margin of the basin, which is also suggested by normal and reversed faults delimiting horsts and grabens in the formations underlying the sedimentary basin (Tairou et al., 2012; Yendaw, 2005; Affaton et al., 1991; Mensah, 2015). This also results in an overall gently asymmetric synclinal shape of the Voltaian Basin containing a somewhat concentric distribution of sediments (Figure 11); around the margins outcrop the oldest sediments, while the youngest outcrop at a more or less central position (Wright et al., 1985). The sedimentary sequence in the western and northern parts of the basin is approximately 3 km thick, while the sequence in the southeast can reach thicknesses of up to 7 km (Affaton et al., 1991).

A subdivision of three supergroups can be recognized in the Voltaian Basin (Affaton et al., 1991), which are the Bombouaka Supergroup, the Pendjari (or Oti) Supergroup and the Tamale (or Obosum) Supergroup in ascending stratigraphic order (Mensah, 2015; Schlüter, 2006). Figure 11 represents a schematic cross section of the Voltaian Basin, showing the three supergroups. Relations to their depositional environment are discussed below.

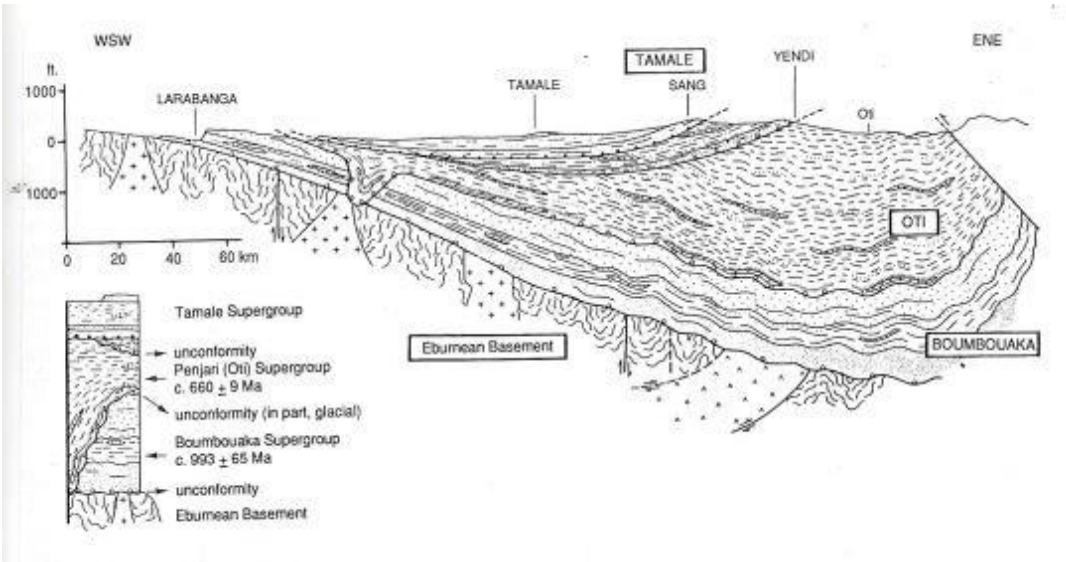

Figure 11: Schematic tectonostratigraphic cross-section of the Voltaian Basin (adapted from Affaton, 1987). The Bombouaka, Oti and Tamale Supergroups are indicated in the cross-section. The stratigraphy of the Voltaian Basin is shown in the lower left corner. The line of section is comparable to the one indicated in Figure 13. From Affaton et al., 1991.

The Bombouaka Supergroup consists of two groups of mainly sandstones enclosing soft clay-siliceous sediments (Affaton et al., 1991) that were deposited on an intracontinental marine platform and range in age from 1000-750 Ma (Wright et al., 1985; Schlüter, 2006). The Pendjari (or Oti) Supergroup rests on both the Bombouake Supergroup, with an erosional unconformity of partly glacial origin, as well as directly on the Birimian and Tarkwaian groups, due to the fill of erosional channels that cut the Bombouaka Supergroup (Affaton et al., 1991; Wright et al., 1985). The Pendjari Supergroup is characterized by shales, siltstones, sandstones and a basal conglomerate, which provides an important stratigraphical marker (Wright et al., 1985) and these were deposited in a relatively deep marine environment on a passive margin that developed east of the West African Craton (Affaton et al., 1991), with an age span estimation between 750-600 Ma.

The Tamale (or Obosum) Supergroup unconformably overlies the Pendjari Supergroup and consists of clays and siltstones overlain by coarser continental rocks (Affaton et al., 1991; Schlüter, 2006). The Pendjari Supergroup is representative of a fore land basin with a molassic sequence partly derived (erosional products) from the Dahomeyide mobile belt (Affaton et al., 1991; Wright et al., 1985). The age of this Supergroup is still open to discussion; some state it is Upper Proterozoic to Paleoproterozoic, while others state it is Lower Paleozoic; Ordovician to Devonian or even younger (Affaton et al., 1991; Wright et al., 1985).

3.1.3 Eastern Province

The Dahomeyide mobile belt, which forms the southern part of the Pan-African mobile belt terrane (Neoproterozoic), forms the Eastern Province (Figure 12) and is located in the eastern and south eastern parts of Ghana and consists of the Dahomeyan system, the Togo formation and the Buem formation (Yendaw, 2005). The Dahomeyide mobile belt forms the southern part of the more extensive Transaharian belt, which extends from Algeria to the Dahomeyan system in Ghana, Togo and Benin, and was developed during the Pan-African orogeny (Affaton et al., 1991) in which the Dahomeyan system was thrusted onto the south eastern margins of the Voltaian Basin (Figure 14). It comprises supracrustal sedimentary and volcanic rocks of late Precambrian to Early Phanerozoic age (Wright et al., 1985), which were deformed and partly metamorphosed during the Pan-African orogeny.

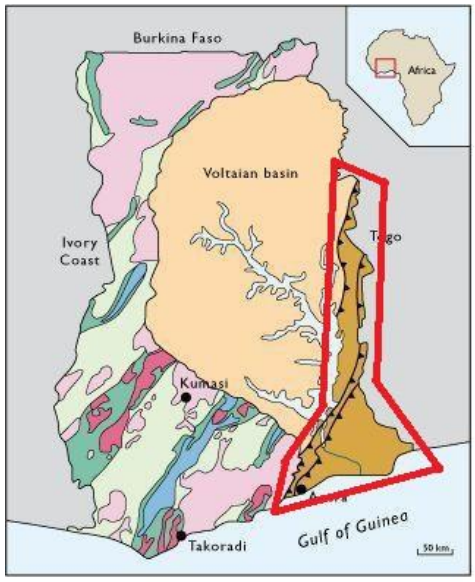

Figure 12: The Eastern geological Province indicated by the red bounding box. Modified from Yendaw, 2005.

The Pan-African Dahomeyide mobile belt is characterised by a sequence of northwest oriented nappes resulting of several folding and thrusting phases. The northern part of the orogenic belt overthrusts the Voltaian Basin while the southern part overthrusts its Eburnean basement (Tairou et al., 2012). External structural units in the West and internal structural units in the East, combined with granulitic massifs in the suture zone (Figure 13 and Figure 14), form the Dahomeyide mobile belt.

It is considered to be a collision belt characterised by an eastward progressive superposition of five different deformation phases, the first being granulitization as a result of the collision between the West African Craton and the Benino-Nigerian metacraton (Tairou et al., 2012). The second phase is the nappe stacking phase which has led to the main or regional foliation. Three postnappe folding phases are associated with the final stages of the Pan-African Dahomeyide orogeny. Three or four compressional axes and one late extensional axis are identified in Eastern Province, resulting from thrust planes associated with reverse faults, strike-slip faults in the suture zone and internal structural units and late normal faults suggesting an extensional episode (Tairou et al., 2012).

The Dahomeyan system (part of the Dahomeyide mobile belt in Ghana) consists of mafic and felsic gneisses that occur as four alternate belts trending in a south-south west to north-north east direction (Yendaw, 2005; Schlüter, 2006) and of ultrabasic intrusives, such as granites and dolerite dykes. The mafic Dahomeyan rocks are made up of two groups: the metabasics, which consists of a thick series of mafic rocks that are strongly colour banded,

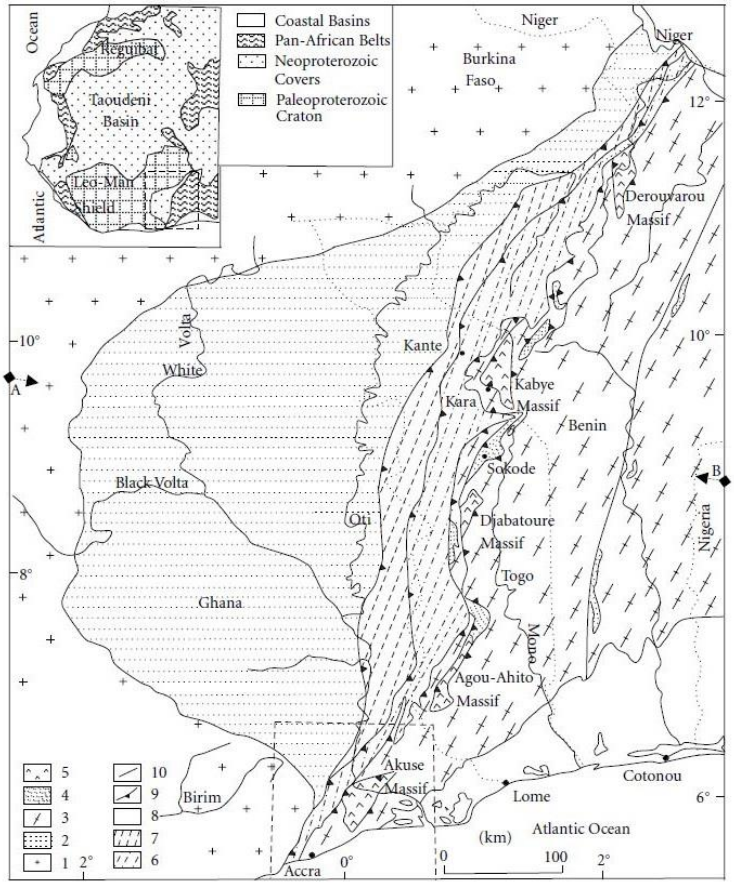

Figure 13: Schematic geological map comprising the Western, Central and Eastern Provinces, with a focus on the Dahomeyide mobile belt (Pan-African mobile zone). 1 = Eburnean basement complex; 2 = Voltaian Basin; 3 = internal and external units of Dahomeyide belt; micaceous quartzites; 5 = basic and ultrabasic massifs of the suture zone; 6 = Akwapim structural unit; 7 = Buem structural unit; 8 = Gulf of Guinea Basin; 9 = thrust contact; 10 = Kandi fault; A-B = schematic cross section line Figure 14. From Tairou et al., 1991.

and the basic intrusives that occur as sills, dykes and minor intrusive bodies in the metabasic rocks (Yendaw, 2005). The geological age of the Dahomeyan system is not quite clear as of yet; Birimian ages of 1700-2050 Ma are reported, but age determinations on gneisses and basic intrusives indicate a wide range of Pan-African ages ranging from 450-580 Ma (Yendaw, 2005). The most probable explanation is that the Dahomeyan system is indeed of Pan-African age and that Birimian ages are derived from Birimian basement rocks that were reactivated during the Pan-African orogeny (Affaton et al., 1991).

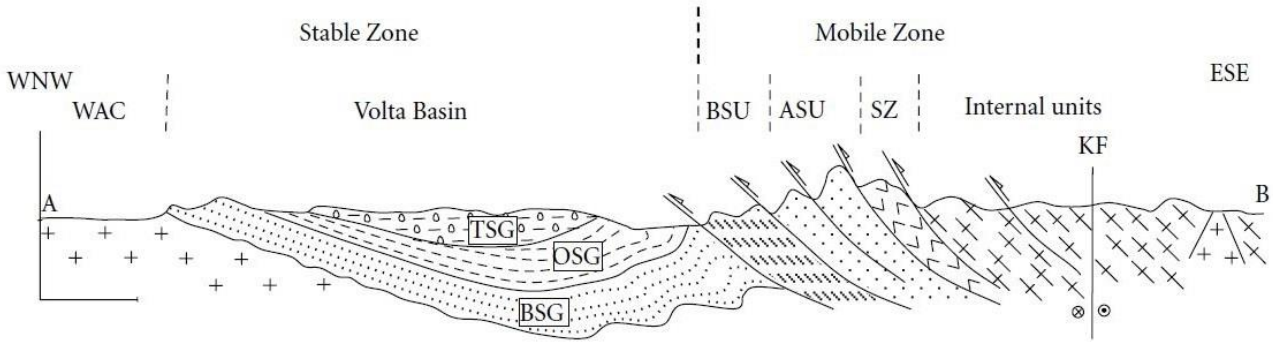

Figure 14: Schematic WNW-ESE cross section showing the relationships between the West African Craton (WAC), the Voltaian Basin (with BSG = Bombouaka Supergroup, OSG = Oti Supergroup, TSG = Tamale Supergroup) and the Dahomeyide orogenic belt (Pan-African Mobile Zone, with BSU = Buem structural unit, ASU = Akwapim structural unit, SZ = Suture Zone and KF is Kandi Fault). From Tairou et al., 2012.

The Buem Formation corresponds to the external structural unit forming the eastern limit of the Voltaian Basin (Central Unit) and consists of a sequence of clastic sediments, mainly sandstones, and shales, but also interstratified volcanics (Wright et al., 1985); the rocks are largely unmetamorphosed. The Togo formation is bordered on both sides by thrust contacts; against the Buem formation on the west and on the east against the Dahomeyan system (Wright et al., 1985) and it includes the Akwapim structural unit in Ghana, where the Togo formation is overthrusted onto the Buem formation (Tairou et al., 2012) and defines the eastern boundary of the Voltaian Basin (Central Unit). The rocks of the Togo formation are more highly metamorphosed and more deformed (Wright et al., 1985), but in some places unaltered shales and sandstones can still be found (Yendaw, 2005). The Togo formation was brought up by thrust faulting to overlie the Buem formation, despite younger age of the Buem rocks.

3.1.4 Coastal Basins

Mostly Mesozoic sediments occur in several places near/along the coast (Figure 15). They consist of Tertiary to Recent unconsolidated, marine, lagoonal and fluvial deposits (Yendaw, 2005; Schlüter, 2006). The different formations found in these coastal basins are summarized by Yendaw (2005) and include: 1) the Accraian Series with ages ranging from Early to Middle Devonian, 2) the Sekondian Series with ages ranging from Middle Devonian to Lower Cretaceous, 3) the Amisian Group with ages ranging from Upper Jurassic to Lower Cretaceous, and 4) the Apollonian Group which is of Upper Cretaceous age.

There are three main coastal basins in Ghana (Sedimentary Basins, n.d.): 1) The Tano-Cape Three Point Basin (also known as the Western Basin) which is a wrench modified pull-apart basin of Cretaceous age, 2) the Saltpond Basin (also known as the Central Basin) which is also a wrench modified pull-apart basin with ages ranging from Ordovician to Cretaceous, including the Sekondian Series, and 3) the Accra-Keta Basin (also known as the Eastern Basin) which is of Cretaceous age, including the Amisian formation. The basins are mainly located offshore, but both the Tano and Keta Basins extend onshore. Extensions of the Saltpond Basin only occur in small strips on/along the coast.

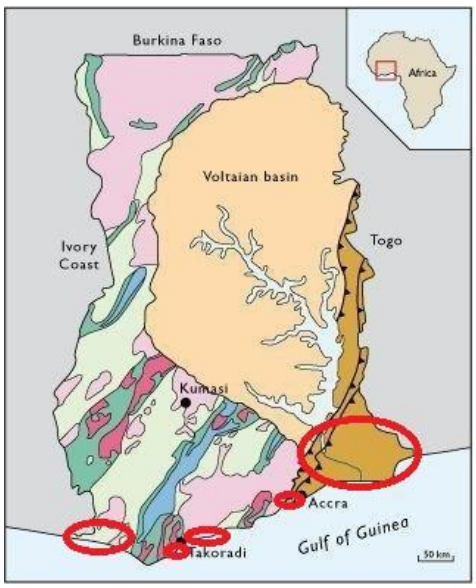

Figure 15: The Coastal Basins indicated by the red bounding circles. Modified from Yendaw, 2005.

3.1.5 Intrusives

Intrusives of granitic or granodioritic composition cover about one-fifth of Ghana (Yendaw, 2005). These granitoids are a heterogeneous association of igneous and metamorphosed rocks and cover a wide range of ages and mineralogical composition (Wright et al., 1985; Yendaw, 2005).

Yendaw (2005) classifies the different intrusions in accordance with their age and composition as follows:

- Post-Devonian and post-Carboniferous basic dykes.
- Post-Buem and pre-Voltaian intrusions of serpentine, pyroxenite, peridotite, gabbro and dolerite.
- Post-Tarkwaian laccoliths, sills and dykes of gabbro, norite and dolerite.
- Metamorphosed pre-Tarkwaian gabbro, norite, serpentinite, peridotite, pyrozenite and dolerite.

In some places, original igneous and sedimentary features are preserved. Such features include pillow structures in lavas and graded bedding and cross stratification in sediments (Wright et al., 1985).

3.1.5.1 Intrusives of Western Province

The Western Unit has been frequently intruded by rocks of granitic and granodioritic composition (Figure 16). They vary in dimensions from elongate batholiths, which are tens of kilometres long and several kilometres across, to small stocks only a kilometre or two across (Wright et al., 1985). The large batholiths occur in the central portion of the metasedimentary basins of the Birimian Supergroup and are known as the Cape Coast type, and as the Winneba type. The smaller masses of granites have intruded the metavolcanic belts of the Birimian and are known as the Dixcove type. In the northern half of the Western Province the rare Bongo type granitoids are found (Wright et al., 1985; Yendaw, 2005; Schlüter, 2006). These are potassic rich granitoids and are intruded in both the Birimian and the Tarkwaian groups (Yendaw, 2005).

The larger batholithic granites of the Cape Coast and Dixcove type are syntectonic; they were emplaced during the climax of the Eburnean orogeny (Affaton et al., 1991). They give ages of about 2100 Ma. The smaller granites of the Bongo type were emplaced after this main climax and give ages of about 1800 Ma (Wright et al., 1985; Yendaw, 2005). The majority of large batholithic granite intrusions are the product of crustal reactivation (Wright et al., 1985).

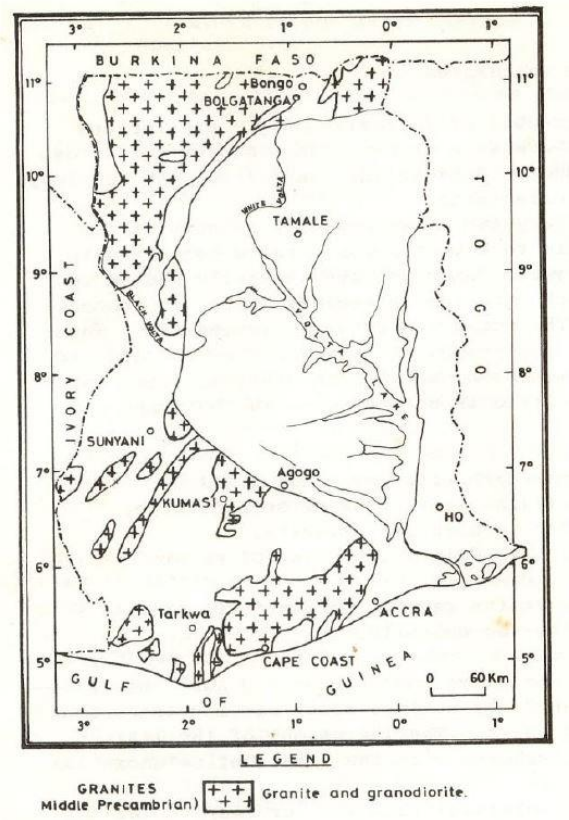

Figure 16: Distribution of intrusives throughout the Western Province. From Yendaw, 2005.

3.1.5.2 Intrusives of Central Province

There is evidence that the Volta basin of the Central Unit has been intruded at depth by igneous rocks in some places (Kesse, 1978). These igneous intrusions could be part of a Permo-Triassic aged system of sills and dykes and other intrusions that are known to occur not only in cratonic basement, but also among Paleozoic sediments overlying the craton (Wright et al., 1985; Yendaw, 2005).

3.1.5.3 Intrusives of Eastern Province

Granites and granitic intrusions are known to occur in the Eastern Province, as Affaton et al. (1991) report that “large amounts of these granitoids were emplaced within the whole Dahomeyide orogeny”.

3.1.5.4 Intrusives in Coastal Basins

At a depth of 3500 meter, a dolerite layer with an approximate thickness of 70 m has been found in the Keta Basin, one of the Coastal Basins of Ghana. The dolerite layer is interpreted as an early Jurassic sill, intruded into the Devonian strata of the basin, with an age of 167 +/- 5 Ma. A similar sill has been found in the Tano Basin further west (Wright et al., 1985). The overall age of these sills ranges between 275 and 175 Ma.

3.1.6 Structural geology

Since the majority of Ghana's geology has been tectonically stable since at least 2000 Ma, the structural geology of the Western Province plays a minor role within the scope of this study. Although the Central Province was influenced by the Pan-African orogeny (600 Ma), its structural geology also plays a minor role. However, the Eastern Province has largely been influenced by the Pan-African orogeny. Since this province relates to the Dahomeyide mobile belt it is worthwhile to elaborate on its evolution, with special attention to the emplacement of granites.

3.1.6.1 Geodynamic evolution of the Dahomeyide orogens

The evolution of the Dahomeyide mobile belt can be explained using plate tectonic models (Affaton et al., 1991). The Pan-African mobile belt terrane was developed by "the closure of an ocean between an active eastern continental margin (Andean type) and a passive western continental margin (i.e., Voltaian Basin) along the eastern side of the West African Craton" (Black et al., 1979b as cited in Affaton et al., 1991, p. 117). This is illustrated in Figure 17.The widespread occurrence of granites in the Dahomeyide mobile belt results from the subduction processes associated with the ocean closure (Affaton et al., 1991) and the granites have many comparable characteristics with modern island arcs and active continental margins (Affaton et al., 1978 as cited in Affaton et al., 1991, p. 117). Thrusting and the development of nappes resulted in crustal thickening and reactivation of the existing basement, in turn resulting in the production and emplacement of granites. Affaton et al. (1991) state that "the eastward dipping subduction process, the partial melting in the thickened crust and the last event of the Pan-African tectonothermal activity produced granitic magmas which were subsequently emplaced as pre-, syn-, late- and post-tectonic Pan-African granitoids". Large amounts of these granitoids were emplaced within the whole Dahomeyide mobile belt.

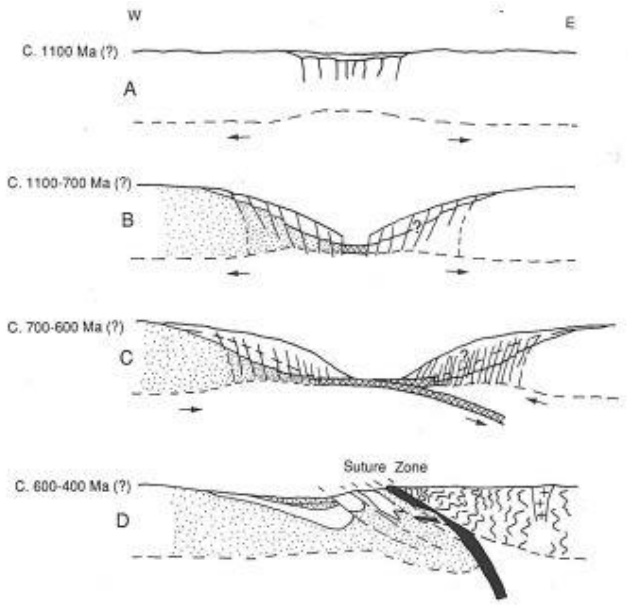

Figure 17: Geodynamic evolution of western portions (I-III) of the Dahomeyide orogeny (adapted from Affaton, 1987). *A* Distention and first stage of rifting; *B* major stage of rifting leading to the creation of the Pan-African proto-ocean; *C* convergence and subduction of the Pan-African oceanic crust; *D* collision, Pan-African ocean closure, folding, thrusting, erosion and development of a molassic basin. From Affaton et al., 1991.

3.2 Thermal features

There are no reports of any active thermal features in Ghana. The only reports mentioning hydrothermally altered areas in formations are related to the many gold resources present in Ghana's subsurface (Harcouët et al., 2005). However, age determinations of these hydrothermal alteration processes give ages corresponding to the Eburnean orogeny (2092 ± 3 and 2086 ± 4 Ma) and are thus no longer of any significance in geothermal exploration.

3.3 Exploration data

Very limited exploration data is openly accessible and therefore available for this study. Well data (including temperature gradient data), gravity and magnetic surveys as well as seismic surveys are present, but not openly available.

Oil and gas exploration programmes have been conducted both onshore and offshore, but the focus lies on the offshore basins, as Ghana is known for its extensive oil and gas fields offshore. All data, which includes temperature logs, bottom hole temperatures and seismic surveys, related to these exploration programmes is stored in the database of the Ghana National Petroleum Company (GNPC), but not openly accessible. Geophysical data, including gravity, radiometric and magnetic surveys, is present in the database of the Geological Survey Department (GSD) of Ghana, which is also not openly accessible. However, maps on a national scale have been acquired (Atta, n.d.) showing gravity and magnetic anomalies and the distribution of radioactive elements (Figure 18). The survey data available from the GSD database is focussed on the Voltaian Basin, but is also related to the mining explorations in the Western Province. A gridded gravity anomaly map can be requested from the Bureau Gravimetrique International (2012) where a grid is extracted from the World Gravity Map of 2012 (Bonvalot et al., 2012) (Figure 18).

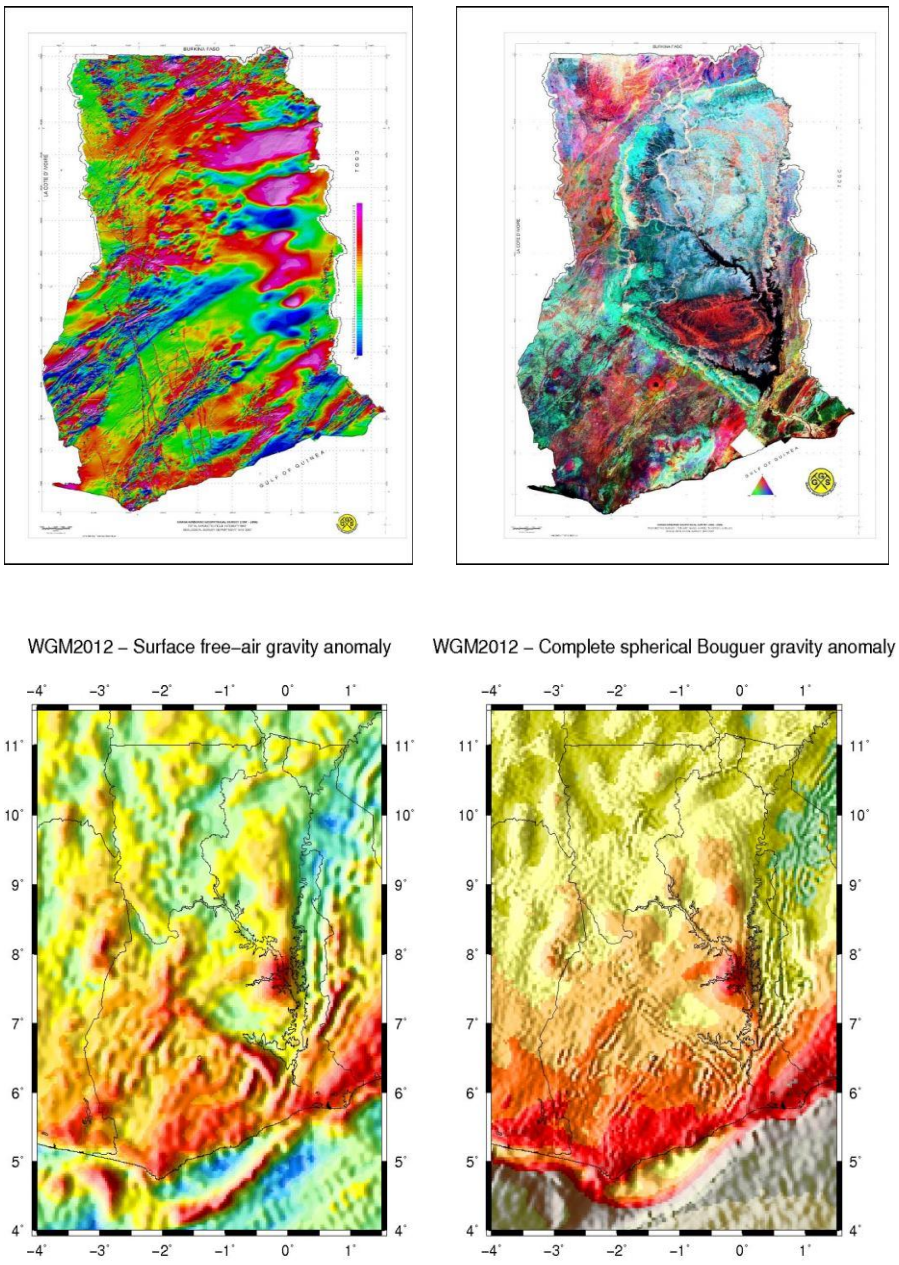

Figure 18: (Top) Magnetic data (left) and radiometric data (right). Both datasets cover the whole of Ghana. From Atta, 2016. (Bottom) Free-air gravity anomaly map (left) and Bouguer gravity anomaly map (right). From http://bgi.obs-mip.fr

3.3.1 Geothermal gradient

As exploration data is very limited, values for heat flow and thermal conductivity are found in and derived from literature. Several publications have been found reporting and/or estimating these values.

3.3.1.1 Heat flow

Heat flow is mostly described as a trend in the context of West Africa (Lucazeau et al., 1991). Only four locations of heat flow measurements exist in Ghana (Beck & Mustonen, 1972). The described trend and data points are shown in Figure 19.

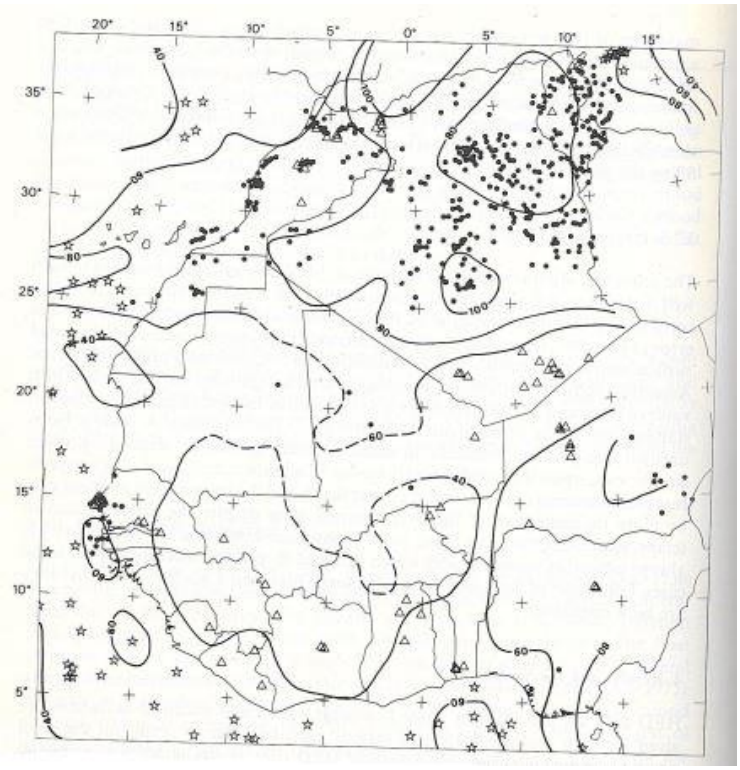

Figure 19: Heat flow contour map. Heat flow values are in mW/m2. *Dots* indicate oil data, *triangles* classical measurements (from literature) and *stars* bottom sea data. Ghana presents only four classical measurements. The described trend of increasing heat flow is clearly visualized over Ghana. From Lucazeau et al., 1991.

Results of these measurements are reported by Beck and Mustonen (1972) as an average value of heat flow for the whole of Ghana of 42 ± 8 mW/m^2. They also set an upper limit to heat flow of 60 mW/m^2. These four locations indicate the only heat flow measurements done in Ghana. Brigaud and Lucazeau (1985) report heat flow values ranging between 30 and 40 mW/m^2, with an average of 37 mW/m^2, for a wide range of Precambrian age formations.

Lucazeau et al. (1991) have adapted these reported values and state that the likely values for heat flow in Ghana range between 37 and 42 mW/m^2. They report a heat flow trend in West Africa of 30-40 mW/m^2 on the West African Craton which increases to 50-60 mW/m^2 in the surrounding mobile belts (Figure 19). They assign an average heat flow value of 38 ± 5 mW/m^2 to the Voltaian Basin and 53 ± 8 mW/m^2 to the Dahomeyide mobile belt.

3.3.1.2 Thermal conductivity

Thermal conductivity is a physical property of a material to conduct heat. When thermal conductivity is low, the heat transfer occurs at a lower rate and vice versa. This means a material with a low conductivity will create a higher potential difference (comparable to electrical resistance), resulting in a higher geothermal gradient, when the heat flow is considered to be constant (Figure 20).

Thermal conductivity measurements have been carried out in the Ashanti belt in Ghana where the conductivities of the Birimian and Tarkwaian have been determined. Harcouët et al. (2005) report values of 2.93 ± 0.74 W/mK for the metavolcanics and 2.89 ± 0.9 W/mK for the metasediments of the Birimian Supergroup. They also report a value of 3.12 ± 0.62 W/mK for the conglomerates of the Tarkwaian Group and a value of 3.10 W/mK for 'monzogranites' found in the Ashanti belt.

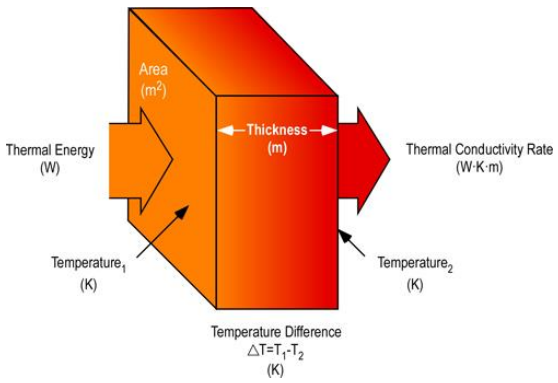

Figure 20: The concept of thermal conductivity. Retrieved from http://cfbt-us.com/wordpress/?p=1110

Beck and Mustonen (1972) have made an attempt to measure thermal conductivity of the sediments in the Central Province, but emphasize their use of an average value of 2.5 W/mK for the thermal conductivity of sedimentary rock in the Voltaian basin.

3.4 Non-resource data

Figure 21 and Figure 22 show a digital elevation model and a population density map (respectively) as these form important non-resource related data at this point. They play an important role in the selection of a geothermal power plant site, and therefore influence the resource identification process. Ghana is a relatively flat-lying country (Figure 21) and thus topography is expected to play a minor role in site location. Population density can have a significant impact on site location, as the demand for electricity increases with the number of people in a certain area (Figure 22). For example, the highest population density is found in the urban centre locations, thus making the region surrounding these centres preferable target areas for geothermal power plant location.

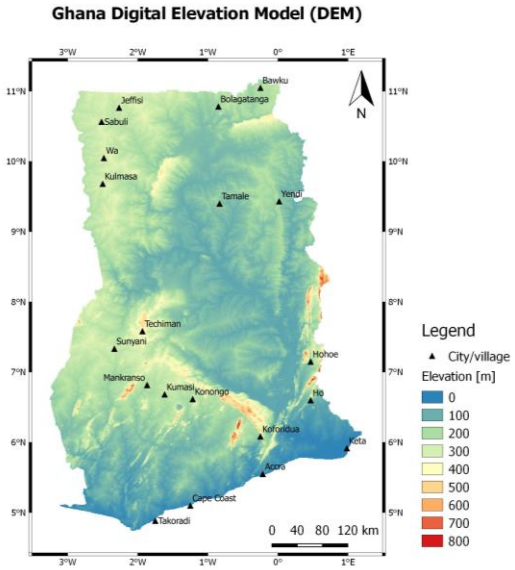

Figure 21: Digital elevation model Ghana indicating topography. Created with QGis, 2016.

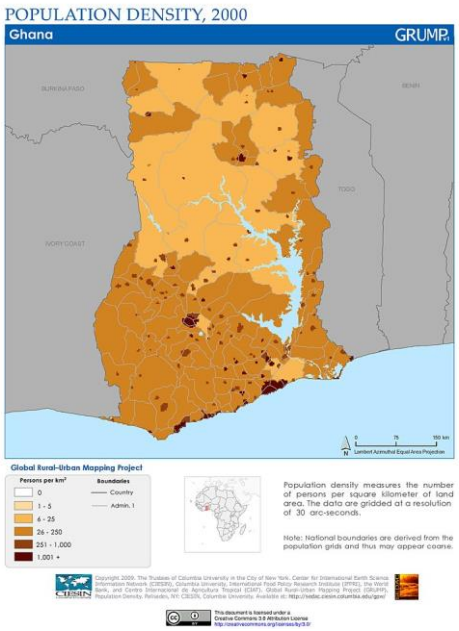

Figure 22: Population density Ghana in the year 2000. Retrieved from http://sedac.ciesin.columbia.edu/data/set/grump-v1-population-density/maps?facets=region:africa

4. Saba Preliminary and exploration

Saba will be discussed in the context of the preliminary survey and exploration phases. A literature review of the following subjects is performed: 1) Regional and local geology, with special attention to the volcanic island arc and its effect on geothermal potential, 2) Thermal features, 3) Exploration data, and 4) non-resource data.

4.1 Regional and local geology

The island of Saba is located on the north eastern edge of the Caribbean oceanic plate (Huttrer, 1998) and forms the most northern island of a volcanic island arc that stretches to Grenada in the south. “These islands are known as the Lesser Antilles” (Huttrer, 1998, p. 7-8).

4.1.1 Volcanic island arc

The Lesser Antilles volcanic island arc is the surface manifestation of a subduction zone, where the westward moving North American plate and northward moving South American plate are underthrusting the Caribbean oceanic plate (Roobol & Smith, 2004; Huttrer, 1998). The volcanic island chain has a multiple arc nature. Throughout the subduction process there have been four arc axes, with ages ranging from Eo-Oligocene in the east through Miocene, and Pliocene to Pleistocene-Recent in the west (Roobol & Smith, 2004).

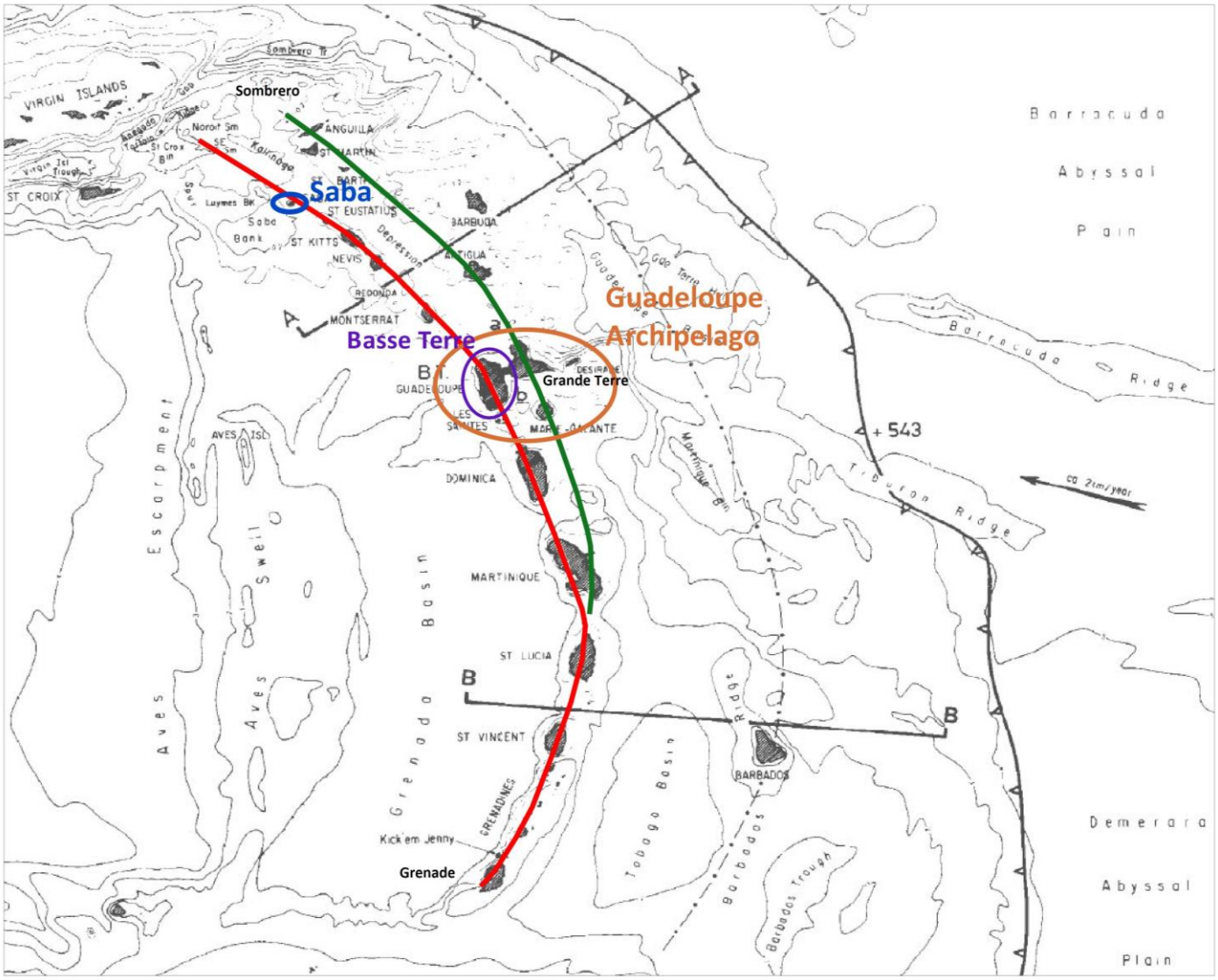

Figure 23: General setting of the Eastern Caribbean and the Lesser Antilles island arc. Red line = Recent, inner volcanic arc (Leeward Islands, Pleistocene-Recent age); Green line = Older, outer volcanic arc (Windward Islands, Eo-Oligocene age). ‘Triangled’ line indicates the subduction zone. Modified from Bouysse & Westercamp, 1990.

At present, the Lesser Antilles volcanic arc is defined by two arcs (Figure 23): an inner, more recent arc in the west, and an outer, older arc in the east. The islands extending from Saba to Basse Terre of Guadeloupe are part of the inner active volcanic arc and are known as the Leeward Islands. The inner arc complies with the most recent arc axis of Pleistocene-Recent age and has been evolving since the Late Miocene (Defant et al., 2001; Roobol & Smith, 2004). The outer arc complies with the oldest arc axis of Eo-Oligocene age and has been inactive since the Late Pliocene (Roobol & Smith, 2004; Defant et al., 2001). It comprises the islands of Sombrero to Grande Terre of Guadeloupe, which are known as the Windward Islands.

In the southern half of the Lesser Antilles (Grenada to St. Lucia) both arcs appear to be tightly superimposed, where the older arc forms the foundation of the islands and the recent arc has continued active volcanism on top of the older, extinct arc (Figure 24). However, in the northern half of the Lesser Antilles (north of Martinique) both arcs start to diverge, which is demonstrated by the two parts, Basse Terre and Grande Terre, of Guadeloupe (Defant et al., 2001; Roobol & Smith, 2004; Bourdon et al., 2011). In the most northern part of the Lesser Antilles, in the vicinity of Saba, both arc axes are separated by a 50 km wide depression known as the Kallinago depression (Roobol & Smith, 2004).

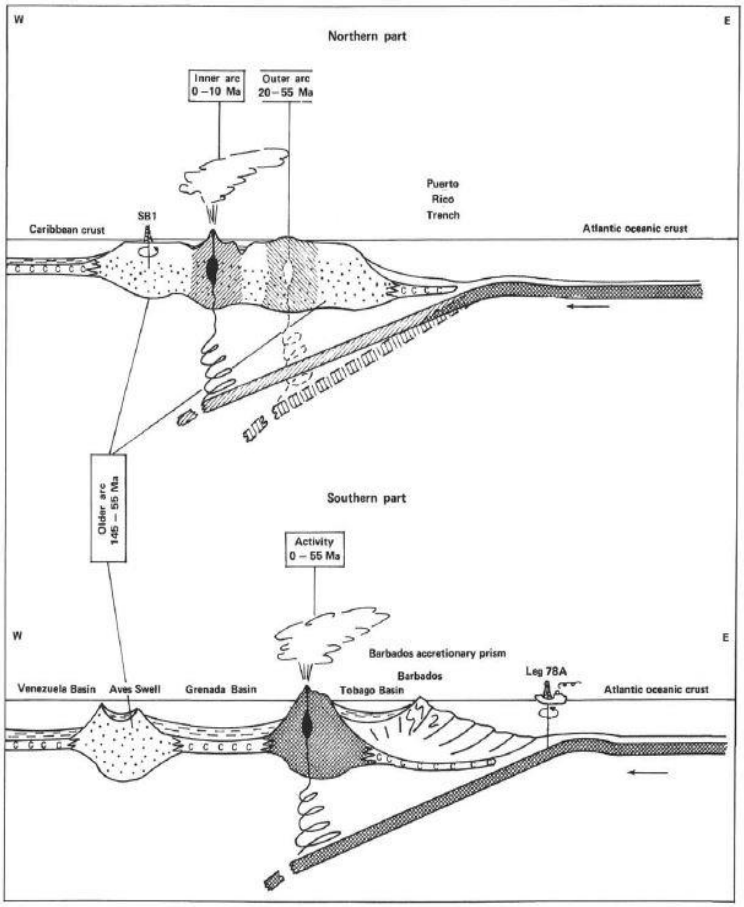

Figure 24: Interpretative schematic sections across the northern and southern Lesser Antilles island arc. In the northern part, the volcanic axis has shifted west (from the outer to inner arc) due to the arrival of the Barracuda Ridge in the subduction zone and consequently interrupting the subduction process. Both arcs were superimposed on an older island arc basement. In the southern part, the subduction process remained undisturbed. SB1 = Saba Bank exploratory well. Caribbean crust is represented by C. From Bouysse, 1984.

This westward shift of the volcanic axis of the Lesser Antilles volcanic island arc (Figure 24) can be explained by the attempted subduction of multiple aseismic ridges that exist on the North American plate (McCann & Sykes, 1984; Westbrook & McCann, 1986, as cited in Roobol & Smith, 2004, p. 6; Bouysse & Westercamp, 1990) . These ridges (Barracuda, Tiburion and St. Lucia ridges) have had a significant effect on the arc north of St. Lucia. These effects have, according to Bouysse and Westercamp (1990), resulted in “a sudden transverse shift of the volcanic front in a westward direction (‘equal’ to the direction of plate movement of the North American plate and due to the initiation of a new subducting slab), centrifugal migration of the eruptive centres on either side of the arc segments above the ridge, gentle uplifts and enhanced seismic and hydrothermal manifestations”.

The arc system of the Lesser Antilles is, as a whole, bordered to the west by an even older, submerged volcanic arc known as the Aves Ridge (Figure 23: indicated as Aves Swell), which formed during the Late Mesozoic and Early Tertiary (Huttrer, 1998; Bouysse, 1984; Roobol and Smith, 2004).

4.1.2 Island geology

The geology of Saba has been described by Westermann and Kiel (1961) and by Roobol and Smith (2004). Both have conducted geological fieldwork on the island, but they differ significantly in their description. Since the work of Westermann and Kiel (1961), the science of volcanology, especially pyroclastic deposits, has been greatly advanced.

Roobol and Smith (2004) interpret the pyroclastic deposits on Saba in terms of styles of volcanic activity. As the geological study by Roobol and Smith (2004) is more recent and takes into account the study by Westermann and Kiel (1961), these findings have been chosen as leading in describing the islands geology. Figure 25 shows the geological map of Saba.

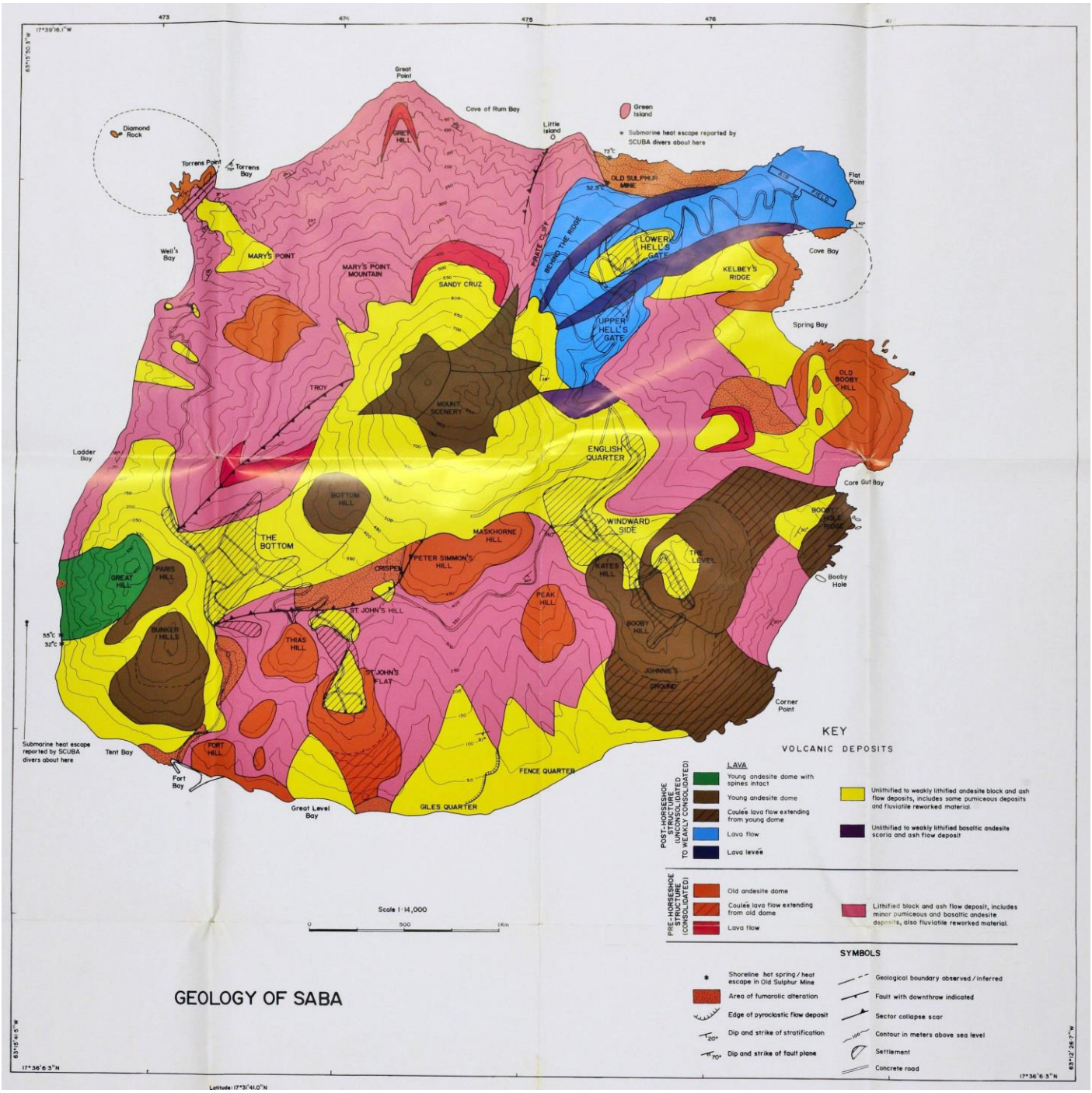

Figure 25: Geological map of Saba. From Roobol & Smith, 2004. (A larger copy of the legend is available in Appendix C).

The Windward Islands, belonging to the outer arc, are composed of “Eocene to Oligocene igneous rocks with a capping of Miocene and younger limestones” (Maury et al., 1990 as cited in Roobol & Smith, 2004, p. 1) and are also referred to as the Limestone Caribbees. The Leeward Islands are part of the inner, active arc and are known as the Volcanic Caribbees (Roobol & Smith, 2004). These islands are composed of “Pliocene and younger volcanic rocks and their reworked equivalents with small amounts of uplifted platform limestones” (Maury et al., 1990 as cited in Roobol & Smith, 2004, p. 1). These volcanic islands, including Saba, have been formed on top of extensive, shallow-water sub-marine banks (Roobol & Smith, 2004; Bouysse, 1984). West of the island of Saba lies the Saba Bank which is defined as a completely submerged carbonate platform (Roobol & Smith, 2004) that consists of a sedimentary sequence as old as early Cretaceous at its base overlain by Eocene and younger sedimentary and volcaniclastic rocks (Warner, 1990 as cited in Roobol & Smith, 2004, p. 2; Roobol & Smith, 2004). The Bank is capped by middle Miocene to early Pliocene platform limestones. Samples of the underlying banks, including Eocene to Plio-Pleistocene aged limestones, occur in the lavas and pyroclastic deposits of the islands, providing direct evidence of the older submarine banks underlying the volcanoes.

The island of Saba is formed by a single stratovolcano, where about twenty andesitic domes dominate the flanks of the volcano (Roobol & Smith, 2004). The main volcano is composed of “a complex of Pelean domes and their surrounding pyroclastic aprons, that sit somewhat eccentrically on top of juxtaposed older Pelean dome complexes”, giving the island a stratovolcano-like appearance (Roobol & Smith, 2004, p. 35). Roobol and Smith (2004) recognize two major geological divisions on the geological map in Figure 25: “an older division composed of lithified rocks that pre-date the formation of a major structure combining a crater with a sector collapse scar, and a younger division of weakly lithified to unlithified rocks that post-dates this structure”.

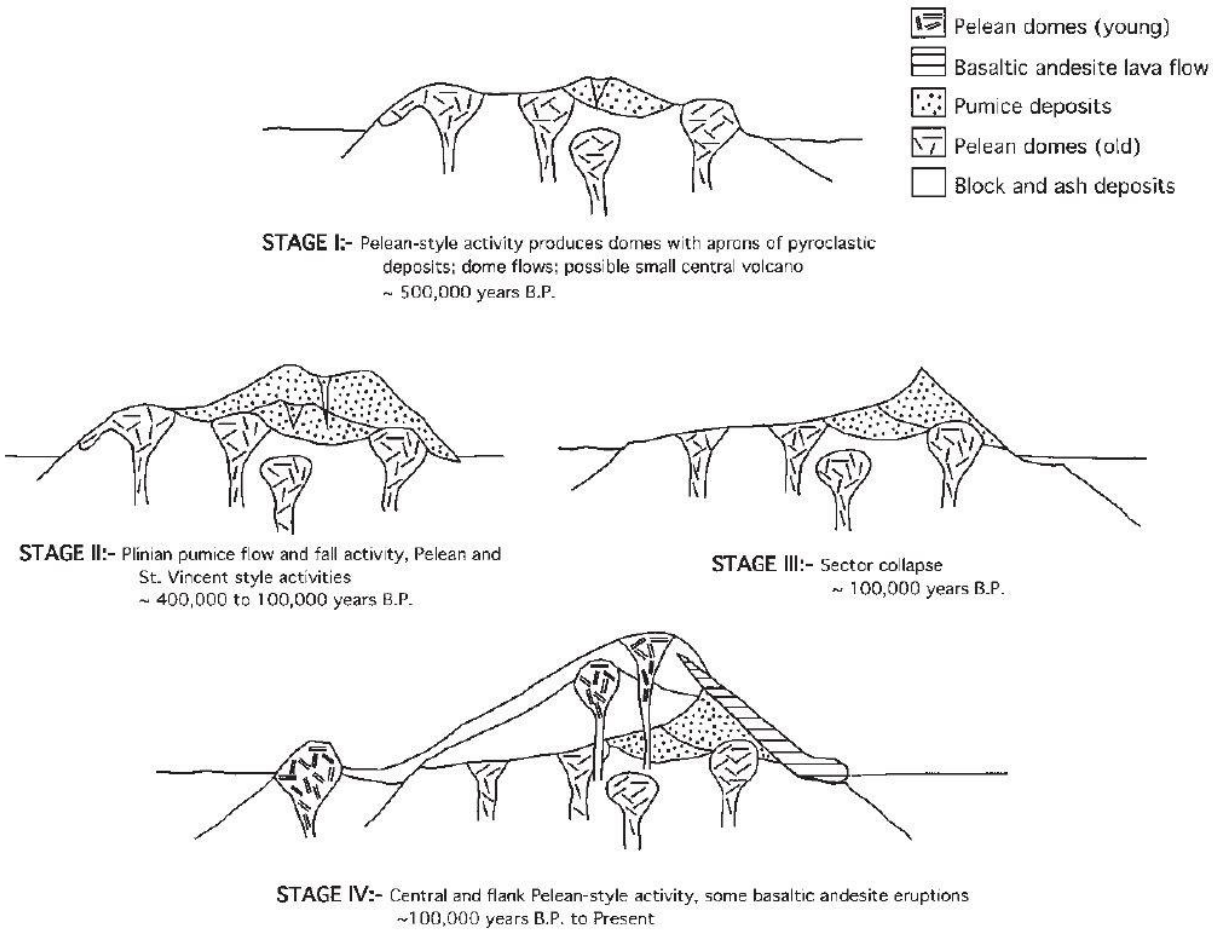

Figure 26: Four stages in the structural evolution of the volcano of Saba. In stage I, at about 500000 years, the island is being formed by a complex of andesitic Pelean domes and pyroclastic dome flows. Stage II, between 400,000 and 100,000 years, is characterized by Plinian-style activity which produced andesitic-dacitic pumineceous fall and flow deposits. At stage III, about 100,000 years, the horseshoe-shaped sector collapse structure formed. Infill of the collapse structure by andesitic domes and pyroclastic material occurred during stage IV, from 100,000 years ago to the present. From Roobol & Smith, 2004.

The older volcanic rocks mainly consist of successions of lithified, coarse block and ash flow deposits with interbedded andesite lava flows. Weakly lithified to unconsolidated block and ash flow deposits form the younger volcanic rocks of Saba (Roobol & Smith, 2004).

The sector collapse structure opens to the southwest and has been largely infilled by the Pelean dome complex of the main volcano and their pyroclastic deposits. According to Roobol and Smith (2004) the structure has an elongate horseshoe shape and they refer to it as the 'horseshoe-shaped sector collapse structure' (Roobol & Smith, 2004, p. 36 'sensu'). This terminology, as well as the geological division, has been adapted in this report. The age of the structure is estimated to be around 100000 years old (Roobol & Smith, 2004) and well preserved basaltic andesite lava flows are truncated by the structure. Hydrothermally altered block and ash flow deposits are located on the southeast wall (sector collapse scar) of this structure (Figure 28).

"In the Lesser Antilles at least five other horseshoe-shaped structures of similar dimensions have been described" (Roobol & Smidt, 2004, p. 37). All of these structures open to the southwest, with the exception of the one on Montserrat, which opens to the east. Such structures (on the west side of the Lesser Antilles islands, opening southwest) are often found adjacent to steep submarine slopes and are therefore considered to originate from gravitational sector collapse. Such mechanisms often result in submarine avalanche deposits, however, such deposits have not been traced adjacent to Saba (Roobol & Smith, 2004).
Roobol and Smith (2004) present a detailed description of the subaerial evolution of the island, which is illustrated in Figure 26.

4.1.3 Structural geology

A horst and graben structure has been indicated as the dominant tectonic style in the region of the Lesser Antilles by faults that are both parallel and transverse to the arc axis. The general direction of faults and lineaments is northeast-southwest and northwest-southeast and the principal tectonic stress directions have been interpreted as being orientated in the same general directions for the entire length of the Lesser Antilles volcanic arc (Figure 27).

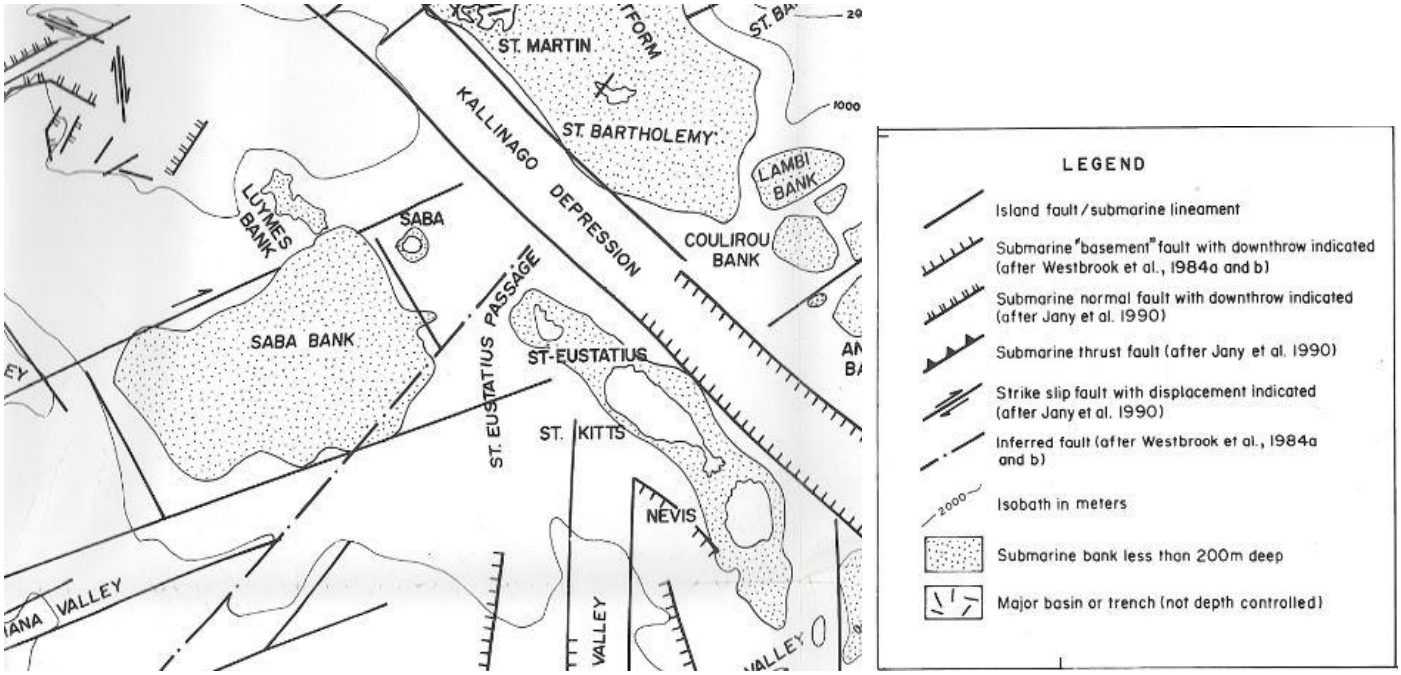

Figure 27: Faults and lineaments in the region surrounding Saba and the Saba Bank. From Roobol & Smith, 2004.

Huttrer (1998), Defant et al. (2001) and Roobol and Smith (2004) propose different ideas as to the structural geology of the island of Saba. Huttrer (1998) has identified three dominant fault trends present on the island of Saba; the first consists of at least 6 faults that transect the entire island following a N10-20W direction, the second trend strikes about N40-45E across the entire island and has a subparallel fault system to the

northwest, and a third fault system is formed by a N65-75E striking 'Rift Zone' (Huttrer, 1998, p. 11 'sensu') that appears to pass through the entire island. Defant et al. (2001) state that there is "one distinct major fault that cuts across the island from southwest to northeast", with small faulting episodes that have occurred north of this fault. Defant et al. (2001) also state that "slickenslides" along the major fault surface indicates that the region to the north of the island has moved up along the fault relative to the southern section". Roobol and Smith (2004) on the other hand, only speak of the horseshoe-shaped sector collapse structure and do not identify any faults that are not associated with this structure. However, they do suggest the existence of a possible fault located along a northeast-southwest direction through the submarine bank beneath the island.

Looking at aerial imagery, using Google Earth, any of these three interpretations can hold valid. In regards to the structural geology of Saba the latest interpretation of Roobol and Smith (2004) has been followed. The sector collapse scars as described in their work can be clearly identified on the aerial images. While the faults proposed by Hutrerr (1998) can be traced on aerial imagery, their existence is inconclusive, as there are many other interpretations possible from the lineaments seen on the aerial imagery.

All three interpretations proposed by the different authors mention a main fault orientated NE-SW that transects the entire island. Looking at a regional map of faults and lineaments given in Figure 27, the existence of such a major fault is unlikely on a regional scale on the basis of the movement along the fault described by Defant et al. (2001). However, on a local scale such a fault could very well exist. Even Roobol and Smith (2004) mention recent seismic data that suggests the island of Saba is located above a fault orientated perpendicular to the volcanic arc. Although Roobol and Smith (2004) only suggest the possibility of such a fault, both other authors clearly interpret its occurrence and therefore the existence of a NE-SW orientated fault, transecting the carbonate platform beneath the island and possibly the volcanic rocks of the island itself, is acknowledged in this report.

4.2 Thermal features

The Volcanic Caribbees (active arc) are characterized by hot springs, fumeroles, solfataras and historic volcanic activity (Roobol & Smith, 2004). As the island of Saba is part of the active arc, there are several thermal features present on the island (Figure 28); 1) several hot springs occurring at and below sea level are known around the coast, 2) Large areas of block and ash flow deposits belonging to the older volcanic rocks, associated with the sector collapse structure, are hydrothermally altered regions, 3) heat is escaping from a sulphur mine adit, 4) areas of former fumerolic activity, and 5) the occurrence of paleo-solfataras (Roobol & Smith, 2004; Huttrer, 1998). All indicate the geothermal potential of Saba.

Roobol and Smith (2004) report the occurrence of several hot springs (Figure 28): 1) hot springs at Well Bay have been reported by Sapper (1903). However, Kruythoff (1939) reported that the hot springs had been overwhelmed by the sea; 2) hot springs between Ladder Bay and Tent Bay occur as two closely-spaced hot springs, 3) hot spring opposite Green Island located on the northern shoreline immediately below the abandoned sulphur mine, and 4) submarine hot springs resulting in two areas of heat escape on the sea bed. The first of these locations is offshore of the Ladder Bay hot spring in Ladder Bay. The second lies on the sea bed between Green Island and the hot spring below the sulphur mine. Huttrer (1998) reports occurrences that agree with Roobol and Smith (2004) in regards to the hot springs between Ladder Bay and Tent Point, and the hot spring below the sulphur mine.

Several temperature measurements have been carried out by different authors in the past century and their results have been summarized in Table 2.

Date	Hot spring, Well Bay	Hot springs between Ladder Bay and Tent Point		Hot spring opposite Green Island	Submarine hot spring, offshore Ladder Bay	Sulfur mine (inside air temperature)	Measured by:
		# 1	# 2				
		°C	°C	°C	°C	°C	
1903	reported						Sapper (1903)
1903			54.2				Sapper (1903)
15/3/1950			55-57				Westermann & Kiel (1961)
22/7/1979						31.5 (20 m inside)	Roobol & Smith (2004)
25/7/1979			51				Roobol & Smith (2004)
27/7/1979			55	72			Roobol & Smith (2004)
26/8/1981			55	66.5			Gunnlaugsson (1981)
9/3/1994				54		32.5 (deepest part)	Roobol & Smith (2004)
10/3/1994		32	54.2				Roobol & Smith (2004)
13/4/1996				80			Johnson
24/9/1996				82			Buchan
30/1/1997		covered	62				Roobol & Smith (2004)
27/8/1997			62				Smith
9/4/1998				79			Johnson
8/5/1998					95.8		Huttrer (1998)

Table 2: Temperature measurement of hot springs and other thermal features. Modified from Roobol & Smith, 2004; adapted from Huttrer, 1998.

Other reports of thermal features made by Roobol and Smith (2004) include an abandoned sulphur mine directly above the hot spring opposite Green Island as the site of heat escape. Measured temperatures of air inside the mine are given in Table 2. They also include a newspaper report in 1995 which noted that a cave in the vicinity of the Ladder Bay hot springs had rocks that were “too hot to touch”.

All thermal and structural features have been mapped (Figure 28) and in total there are six locations of heat escape from the island of Saba and off its shores. There are groups of three features on opposite sides of the island, along a NE-SW line (Roobol & Smith, 2004). The sulphur mine adit, the hot spring opposite Green Island and the submarine hot spring near Green Island cover a horizontal length of 300 m and are located on the northeast corner. Occupying a horizontal distance of 600 m in the southwest are the hot springs between Ladder Bay and Tent Point (both on the shoreline and submarine) and the cave with the reported ‘hot rocks’.

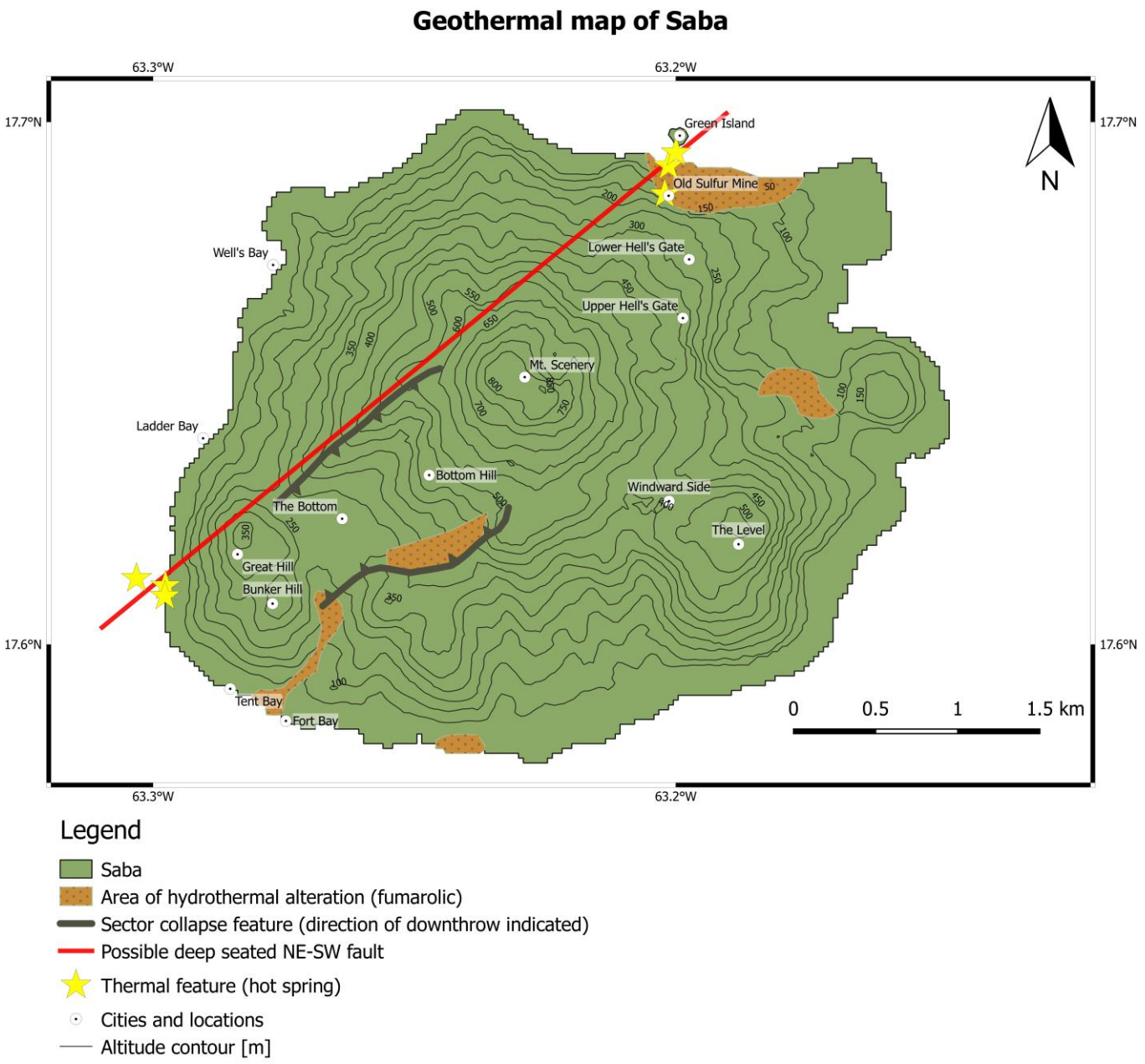

Figure 28: Geothermal potential map of Saba indicating locations of thermal and structural features. Created with QGis, 2016 and adapted from Roobol & Smith, 2010.

4.3 Geochemistry

Huttrer (1998) reports selective conclusions of a geochemical and geothermometric analysis of the samples taken during his study, on the basis of water chemistry only. Key findings from these conclusions are: 1) "all samples have variations in chemistry that suggest possible geothermal interaction with recycled or thermally modified seawater", 2) the sample taken at the hot spring below the sulphur mine has higher concentrations of major components (Br, Ca, Cl, K, Na) and major trace elements. "The fluid in the sample may have a reservoir temperature of 190 ^{o}C"; and 3) the sample from a hot spring between Ladder Bay and Tent Point "suggests a temperature as high as 185 ^{o}C".

4.4 Exploration data

At present, two geothermal exploration programmes have been conducted on the island of Saba: 1) by Huttrer in 1998, and 2) by Roobol and Smith in 2004. Their exploration programmes were focussed on geology, active features and geochemistry as part of the exploration phase (Figure 6). However, geophysical surveys have not been part of these explorations and thus there is no geophysical data available for or from the island of Saba. As mentioned above, a Bouguer gravity anomaly map derived from the WGS2012 map can be obtained from the BGI (2012), but only for marine gravity data. Land gravity data is not available at a scale suitable for the island of Saba.

Multiple, extensive exploration programmes have been conducted for oil and gas on the Saba Bank (Church & Allison, 2004). The acquired data consists of seismics, gravity and magnetic data and two exploratory wells were drilled in the Saba Bank, resulting in a wide variety of well data. Church and Allison (2004) report geothermal gradients of 3.3 ^{o}C/100 m for the SB-2 well and a slightly higher gradient of 3.8 ^{o}C/100 m for the SB-1 well.

4.5 Non-resource data

Figure 29 shows a digital elevation model of Saba (top) and a slope terrain analysis of Saba's topography (bottom). As can be seen from the figures, the topography of the island is very steep and highly irregular, and thus plays a major role in the site selection for a geothermal power plant.

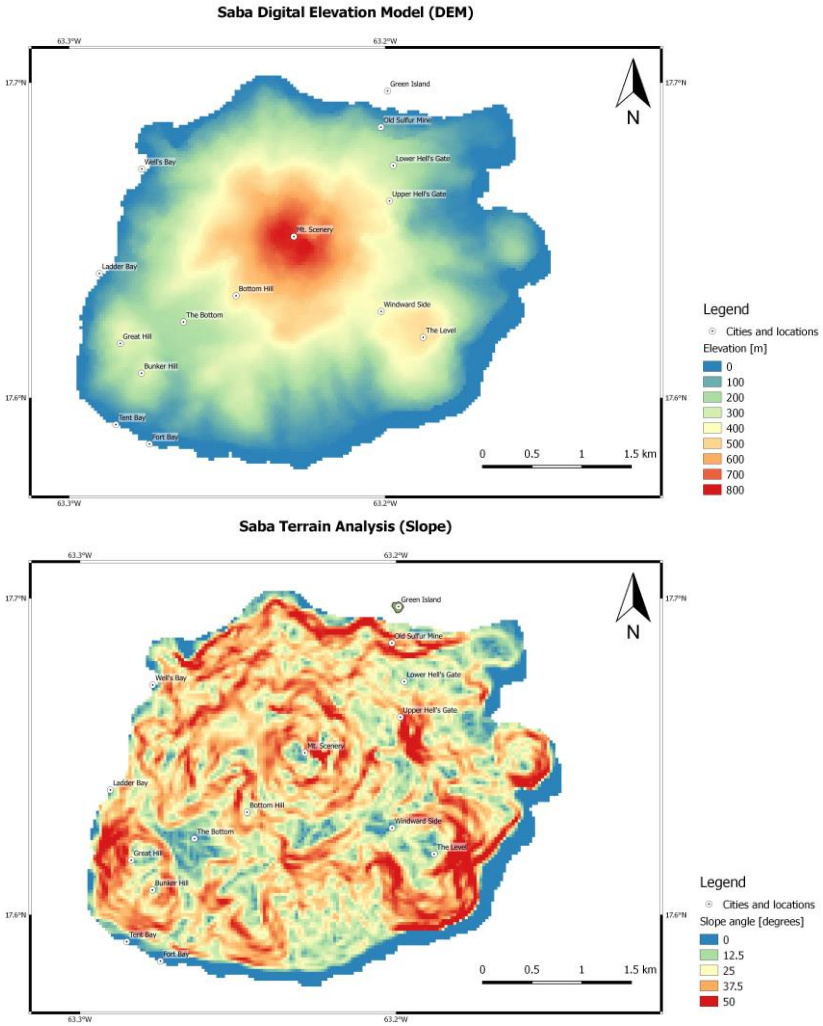

Figure 29: Digital elevation model (top) and Slope analysis (bottom) of the island of Saba. Created with QGis, 2016.

5. Data assembly

An overview of important results obtained from the preliminary survey and exploration phases is presented together with suitable development analogues that provide data that has not been acquired in the initial phases. The results presented in this chapter play an important role in the final phases of this geothermal energy screening study (Figure 6); 1) the classification and identification of potential geothermal systems, and 2) the estimation of the geothermal potential of available resources

5.1 Results exploration phase

An important objective of the exploration phase is determining subsurface temperatures, and their distribution and depth. Exploration data for Ghana allows for a subsurface temperature assessment by means of a geothermal gradient and results are presented below. Exploration data for Saba is limited in terms of determining a geothermal gradient. Therefore, subsurface temperature assessment in based on temperatures and reservoir depths associated with the Bouillante Geothermal field on Guadeloupe.

5.1.1 Results Ghana

After establishing input parameters, a geothermal gradient has been calculated for each of the dominant formations in the Western, Central and Eastern Provinces in Ghana. Although the Coastal Basins are geologically rather different from the other geological provinces described in Ghana, due to a lack in discrimination data regarding these basins, they are considered to be part of the respective provinces in which they are located. Outcrop distributions of the dominant formations in the geological provinces of Ghana have been illustrated in Figure 9, Figure 10 and Figure 12. The annual average surface temperature in Ghana is 26.5 ^{o}C ("Accra: Annual Weather Averages", n.d.).

5.1.1.1 Heat flow

The values reported by Lucazeau et al. (1991) form the most recent reports of heat flow in Ghana, combining classical measurements of heat flow reported in literature and temperature measurements from an extensive database of (exploration) well data.

These values have therefore been adapted in the thermal gradient calculations for the low-, base- and high case scenario's (Table 3). Heat flow values used in the best case scenario form the upper limits of heat flow and are adapted from Beck and Mustonen (1972). When a correlation is made between the Dahomeyide mobile belt and the Namaqua-Natal mobile belt in South Africa on the basis of similar geological features and age, an upper limit of 80 mW/m^2 would apply to the Dahomeyide orogenic belt (Table 3).

Heat flow [mW/m2]	Low case	Base case	High case	Best case
Western Province	37	40	42	60
Central Province (Voltaian Basin)	33	38	43	60
Eastern Province (Dahomeyide orogenic belt)	45	53	61	80

Table 3: Selected heat flow values for the main geological provinces according to the scenario considered.

5.1.1.2 Thermal conductivity

The reported thermal conductivity values as described in chapter 0 have been adapted in the geothermal gradient calculations for the different scenario's (Table 4), with the exception of the thermal conductivity value of 'monzogranites'. This value is not considered representative for the granitoids of the Western Province as they are composed of different types with varying compositions. Since there are no further reports on thermal conductivities of these granitoids, they have not been taken into account for the gradient distribution in the Western Province.

There are no reports of thermal conductivity measurements or values related to the Dahomeyide mobile belt of the Eastern Province. Since the rocks have an overall metamorphic composition, are known to be highly

deformed in some parts, and were formed as reactivated Birimian basement, a value comparable to the Western Province has been chosen for the thermal conductivity in the mobile belt terrane; 2.9 W/mK with a comparable error of ± 0.8 W/mK (Table 4). An error of ± 0.8 W/mK has also been applied to the thermal conductivity value of the sedimentary rocks in the Voltaian Basin in order to account for a wide range of conductivities.

Thermal conductivity [W/mK]	Province	Low case	Base case	High case	Best case
Metavolcanics	Western	3.67	2.93	2.19	2.19
Metasediments	Western	3.79	2.89	1.99	1.99
Tarkwaian	Western	3.74	3.12	2.5	2.5
Voltaian Basin	Central	3.3	2.5	1.7	1.7
Dahomeyide orogenic belt	Eastern	3.7	2.9	2.1	2.1

Table 4: Selected thermal conductivity values for the main geological provinces according to the scenario considered.

5.1.1.3 Calculated geothermal gradient

The low case resource maps show the lowest values of temperature distribution in the subsurface of Ghana. Temperatures range between 56 and 75 degrees Celsius at depths of 3-4 km. This is the result of low geothermal gradients which range from 9.8 to 12.2 ^{o}C/km.

The base case resource maps indicate the average values of temperature distribution at depth. Temperatures range between 65 and 100 degrees Celsius at depths of 3-4 km. Average geothermal gradients vary from 12.8 to 18.3 ^{o}C/km.

High values of temperature distribution in the subsurface are indicated on the high case resource maps. Temperatures range between 77 and 143 degrees Celsius at 3-4 km depths. These higher temperatures are the result of relatively higher geothermal gradients, which vary from 16.8 to 29 ^{o}C/km.

The resource maps belonging to the best case scenario show the upper limits of estimated subsurface temperature distribution in Ghana. At depths of 3-4 km temperatures range between 99 and 179 degrees Celsius, due to the high geothermal gradients derived from the upper limits of heat flow in Ghana. Geothermal gradients range from 24 to 38.1 ^{o}C/km.

Geothermal gradients are presented in Table 5 and estimated temperatures are quantified in appendix A. Examples of the resource maps for the different scenarios are given at a depth of 3km in Figure 30 and Figure 31. The resource maps related to all scenarios and all depths are presented in appendix B.

Geothermal gradient [^{o}C/km]	Province	Low case	Base case	High case	Best case
Metavolcanics	Western	10.1	13.7	19.2	27.4
Metasediments	Western	9.8	13.8	21.1	30.2
Tarkwaian	Western	9.9	12.8	16.8	24
Voltaian Basin	Central	10	15.2	25.3	35.3
Dahomeyide orogenic belt	Eastern	12.2	18.3	29	38.1

Table 5: Geothermal gradient distribution throughout the main geological provinces according to the scenario considered. The global average temperature gradient equals 25-30 ^{o}C/km.

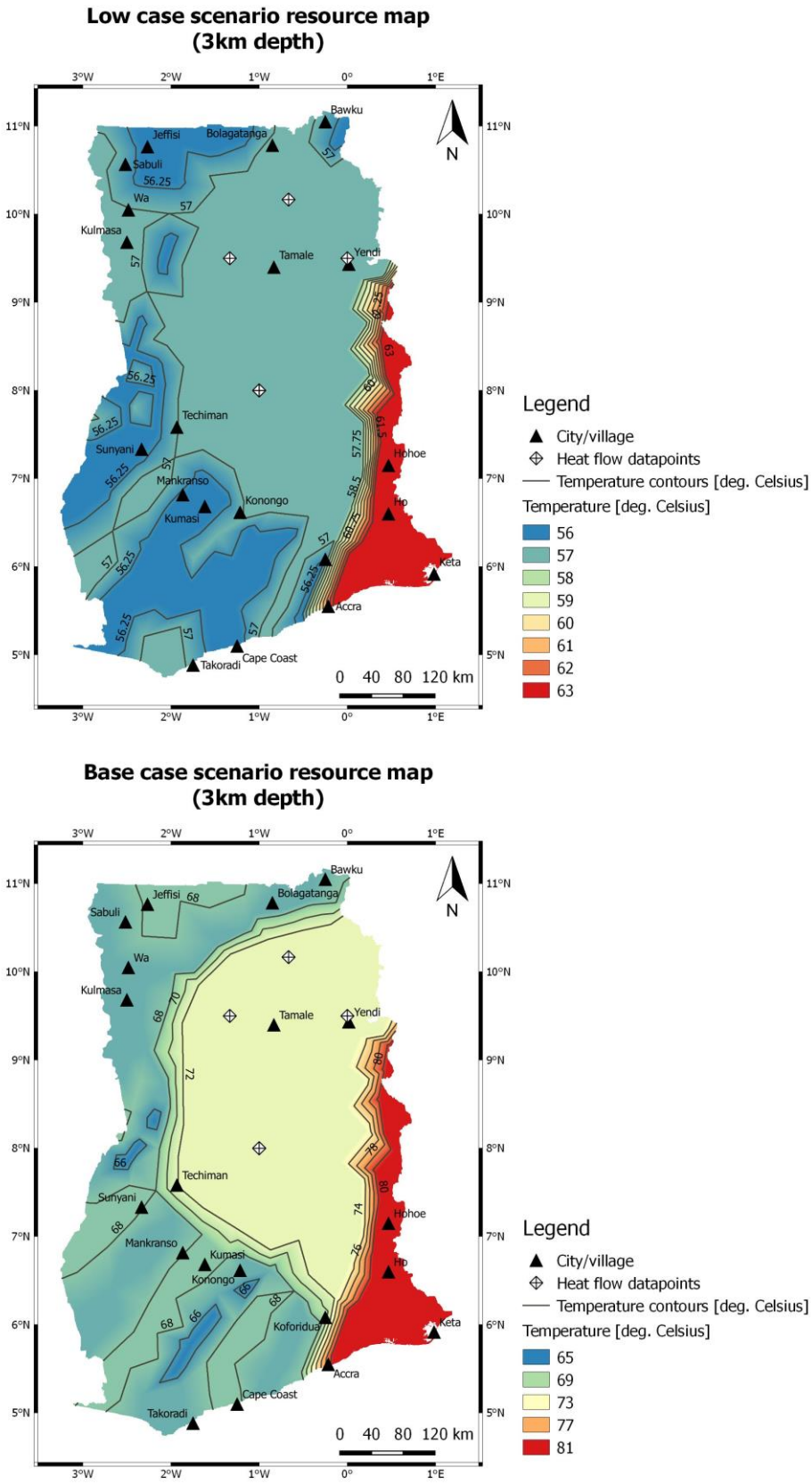

Figure 30: Subsurface temperature distribution at a depth of 3km for the low case scenario (top) and for the base case scenario (bottom). Created with QGis, 2016.

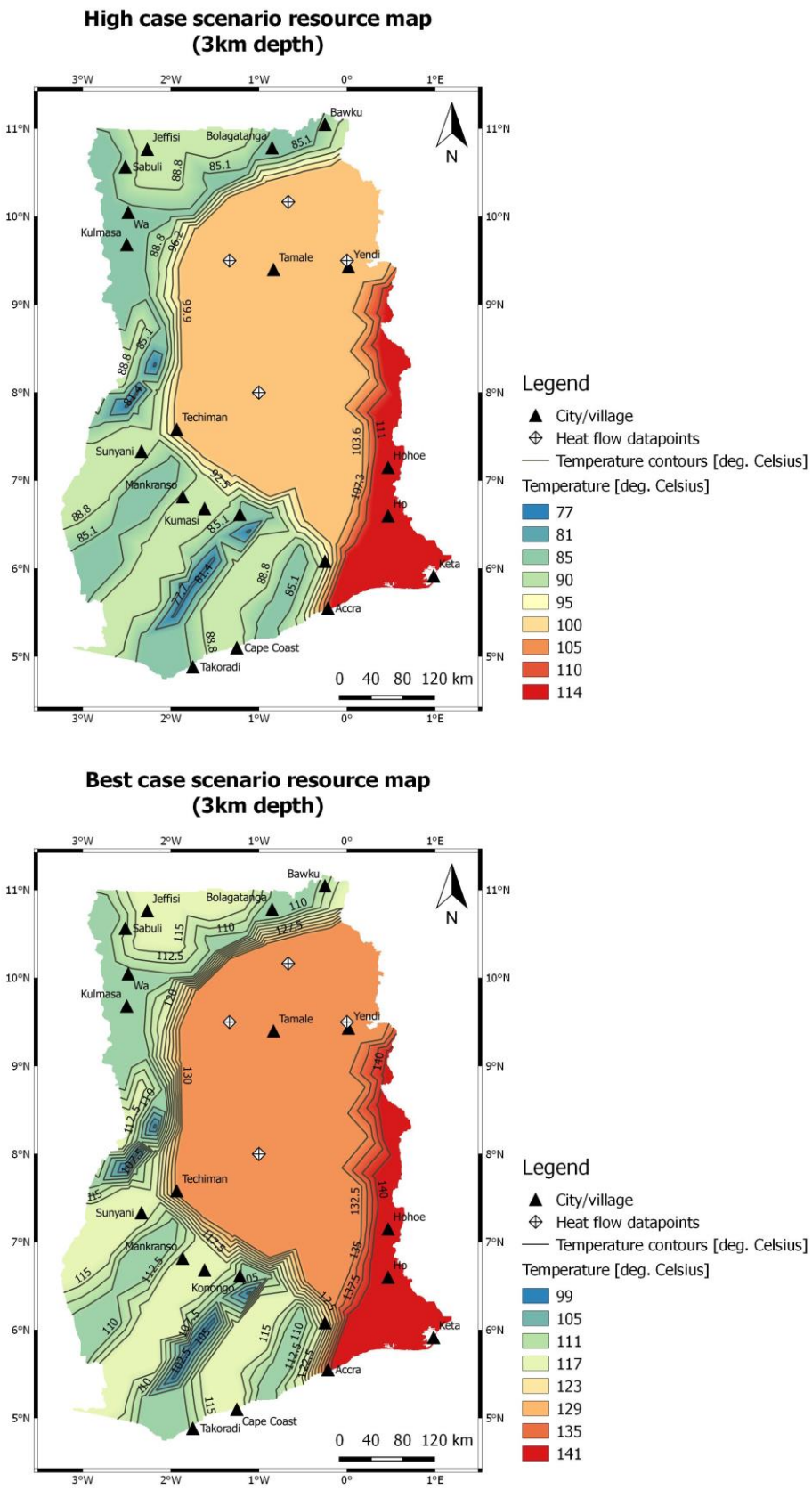

Figure 31: Subsurface temperature distribution at a depth of 3km for the high case scenario (top) and for the best case scenario (bottom). Created with QGis, 2016.

5.2 Development analogues

An evaluation study on the geothermal potential of the Limpopo Province in South Africa and a case study of the Bouillante geothermal field on Guadeloupe provide suitable development analogues.

5.2.1 Limpopo Province geothermal potential, South Africa – evaluation study

A geothermal evaluation study in the Limpopo Province, South Africa is used as an analogue for heat flow in Ghana. According to the findings described below, an upper limit of heat flow is estimated for the Eastern Province in Ghana, based on a similar geologic setting and comparable geologic age.

5.2.1.1 Geological setting

The majority of South African geology is comprised of the Archean-aged Kaapvaal Craton (Dhansay et al., 2014). The craton has formed a nucleus for continental growth by accretion of younger rock formations (between 1000 and 2000 Ma) to the craton, known as the Namaqua-Natal Mobile Belt.

5.2.1.2 Heat flow

The Kaapvaal Craton has low thermal conductivity and most of the heat is deflected from the underlying convective mantle away from the craton and towards the younger surrounding regions (Dhansay et al., 2014). Early heat flow measurements on the craton showed a relatively low heat flow profile. The heat flow profile increased significantly when measurements were done on the surrounding Proterozoic mobile belts. Heat flow increased from 45 mW/m^2 to 80 mW/m^2 along the Namaqua-Natal Mobile Belt (Figure 32). The higher heat flow in the Proterozoic mobile belt can also be the result of the high concentrations of heat producing elements found in the younger Proterozoic granites (Dhansay et al., 2014). Other examples of Proterozoic mobile belts in South Africa that show significantly higher heat flow measurements include the Limpopo Belt and Cape Fold Belt.

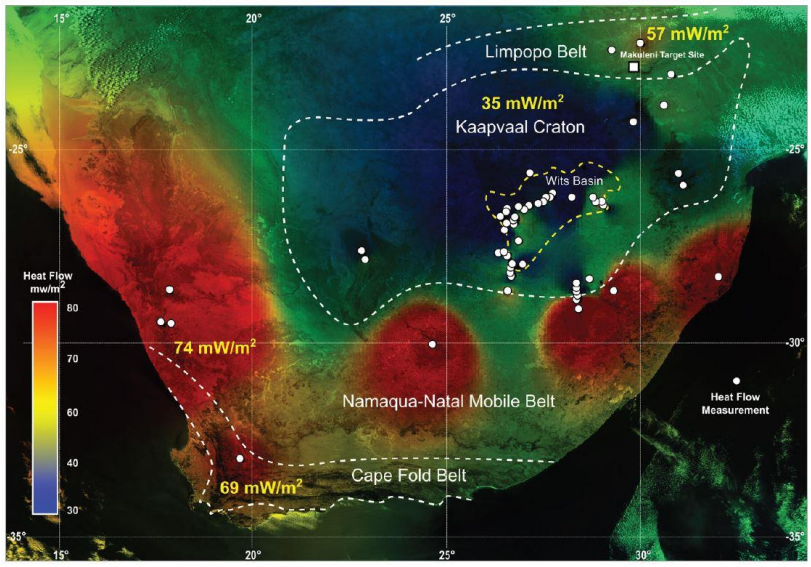

Figure 32: Geothermal potential map showing heat flow contours and measurement locations in South Africa. From Dhansay et al., 2014.

5.2.2 Bouillante geothermal field, Guadeloupe – case study

A case study of the Bouillante geothermal field on Guadeloupe is used as an analogue for reservoir conditions such as temperature, depth and location on Saba. The Bouillante field, located on the Basse Terre island of Guadeloupe, is also part of the inner, more recent and active volcanic arc (Figure 23) and therefore poses an excellent analogue. This case study is used to indicate the location of potential resources and estimate important parameters, such as resource temperature, for geothermal resource assessment on Saba.

5.2.2.1 Geological setting

The Guadeloupe archipelago is formed by the islands of Basse-Terre, Grande-terre, les Saintes, Marie-Galante and la Désirade (Figure 23). The archipelago is located in the northern part of the Lesser Antilles (Bourdon et al., 2011). “The Guadeloupe archipelago is a unique setting displaying both the older, extinct and younger, active volcanic arcs” (Bourdon et al., 2011, p. 4) (Figure 23). The islands of Grande-Terre and Marie-Galante are part of the older, extinct arc while the island of Basse-Terre, lying to the west, is part of the active volcanic arc which includes Saba. The basement of Grande-Terre is composed of volcanic formations and is overlain by a thick carbonate platform (Bourdon et al., 2011) identical to the carbonate

platform found on the island of Basse-Terre. Six main volcanic complexes have been identified on Basse-Terre forming the NNW-SSE trending Bouillante volcanic chain. It is believed that a two level magmatic reservoir is located below this volcanic chain with the same orientation (Bourdon et al., 2011).

The Bouillante geothermal field is located at the intersection between a major (sinistral) strike-slip fault, belonging to the Bouillante-Les Saintes system, and the Bouillante-Capesterre normal fault (Bourdon et al., 2011). The geothermal field has been developed in a small graben which is part of the large E-W Marie-Galante graben system (Figure 33, Left). The graben is made of a network of faults (Figure 33, Right) that favour tension opening, due to NNE-SSW extension along the strike-slip fault, and the circulation of geothermal fluids.

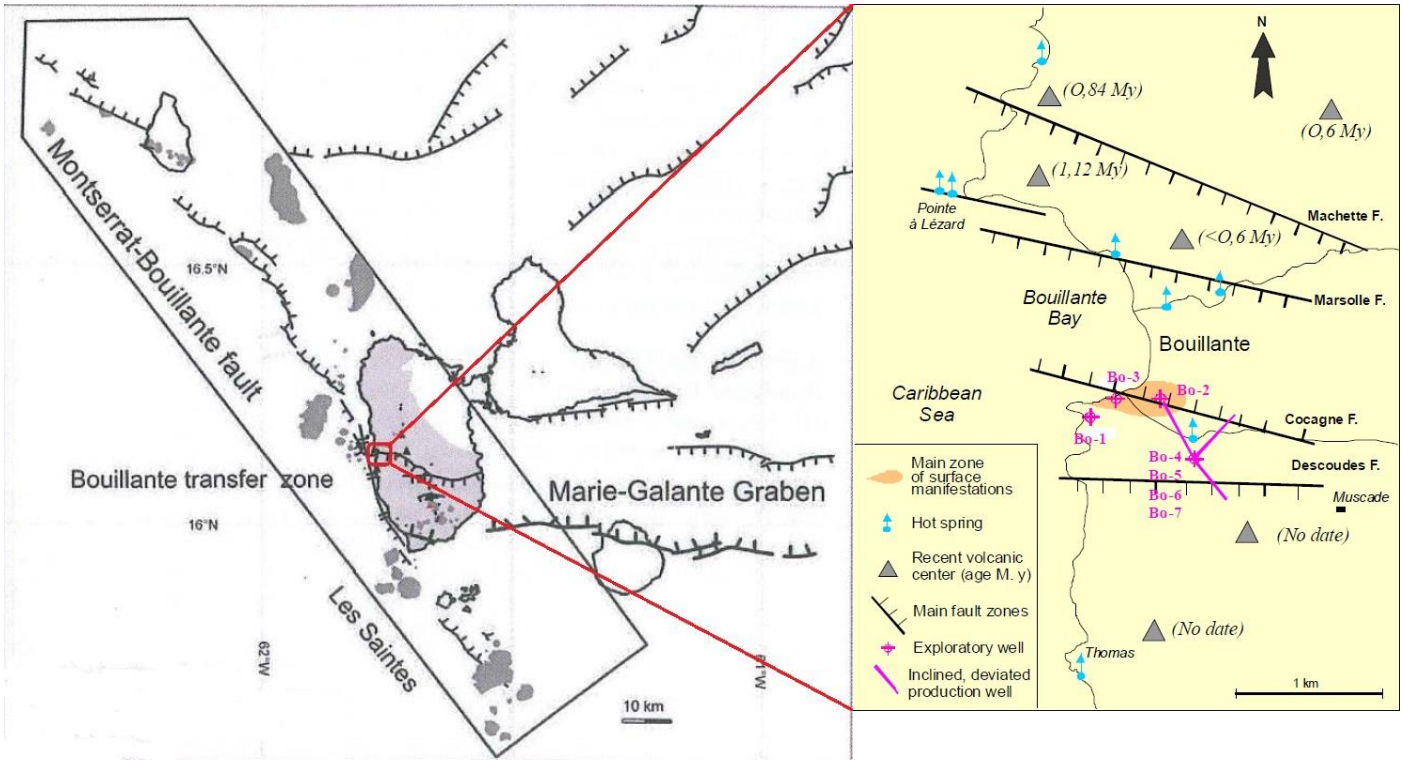

Figure 33: (Left) Regional and tectonic settings of the Bouillante geothermal field, indicated by the red bounding box. From Bourdon et al., 2011. (Right) Tectonic setting of the small graben in which the Bouillante geothermal field is located. From Beutin & LaPlaige, 2006.

There are a lot of thermal features indicating this geothermal reservoir at depth: hot soils, hot springs and fumaroles (Bourdon et al., 2011). Measurements of a hot spring show a temperature of 120 °C (Sanjuan et al., 2002 as cited in Traineau et al., 2015, p. 2). Hydrothermally altered rocks are indicative of temperatures in excess of 250 °C (Patrier et al., 2003 as cited in Traineau et al., 2015, p. 2).

5.2.2.2 Geothermal model

"The reservoir of the Bouillante geothermal field can be defined by two units: 1) a heat reservoir corresponding to the total rock volume affected by intense pervasive hydrothermal alteration with a homogenized temperature of 250-260 °C at less than 400 m depth and 2) a hydraulic network of permeable faults and porous aquifers in which the geothermal fluids circulate in the heat reservoir" (Figure 34) (Bourdon et al., 2011, p. 10).

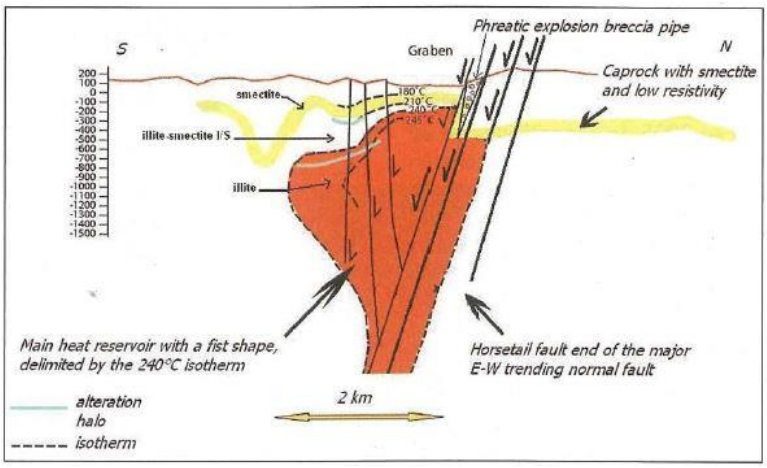

Figure 34: 2D conceptual model of the Bouillante geothermal field. The 240 °C isotherm roughly delimits the geothermal reservoir. From Bourdon et al., 2011.

The working fluid (or thermal fluid) forms a mixture of seawater (58%) and freshwater (42%) and occurs at a temperature of about 260 °C in the reservoir (Bourdon et al., 2011). The working fluid occurs mainly in the liquid phase, but can also occur in the vapour phase forming a water-steam mixture. “The process of mixing between seawater and meteoric water is in good accordance with the regional W-E Bouillante-Capesterre fault system extending both onshore and offshore” (Bourdon et al., 2011, p. 8).

Major faults have a strong control on the geothermal reservoir and migration of the thermal fluid within the reservoir. Wells have been drilled intersecting these major faults (Bourdon et al., 2011; Jaud & Lamethe, 1985); only three of which showed good productivity. The other wells did not show any productivity even though some did intersect a major fault. Figure 35 shows the well trajectories of some of these wells intersecting major faults.

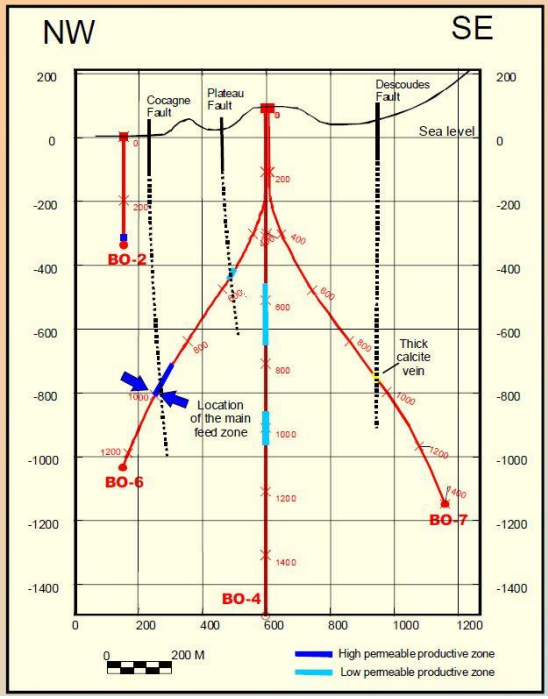

Figure 35: Cross sections along a NW-SE profile showing well trajectories, location and quality of permeable zones in relation with faults deduced from surface geology. Only Cocagne Fault appears to be highly permeable, Descoudes Fault has no permeability; possibly due to carbonates scaling. From Beutin & LaPlaige, 2006.

5.2.2.3 Resource and production parameters

The resource is classified as a high-enthalpy water-dominated dynamic system with a reservoir temperature of 230-250 °C at a depth of 600-2500 m (Jaud & Lamethe, 1985). The surface area of the field should not be less than 2.5 square km as its width is known to be 1 km and its length extends 2.5 km to the south (Jaud & Lamethe, 1985). The geothermal reservoir itself spans an area of less than 1 square kilometre (Traineau et al., 2015).There are four wells in production, two of which are steam productive.

The geothermal reservoir consists of sand and tuffs of low porosity, crossed by faults. The produced geothermal water has a temperature of 160 °C when entering the power plant and is discharged at 100 °C. As an example the productivity of two wells is given by Jaud and Lamethe (1985): 1) “the BO-2 well intersects a very productive fault and produces over 30 tons/hour of steam, together with 120 t/h of water at a pressure of 6 bars; The flow rate of this water-steam mixture equals 42 L/sec”, and 2) “the BO-4 well produces ‘only’ 13 t/h of steam and 50 t/h of water at a pressure of 5 bars; this equals a flow rate of 17.5 L/s”.

The Bouillante power plant consists of 2 units: 1) unit 1 has an installed capacity of 4.5 MWe, uses a single well (BO-2 well to a depth of 350 m) and a double flash unit, its nominal power capacity is 4.7 MW and the Bouillante 1 unit produces 30 GWh/year, and 2) unit 2 has an installed capacity of 11 MWe, uses three wells (including BO-4 well to depths of 1000-1150 m) and a single flash unit, its nominal power capacity is 11 MW and the Bouillante 2 unit produces 72 GWh/y (Jaud & Lamethe, 1985; Beutin & LaPlaige, 2006).

Specific reservoir parameters of the Bouillante geothermal field are reported by Traineau et al. (2015).

6. Resource identification

In order to identify potential resources for geothermal energy extraction, they have to be located and resources have to be classified on the basis of their corresponding geothermal system. In addition, a preliminary conceptual model of the expected system is proposed.

6.1 Ghana

As the available data only allows for a distinction between the different geological provinces, resource identification is limited to these provinces and thus based on a rather large scale. Lack of discrimination data within the provinces permits identification on a smaller scale.

6.1.1 Classification

Estimated temperatures in the subsurface of Ghana were calculated from 36 to 179 ^{o}C at depths ranging from 1 to 4 km. As the aim is to generate electricity, a minimum resource temperature of 90 ^{o}C, according to Figure 5, is required when using a binary plant. Temperatures of viable resources thus range from 90 to 179 ^{o}C in Ghana. Setting the boundary between low and high enthalpy resources roughly halfway, all geothermal resources with temperatures equal to or greater than 130 ^{o}C are classified as high enthalpy resources. Resources in the different geological provinces in Ghana can be classified as low- and/or high enthalpy resources, depending on the province and, more importantly, the scenario considered. All resources are assumed to be water dominated and can be based on either a static- or dynamic geothermal system, depending on the rate of natural recharge.

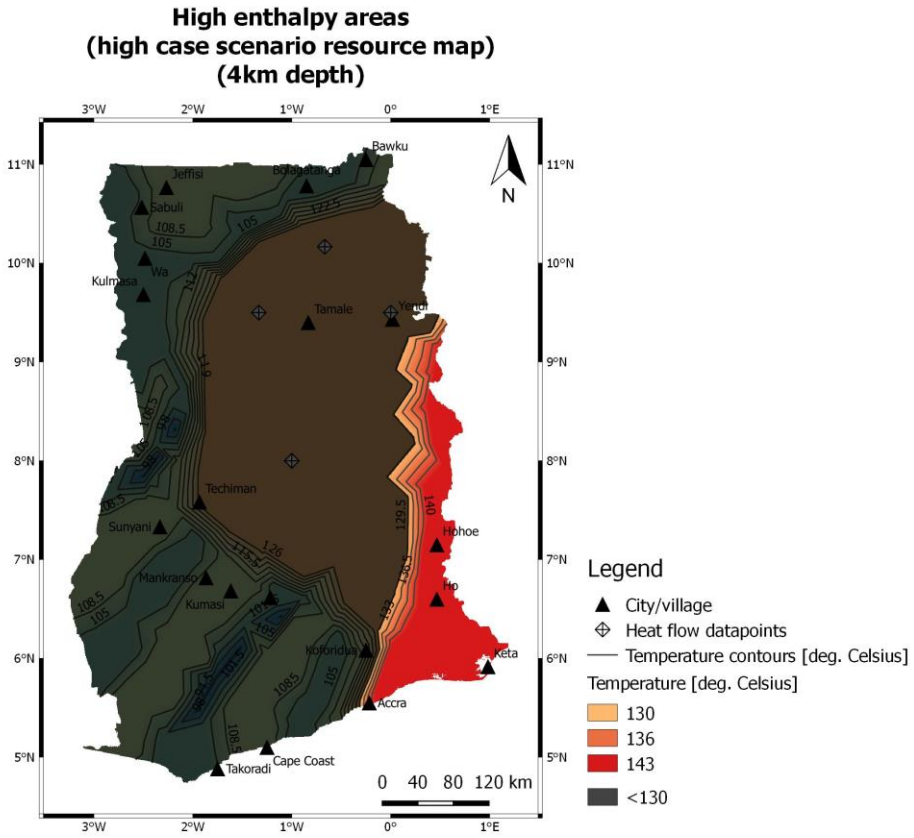

Figure 36: Location of high enthalpy areas for the high case scenario at a depth of 4km. Created with QGIS, 2016.

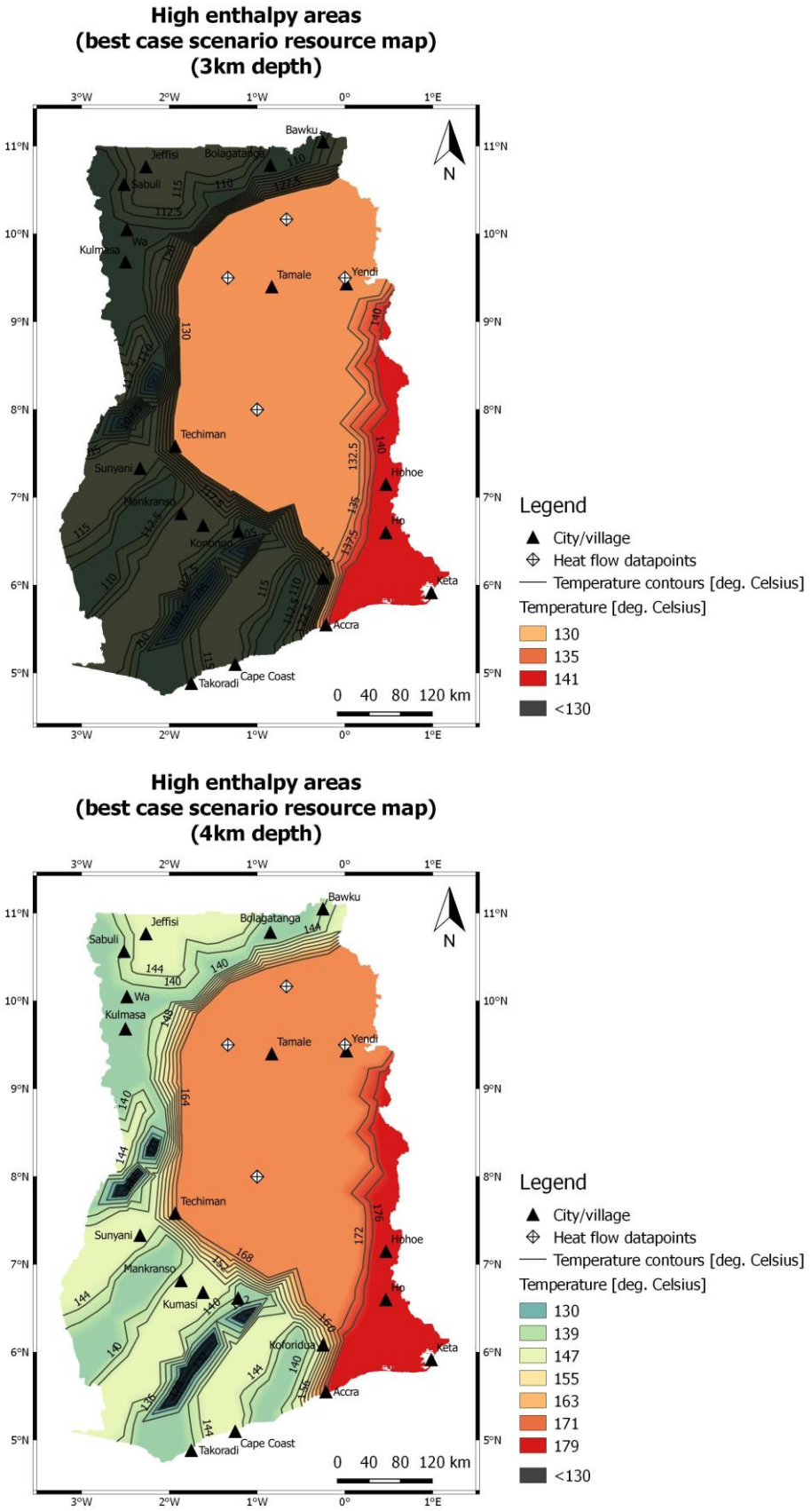

Figure 37: Location of high enthalpy areas for the best case scenario. At a depth of 3km (top) and at a depth of 4km (bottom). Created with QGIS, 2016.

6.1.2 Location

Location selection is restricted to areas where temperatures exceed 130 ^{o}C, as this screening study focusses on high enthalpy resources only. These areas include; 1) the Eastern Province when the high case scenario is considered at a depth of 4km, 2) the Central and Eastern Province when the best case scenario is considered at a depth of 3 km, and 3) all Provinces when the best case scenario is considered at a depth of 4 km, with the exception of the areas where the Tarkwaian Group outcrops. These areas are illustrated in Figure 37 and Figure 36.

When population density is taken into account, it becomes clear that potential resources should be located in the Eastern Province and in the southern half of the Western and Central province as population density is relatively high in these areas. Preferably, potential resources and their respective power plants should be located in the vicinity of the urban center locations and thus mainly along the southern coast.

6.1.3 Conceptual model

Depending on the natural occurrence of the remaining two components of any geothermal system, a reservoir with sufficient permeability and a naturally occurring working fluid, either a “conventional” geothermal system or an enhanced geothermal system can be considered. Both will be discussed in the conceptual model in the context of high enthalpy resources, which occur only at great depths in Ghana.

- Thermal waters can either infiltrate, be trapped in, or are injected into permeable layers at depth, depending on natural recharge.
- Temperatures of thermal waters are in excess of 130 ^{o}C as they have been trapped in high temperature zones or are heated as they infiltrate, or are injected into, high temperature zones.
- Independent of the presence of thermal waters, with sufficient permeability the resource forms a “conventional” geothermal system. When permeable formations in/near the high temperature zones are absent, permeability has to be created by hydraulic stimulation and the resource becomes an enhanced geothermal system.
- Thermal waters are transported to the surface where they can be used to generate electricity, assuming sufficient thermal water production capacity.
- After the thermal water has been cooled to a temperature of 90 ^{o}C it is re-injected into the (artificial) reservoir to prevent depletion.
- Waters are re-heated to reservoir temperature and the cycle starts over, creating a closed loop.

6.2 Saba

As the island of Saba is formed by a geologically active volcano, the entire surface area of the island can be identified as a potential resource. Traineau et al. (2015) state that “a combination of recent volcanic activity and tectonic activity is highly favourable for the emplacement of shallow magmatic intrusions which would represent a heat source for the development of the geothermal system”. Thus, the sector collapse zone and the NE-SW trending fault are ideal structural features in the subsurface that allow for thermal waters, heated by shallow magmatic intrusions, to rise to the shallow subsurface, greatly increasing the geothermal potential in these areas. The thermal features present on the island give a good indication as to where such processes might be taking place, as the development analogue on Guadeloupe and the example from Nevis illustrate that the thermal features can be associated with structural features in the subsurface.

6.2.1 Classification

As temperatures in the subsurface are expected to be in excess of 185 ^{o}C, geothermal resources on Saba can be classified as high enthalpy resources. Considering the development analogue on Guadeloupe, temperatures range from 230 to 250 ^{o}C, the phase of the working fluid is expected to be liquid dominated (water), but could also be vapour dominated (producing a water-steam mixture), and a dynamic geothermal system is assumed.

6.2.2 Location

There are six locations of heat escape from the island and off its shores (Figure 28). Combined with the main NE-SW trending fault system and the ‘horseshoe-shaped’ sector collapse structure, their location poses two areas of significant geothermal potential, as thermal waters are able to rise to the

(shallower sub-) surface through permeable faults and fractures associated with these structures, and thus greatly decreasing drilling depth. As the Guadeloupe analogue shows, potential resources are most likely located in the vicinity of these permeable fault systems. The topography of the island is steep and highly irregular and thus plays a major role in selecting a power plant location (Huttrer, 1998).

6.2.3 Conceptual model

Huttrer (1998) has proposed a preliminary geothermal model which has been adapted in this study. Some key principals have been slightly modified to fit new insights.

- Thermal waters originate as precipitation that falls onto the island and/or from thermally altered seawater intruding permeable layers beneath the island.
- Rainwater and/or seawater may be heated to an excess of 185 ^{o}C as it percolates through high-temperature zones at unknown depths beneath and/or near the island.
- “Beginning at various depths within/around the volcano, the heated waters then move down-gradient through permeable pyroclastic materials, open/permeable fracture systems and aquifers that overlie relatively impermeable deposits.
- “Some of the thermal waters flow down the hydraulic gradient within permeable volcanic aquifers and then upward along fractures”. These can be the waters sampled at the hot spring beneath the sulphur mine, the hot springs between Ladder Bay and Tent Point and the submarine hot springs.
- “Rising thermal waters saturate permeable zones of limited extent in pyroclastic deposits” and alter them so as to create the hydrothermally altered regions associated with the sector collapse structure found on the island and the area near the old sulphur mine (Figure 28).

7. Geothermal resource assessment

In order to assess and compare the geothermal potential of the potential high enthalpy resources of Ghana and Saba defined above, the available energy, or installed power, for a single geothermal power plant, over a period of 30 years, is quantified by estimating the amount of heat stored in such resources and the amount of heat that can be extracted from these resources.

7.1 Parameter estimation

The resource parameters that have to be estimated are: 1) density and heat capacity of the reservoir rock and the working fluid of the geothermal system, 2) reservoir porosity and volume, and 3) resource temperature and base temperature. Water is used as the working fluid in all estimations and its heat capacity is based on temperature of the water at reservoir conditions, i.e. resource temperature.

The recovery factor and conversion efficiency depend on the geothermal system and the resource temperature respectively. Mendrinos et al. (2008) state that for a “conventional” geothermal system the recovery factor is 25% and for an enhanced geothermal system the recovery factor is 40%.

7.1.1 Ghana

All three major geological provinces represent possible high enthalpy resources depending on scenario and depth; the high- and best case scenarios at depths of 3 and 4 km are considered for geothermal resources assessment. Two cases are considered for all provinces: 1) there is sufficient reservoir permeability, resulting in a “conventional” system and a recovery factor of 25%, and 2) there is insufficient reservoir permeability, resulting in an enhanced system and thus a recovery factor of 40%. The rock density is based on the main lithological unit in the province; for the Central Province the average density of sandstone is used and for the Eastern Province the average density of metamorphic rock is used. The density of water is based on reservoir conditions, i.e. temperature. Conservative values for porosity have been estimated; 5% porosity for the Western- and Eastern Province and 10% porosity for the Central Province, as there is no porosity and/or permeability (neither matrix- or fracture dominated) data available. A reservoir volume of 1 km^3 is assumed in all cases. Resource temperatures are derived from the high enthalpy resource maps presented in section 0 and the base temperature is set at the minimum operating temperature for electricity generation (Figure 5). All parameters and their sources are listed in Table 6 to Table 9.

Parameters Western Province	Assumed value	Source
Best case scenario		
φ, Porosity [%]	5	Estimated
ρ_r, Rock density [kg/m^3]	2750	http://www.comparerocks.com/en/sandstone-rock/model-8-0
ρ_w, Water density [kg/m^3]	922	http://www.engineeringtoolbox.com/water-thermal-properties-d_162.html
C_r, Rock heat capacity [kJ/kg^{o}C]	1.1	http://www.comparerocks.com/en/metamorphic-rocks/style-3?languageCode=en&parameter=Category&categoryId=3
C_w, Water heat capacity [kJ/kg^{o}C]	4.3	http://www.engineeringtoolbox.com/water-thermal-properties-d_162.html
V, Rock Volume [m^3]	$1 \cdot 10^9$	Estimated
T, Rock natural state temperature [^{o}C]	145	Figure 37
T_b, Base temperature [^{o}C]	90	Figure 5
R, Recovery factor	0.25/0.40	Mendrinos et al. (2008)
N, Conversion efficiency	0.11	Tester et al. (2006)
F, Load factor	0.95	Mendrinos et al. (2008)
T, Commercial life span of the plant [msec]	$9.48 \cdot 10^{11}$	Tester et al. (2006)

Table 6: Estimated parameters for high enthalpy resource assessment in the Western Province for the best case scenario. Sources are listed in table.

Parameters Central Province	Assumed value		Source
Best case scenario	**3km**	**4km**	
φ, Porosity [%]	10	10	Estimated
ρ_r, Rock density [kg/m^3]	2650	2650	http://www.comparerocks.com/en/sandstone-rock/model-8-0
ρ_w, Water density [kg/m^3]	935	902	http://www.engineeringtoolbox.com/water-thermal-properties-d_162.html
C_r, Rock heat capacity [kJ/kg^{o}C]	0.92	0.92	http://www.comparerocks.com/en/sandstone-rock/model-8-0
C_w, Water heat capacity [kJ/kg^{o}C]	4.27	4.36	http://www.engineeringtoolbox.com/water-thermal-properties-d_162.html
V, Rock Volume [m^3]	$1 \cdot 10^9$	$1 \cdot 10^9$	Estimated
T, Rock natural state temperature [^{o}C]	130	165	Figure 37
T_b, Base temperature [^{o}C]	90	90	Figure 5
R, Recovery factor	0.25/0.40	0.25/0.40	Mendrinos et al. (2008)
N, Conversion efficiency	0.1	0.12	Tester et al. (2006)
F, Load factor	0.95	0.95	Mendrinos et al. (2008)
T, Commercial life span of the plant [msec]	$9.48 \cdot 10^{11}$	$9.48 \cdot 10^{11}$	Tester et al. (2006)

Table 7: Estimated parameters for high enthalpy resource assessment in the Central Province for the best case scenario. Sources are listed in table.

Parameters Eastern Province	Assumed value	Source
High case scenario		
φ, Porosity [%]	5	Estimated
ρ_r, Rock density [kg/m^3]	2750	Smithson (1971)
ρ_w, Water density [kg/m^3]	926	http://www.engineeringtoolbox.com/water-thermal-properties-d_162.html
C_r, Rock heat capacity [kJ/kg^{o}C]	1.1	http://www.comparerocks.com/en/metamorphic-rocks/style-3?languageCode=en&parameter=Category&categoryId=3
C_w, Water heat capacity [kJ/kg^{o}C]	4.29	http://www.engineeringtoolbox.com/water-thermal-propertiesd_162.html
V, Rock Volume [m^3]	$1 \cdot 10^9$	Estimated
T, Rock natural state temperature [^{o}C]	140	Figure 36
T_b, Base temperature [^{o}C]	90	Figure 5
R, Recovery factor	0.25/0.40	Mendrinos et al. (2008)
N, Conversion efficiency	0.1	Tester et al. (2006)
F, Load factor	0.95	Mendrinos et al. (2008)
T, Commercial life span of the plant [msec]	$9.48 \cdot 10^{11}$	Tester et al. (2006)

Table 8: Estimated parameters for high enthalpy resource assessment in the Eastern Province for the high case scenario. Sources are listed in table.

Parameters Eastern Province	Assumed value		Source
Best case scenario	**3km**	**4km**	
φ, Porosity [%]	5	5	Estimated
ρ_r, Rock density [kg/m^3]	2750	2750	Smithson (1971)
ρ_w, Water density [kg/m^3]	926	893	http://www.engineeringtoolbox.com/water-thermal-properties-d_162.html
C_r, Rock heat capacity [kJ/kg^{o}C]	1.1	1.1	http://www.comparerocks.com/en/metamorphic-rocks/style-3?languageCode=en&parameter=Category&categoryId=3
C_w, Water heat capacity [kJ/kg^{o}C]	4.29	4.39	http://www.engineeringtoolbox.com/water-thermal-properties-d_162.html
V, Rock Volume [m^3]	$1 \cdot 10^9$	$1 \cdot 10^9$	Estimated
T, Rock natural state temperature [^{o}C]	140	178	Figure 37
T_b, Base temperature [^{o}C]	90	90	Figure 5
R, Recovery factor	0.25/0.40	0.25/0.40	Mendrinos et al. (2008)
N, Conversion efficiency	0.1	0.13	Tester et al. (2006)
F, Load factor	0.95	0.95	Mendrinos et al. (2008)
T, Commercial life span of the plant [msec]	$9.48 \cdot 10^{11}$	$9.48 \cdot 10^{11}$	Tester et al. (2006)

Table 9: Estimated parameters for high enthalpy resource assessment in the Eastern Province for the best case scenario. Sources are listed in table.

7.1.2 Saba

Traineau et al. (2015) report results of a long-term monitoring of the Bouillante geothermal reservoir and quantify several reservoir characteristics, such as porosity, water density and volume. These values have been adapted in the parameter estimation, as the Bouillante geothermal field acts as a development analogue for geothermal resources on Saba.
Rock density of the reservoir is estimated using the average density of andesite as most of Saba's geology is composed of andesitic domes. The potential resource on Saba is part of a "conventional" geothermal system and therefore the recovery factor is set at 25%. All parameters and their sources are listed in Table 10.

Parameters Saba	**Assumed value**	**Source**
φ, Porosity [%]	10	Traineau et al. (2015)
ρ_r, Rock density [kg/m^3]	2700	http://geology.about.com/cs/rock_types/a/aarockspecgrav.htm
ρ_w, Water density [kg/m^3]	820	Traineau et al. (2015)
C_r, Rock heat capacity [kJ/kg^{o}C]	2.39	http://www.comparerocks.com/en/andesite-rock/model-21-0
C_w, Water heat capacity [kJ/kg^{o}C]	4.87	http://www.engineeringtoolbox.com/water-thermal-properties-d_162.html
V, Rock Volume [m^3]	$0.7 \cdot 10^9$	Traineau et al. (2015)
T, Rock natural state temperature [^{o}C]	250	Traineau et al. (2015)
T_b, Base temperature [^{o}C]	160	Traineau et al. (2015)
R, Recovery factor	0.25	Mendrinos et al. (2008)
N, Conversion efficiency	0.16	Tester et al. (2006)
F, Load factor	0.95	Mendrinos et al. (2008)
T, Commercial life span of the plant [msec]	$9.48 \cdot 10^{11}$	Tester et al. (2006)

Table 10: Estimated parameters for high enthalpy resource assessment on Saba at an average temperature based on the Bouillante geothermal field analogue. Sources are listed in table.

7.2 Results

The resulting installed power capacity estimates are representative for specific and/or generalized resource conditions and are indicative of the geothermal potential of Ghana and Saba.

7.2.1 Ghana

The estimated installed power capacity of a resource in the Eastern Province, when the high case scenario is considered, is either 4.3 or 6.8 MW_e depending on the geothermal system (recovery factor). The best case scenario at 3 km depth yields power capacity estimates ranging from 2.9 to 6.8 MW_e, depending on the geological province and the geothermal system. At a depth of 4 km, the best case scenario yields power capacity estimates ranging from 5.2 to 15.6 MW_e, again depending on the geological province and the geothermal system. All power capacity estimates are presented in Table 11 for the different scenarios, depths and geological provinces considered. They are given for the different recovery factors that apply to the two geothermal systems considered.

Installed power capacity estimates [MW_e]	**High case scenario**	**Best case scenario**	
		3km	**4km**
Western Province	-	-	5.2 / 8.3
Central Province	-	2.9 / 4.6	6.5 / 10.4
Eastern Province	4.3 / 6.8	4.3 / 6.8	9.8 / 15.6

Table 11: Estimated installed power capacities for the different geological provinces according to scenario and depth. Power capacities are given for the 0.25 / 0.40 recovery factors respectively.

7.2.2 Saba

The estimated power plant capacity for Saba is 16.8 MW_e, based on a reservoir volume of 0.7 km^3. The depth of the resource is expected to be less than 1 km.

8. Discussion

8.1 Sensitivity analysis

This section will address the uncertainties related to estimates and computations made in this study, how these uncertainties have been dealt with and what their consequences are.

8.1.1 Ghana

Heat flow and thermal conductivity values are all reported as an average value and include large error margins. For example, Beck and Mustonen report "the correct value for heat flow being within 20% of 42 mW/m^2". Heat flow values for the Central and Eastern Province reported by Lucazeau et al. (1991) come with an error margin of 15% from the average value. The average value that applies to Ghana has been reported by multiple authors (Beck & Mustonen 1972; Brigaud & Lucazeau, 1985; Lucazeau et al., 1991) and therefore comes with an error margin of 7.5% of the average value. The same applies to thermal conductivity values, where the error margin is roughly 25% from the average value in all cases. These large error margins allow for a range of parameters that can be used to arrive at an estimate for the geothermal gradient. Propagation of these error margins results in geothermal gradient values with a 30% error margin. The resulting uncertainty has been taken into account by the different scenarios used for subsurface temperature distributions.

The quality of the geological maps showing the outcrop distributions of dominant formations in the different provinces results in a weak horizontal resolution of the resource maps. The vertical resolution of these maps is also weak, because the use of a geothermal gradient based on a single layer model suggests a constant gradient in the subsurface, thus disregarding stratigraphy and lithology. The possibility of finding a high temperature zone, a so called 'hot spot', is eliminated due to the weak horizontal and vertical resolution of the resource maps. By incorporating the Coastal Basins in the respective provinces in which they are located, the geothermal potential of these basins has been disregarded.

Probability distributions of the geothermal gradient in the different geological provinces are used to determine the sensitivity of the different case scenarios. The distributions are presented in appendix D. An example is given in Figure 38, which shows the probability distribution for the gradient of the Central province. The sensitivity of the scenarios displayed in this figure is comparable to the other geological provinces. The best case scenario shows little room for improvement, as there is a probability of 0.01% that the gradient will be higher than the value considered in this scenario. The low case scenario shows a probability of 99.99% that the gradient will be higher than the value considered and can therefore be regarded as the worst case scenario. Although the gradient and resulting subsurface temperatures at depth presented for the best case scenario appear to be very optimistic, they are in fact possible, when, for example, a 'hot spot' is located and considered.

There is roughly a 75% probability that the gradient is higher than the one considered in the base case scenario. This means that the gradient considered in the base case scenario is not overly optimistic and leaves significant room for improvement. Therefore the gradients and resulting subsurface temperatures related to the base case scenario should be considered as most representative of what applies to Ghana.

The high case scenario also appears to be a little optimistic, as there is only a 5-10% probability of the gradient being higher than the value considered in this scenario. The mode (value with the highest count) and the mean (average value of distribution) of the geothermal gradient are derived from the probability distributions and show a 60% and 30% probability respectively of the gradient being higher than the mode and mean value.

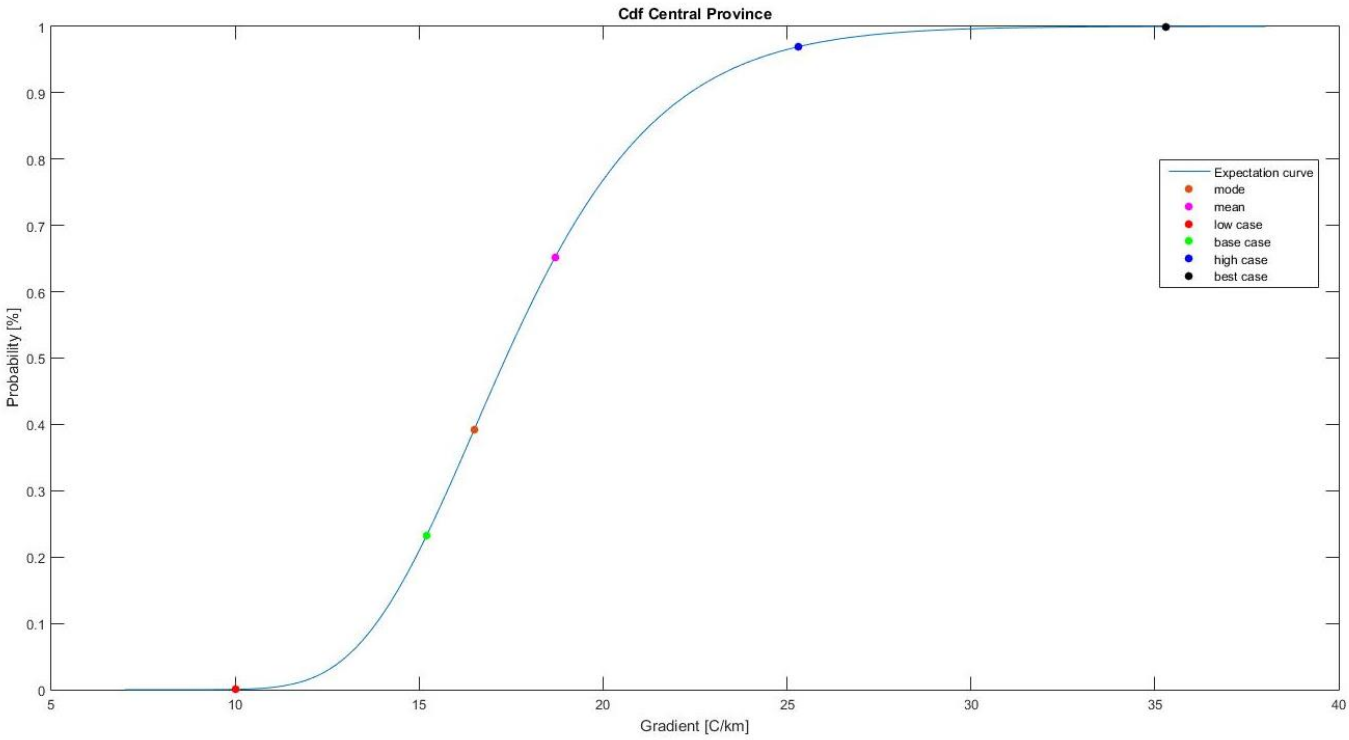

Figure 38: Cumulative probability density function for the geothermal gradient in the Central Province as representation of the sensitivity of the scenario's considered. Deterministic gradients according to the different scenarios are plotted. Created with Matlab R2015a.

The parameters used for the installed power capacity estimation represent a large generalization of resource characteristics and conditions, as general values have been used for the density and heat capacity of reservoir rock(s) and fluid(s). Although the reservoir volume seems a bit large, it is comparable to the reservoir size of the Middenmeer geothermal field in The Netherlands.

8.1.2 Saba

The parameters used in the geothermal resource assessment are mostly based on the Bouillante geothermal field analogue, with the exception of the reservoir rock properties. The use of these parameters significantly reduces uncertainty in estimating the installed power capacity on Saba. The geothermal resource assessment is therefore considered to be reliable, as it is supported by the total installed capacity of the Bouillante geothermal field, 15.5 MWe compared to an estimated 16.8 MWe on Saba.

8.2 Geothermal potential

The geothermal potential, in terms of electricity generation, displayed by Ghana may be lacking and is poorly constrained. Saba shows a geothermal potential, but issues remain related to (thermal) fluid migration.

8.2.1 Ghana

The heat source in Ghana is most likely latent heat encapsulated in the earth's crust, with a possible additional component of heat produced by radioactive elements. The working fluid of geothermal resources is assumed to be water. Reservoir conditions may vary significantly as the geology is very different throughout the geological provinces. Geothermal systems in Ghana can be classified as conventional and/or enhanced, and subsurface temperatures suggest both low- and high enthalpy resources.

The geothermal gradients considered in the base case scenario range from 12.8 to 18.3 ^{o}C/km, which are lower than the global average gradient of 20-30 ^{o}C/km, and yield subsurface temperatures ranging from 39 to 100 ^{o}C at depths up to 4 km. The high case scenario shows gradients that vary from 16.8 to 29 ^{o}C/km resulting in temperatures between 77 and 114 ^{o}C at a depth of 3 km and between 94 and 143 ^{o}C at a depth of 4 km. These gradients are lower than the average geothermal gradient in The Netherlands (31 ^{o}C/km),

but do show similarities to the average global gradient. The best case scenario is characterized by gradients varying between 24 and 38.1 ^{o}C/km which results in temperatures ranging from 99 to 141 ^{o}C at 3 km depth and from 123 to 179 ^{o}C at a depth of 4 km. The range of gradients reported for the best case scenario are comparable with the average gradient in The Netherlands, but only the high end of the range compares with the gradient that applies to the Middenmeer geothermal field (38 ^{o}C/km). The full range of geothermal gradients is presented in Table 5. As a direct consequence of the trend in heat flow, thermal gradients and related subsurface temperatures also display a similar trend, i.e. increasing towards the Eastern Province.

The base case scenario yields no high enthalpy resources as classified above. Resource assessment based on the highest estimated temperature (which is present at 4 km depth) shows installed power capacities of 0.7 and 1.1 MW_e for a conventional and enhanced geothermal system respectively, based on the reservoir characteristics estimated above.

The temperatures at 3 and 4 km depth related to the high- and best case scenarios do present possible zones of high enthalpy resources in the Central- and Eastern Provinces as these temperatures exceed 130 ^{o}C. Geothermal resource assessment of these areas shows a varying potential for geothermal energy exploitation as the installed power capacity for a period of 30 years ranges from 2.9 to 9.8 MW_e for a conventional geothermal system. When an enhanced geothermal system is considered, the installed power capacity ranges from 4.3 MWe to 15.6 MW_e. All estimated power capacities, depending on scenario, location and depth, are presented in Table 11. When both geothermal systems are considered, the high case scenario shows moderate- to weak geothermal potential (4.3 to 6.8 MW_e) and the best case scenario shows weak- to a geothermal potential (2.9 to 15.6 MW_e). The overall geothermal potential of Ghana is considered moderate to weak as power capacities related to the best case scenario are considered highly optimistic.

As the base case scenario is considered to best represent the geothermal gradient in Ghana, the occurrence of high enthalpy resources as classified above can be considered doubtful. The power capacities stated above could therefore be regarded as poorly constraining geothermal potential, as the base case yields significantly lower power outputs.

There are two significant challenges related to geothermal energy exploitation is Ghana, besides the great depths at which high enthalpy resources occur in the Central- and Eastern Province.
A significant challenge is formed by the reservoir permeability of a potential resource. At this point, any indication on reservoir permeability is absent and thus reservoir permeability is only speculated. In case the reservoir is a sandstone layer at a depth of 4 km in the Central Province, sufficient naturally occurring matrix dominated permeability could be present, as Kesse (1978) reports findings of bitumen in the Voltaian Basin and oil and gas are known to be produced from PreCambrian reservoir rocks in the northern part of West Africa and the Middle East. The presence of a dense fracture network facilitating permeability in such a reservoir can not be excluded at this point. Considering a reservoir of undefined strata at a depth of 3 km in the Eastern Province, naturally occurring matrix dominated permeability is most likely very low or even absent due to the highly metamorphosed nature of the rocks in this province. However, structural features related to Dahomeyide mobile belt terrane may provide reservoirs with sufficient naturally occurring fracture dominated permeability. The Buem Sandstone formation in this province could contain reservoirs with sufficient naturally occurring matrix- and/or fracture-dominated permeability, but at this point it is not clear whether these sandstones occur at the depths considered.

Secondly, as data on hydrogeological conditions is lacking, the presence (aquifers) of a naturally occurring working fluid (water) cannot be indicated. The same applies to the natural recharge of such aquifers. It is assumed that the presence of thermal waters is most likely in the Central Province, and assumed very limited in the Western and Eastern Provinces.

These challenges minimize the possibility of a conventional geothermal system and, at this point, limit its possible occurrence to the Central Province. It is therefore most likely to assume Enhanced Geothermal Systems facilitating high enthalpy resources in Ghana, greatly increasing costs (especially at these depths) but also increasing the installed power capacity.

8.2.1.1 Possible increase in Ghana's geothermal potential

The various intrusives of granitic or granodioritic composition form a large part of Ghanaian geology and are emplaced throughout all geological provinces. Their potential for containing high concentrations of heat producing elements can increase the heat flow locally as the radioactive component of heat flow increases, thus increasing the geothermal gradient in areas associated with these intrusives. As the heat production of such elements is the result of their radioactive decay, the amount of heat that is being produced is dependent on the age of these elements and therefore the time of emplacement of these intrusives.

Lesquer and Vasseur (1992) state that in general the heat production values of granitoids have a maximum between 1 and 2 $\mu W/m^3$ in Ghana. A comparable value of 1.05 +/- 0.9 $\mu W/m^3$ for 'monzogranites' has been reported by Harcouët et al. (2005). These relatively low values can be explained by the geologically old age of these intrusives. However, Lesquer and Vasseur (1992) also report higher values of 3 to 5 $\mu W/m^3$ of radioactive heat production for some small enriched late granitoids in the Eburnean province (the area affected by the Eburnean orogeny). According to a feasibility study for a geothermal energy project in the Hill of Banchory in Scotland (Milligan et al., 2016), "granites with heat production rates of 4 $\mu W/m^3$ or more are generally considered promising geothermal prospects".

More important is however the depth at which these intrusives occur. As radioactive heat is produced from elements in a layer at a certain depth, high heat producing intrusives can significantly lower the depth at which a geothermal resource occurs. For example; Kesse (1978) reports the occurrence of several igneous rock intrusions at depth in the Central Province. If these intrusives have a high radioactive heat production it can significantly increase the temperature at that depth and the thermal gradient in that area, therefore greatly increasing geothermal potential.

The geothermal potential of the Coastal Basins has been left out of consideration. Since these are comprised of the youngest rocks in Ghana, the youngest intrusives are found in these basins and are likely to have high(est) heat production values. In addition, their offshore extensions, where present, have proven to facilitate excellent reservoir conditions. The Coastal Basins can therefore play an important role in increasing the geothermal potential of Ghana.

8.2.2 Saba

The heat source on Saba is a magmatic intrusion which means heat is directly derived from the earth's mantle. On Saba a conventional, or hydrothermal, system is assumed and due to high temperatures the resources are clearly defined as high enthalpy resources. The working fluid of the geothermal resource is assumed to be water, but can also be a water-steam mixture.

Subsurface temperatures and their depths are derived from the Bouillante geothermal field on Guadeloupe and are related to zones of high temperature waters in the (shallow) subsurface. As temperatures are assumed to vary from 230 to 250 ^oC at depths of 600-2500 m, these zones are easily classified as high enthalpy resources. A conventional (hydro-) geothermal system is assumed with a dynamic, water-dominated reservoir and the possibility of steam produced from a reservoir is not excluded.

Saba's geothermal potential is clearly indicated by the presence of several thermal features such as 3 onshore- and 2 offshore hot spring locations and several areas of hydrothermal alteration indicating possible locations of these shallow high enthalpy resources. Geothermal resource assessment of such resources shows a potential for geothermal energy exploitation as the installed power capacity for a period of 30 years is estimated at 16.8 MW_e. This estimate is based on the occurrence of a resource with a temperature of 250 ^oC at a depth less than 1 km.

Such resources originate from waters that are heated at great(er) depths and flow upward through permeable layers and/or faults saturating formations at relatively low depths. The occurrence of shallow resources is thus mainly dependent on fracture/fault dominated permeability. As volcanic rocks and/or deposits are generally not associated with having high matrix dominated permeabilities (most likely permeability anisotropy), fault zones are most likely to act as the primary conduits for fluid flow in the subsurface and ensure the migration of fluids within the reservoir. The deep seated NE-SW orientated fault zone and (shallow) faults associated with the sector collapse structure on the southwest corner of the island

are ideal features to facilitate the migration of thermal fluids in the subsurface. The distribution of hot springs and zones of thermally altered rock can be clearly correlated to these structures, thus making it safe to assume shallow resources do occur on Saba, especially in the sector collapse area. Such an assumption also holds valid compared to the geological setting of the Bouillante geothermal field and the areas of interest for geothermal development indicated on the island of Nevis (LaFleur & Hoag, 2010).

A significant challenge, or significant risk (of failure), related to power capacity is thus formed by the permeability of the faults themselves. As becomes clear from the Bouillante analogue, not all faults and/or fractures are highly permeable, some are not permeable at all. Fractures and faults that have low permeability, or where permeability is absent, can greatly decrease the power capacity of the reservoir by decreasing the flow rate of the geothermal well. One the other hand, very permeable faults are able to greatly increase the power capacity of a single well.

8.3 Non-resource related challenges

Non-resource data shows that topography and population density can affect geothermal potential significantly by increasing the number of challenges that have to be dealt with.

8.3.1 Ghana

Population density plays an important role in site location for geothermal exploitation in Ghana. Figure 22 shows that the majority of people live in the southern half of Ghana and along the eastern border. Industry is mainly located in the south, in the vicinity of the urban centre locations. Therefore site location is restricted to the Eastern Province and the southern half of the Western and Central province.

Most preferably, a high enthalpy geothermal resource and its power plant are located near the urban centre locations along the south coast. Again, the Coastal Basins become interesting sites for geothermal exploration as they are located in the vicinity of these urban centres.

8.3.2 Saba

A major challenge to geothermal development on Saba is the steep and highly irregular topography of the island, resulting in limited land availability, and its remote location. In addition the area of interest defined on the northeast corner of the island is located in a national park and therefore most likely to be off limits for geothermal exploitation.

9. Conclusion

The aim of this study is to identify high enthalpy geothermal resources on the basis of geological setting and subsurface temperature, and to assess the geothermal potential of both Ghana and Saba by classifying the potential geothermal systems and estimating the (minimum) installed power capacity of potential high enthalpy resources.

Ghana has experienced its last major tectonic activity (i.e. period of crustal reactivation) about 600 Ma and has been tectonically stable since. Heat flow is low on the Archean age craton and increases towards its surrounding mobile belts. A tectonic component of heat flow appears absent, but many geological formations in Ghana are largely intruded by rocks of granitic and granodioritic composition, with varying reported radioactive heat production capabilities.
Saba, on the other hand, is part of a volcanic island arc related to a subduction zone and the island is formed by a geologically active stratovolcano. There is a clear tectonic component of heat flow present on the island. Ghana and Saba show different settings geologically and geothermally.

Results of this study show a wide range of estimated temperatures in the subsurface of Ghana; from 36 to 179 ^{o}C at varying depths. Subsurface temperatures related to Saba appear to be at a minimum of approximately 200 ^{o}C, with a most likely temperature of 250 ^{o}C, and are situated at shallow depths.

Geothermal systems in Ghana are classified as either conventional and/or enhanced geothermal systems, and subsurface temperatures suggest both low- and high enthalpy resources. On Saba a conventional, or hydrothermal, system is classified for what are clearly high enthalpy resources.

The estimated power capacity of Saba (16.8 MW_e) exceeds the range of power capacities estimated for Ghana (2.9 MW_e to 15.6 MW_e depending on scenario, location and depth). The estimated geothermal potential in Saba holds valid, as the concept is proven by the Bouillante geothermal field on Guadeloupe.
The estimated geothermal potential of Ghana is based on the two most optimistic scenario's, indicated by the small probability of the gradient being higher than the value considered. The least optimistic of these two scenario's yields significantly lower power capacity estimates of 4.3 to 6.8 MW_e, when compared to Saba.

In terms of technical feasibility, Saba shows a potential for geothermal energy exploitation compared to an overall moderate- to weak geothermal potential displayed by Ghana.

10. Recommendations

As Saba shows a clear potential for geothermal energy exploitation but incorporates a significant risk of failure, and Ghana only shows moderate- to weak geothermal potential, recommendations are given to decrease the uncertainties and risks related to initial estimations and geothermal resource assessments described above. In addition, promising areas for future exploration are recommended.

10.1 Decreasing uncertainties

A first step in decreasing uncertainties is to compare the estimates presented in this report with existing or gathered exploration data from wells or geophysical surveys, in order to confirm or correct the initial estimates.

10.1.1 Ghana

Temperature data from exploration wells is available from the database of the GNPC. Although most of their exploration is focussed offshore, multiple exploration wells have been drilled onshore and data is available from the GNPC. This temperature data poses an excellent means to confirm or correct initial gradient estimates made and eliminate uncertainties. In addition, such data allows for vertical extrapolation based on a multiple layer model, increasing the accuracy of subsurface temperatures at depth. Offshore well data can provide discrimination data for the Coastal Basins by giving a much more robust thermal gradient for these basins.

Regarding the various intrusives present in the subsurface of Ghana, data corresponding to the concentrations of radioactive elements in these intrusives and their radioactive heat production can be used to confirm or correct their ability for increasing geothermal potential. When radioactive heat production is known, uncertainty related to subsurface temperature distribution can be further reduced by incorporating these values in temperature estimations. The database of the GSD is the most likely place to obtain such data.
As high radioactive heat production can increase the geothermal gradient significantly, the potential of the intrusives should also become clear from (more common) temperature gradient data, but the location of measurement may be required to be in the vicinity of such intrusives.

10.1.2 Saba

The presence of several thermal features indicates there is a clear geothermal potential on Saba. Risks involved in the geothermal potential and technical feasibility mainly depend on depth and permeability of the reservoir, so therefore two things are recommended in order to significantly reduce risks: 1) an electromagnetic survey (CSAMT) in order to locate thermal waters stored in the subsurface, and 2) geological studies (or 'slim hole' drillings) focussed on the permeability of faults and fractures related to the sector collapse zone and faults related to the possible deep seated NE-SW trending fault.

10.2 Low enthalpy resources in Ghana

In the case of Ghana, it might be worthwhile to investigate the possibilities of electricity generation from low enthalpy resources. As the minimum temperature required for electricity generation is 90 ^{o}C, small installed power capacities can still be achieved using temperatures lower than 130 ^{o}C. When thermal efficiencies can be increased by optimizing the energy conversion process, hot water production capacities are increased by hydraulic stimulation (which also increases the recoverable heat) or the reservoir volume is increased, lower resource temperatures do not necessarily result in lower installed power capacities and may even be higher.
An important first step in investigating low enthalpy resources is optimizing power plant processes. The base temperature can be lowered to increase the amount of heat that can be extracted from thermal fluids, but the temperature to which these fluids are lowered is dependent on the type of power plant used. For example, the base temperature of thermal fluids can be lowered to atmospheric temperatures, significantly increasing the extractable heat, but this can have a strong negative influence on power plant processes.

10.3 Areas of interest for future exploration

There are certain areas or regions in both countries that hold significant potential for geothermal energy exploitation or show promising features that could increase the initially estimated geothermal potential.

10.3.1 Ghana

The Coastal Basins along the southern coast of Ghana are important areas for future exploration as they are promising for increasing geothermal potential. Acquisition of data that can distinct them from the respective geological provinces in which they are located is an important step in assessing their geothermal potential. It is recommended to focus on the Tano and Keta Basins, but especially the Keta Basin as it has been intruded at depth and is closest the country capital (main urban centre location). Based on the temperature estimates made in this report, future exploration is recommended on the Dahomeyide mobile belt terrane of the Eastern Province, if/when these estimates hold valid.

Looking at the Bouguer gravity anomaly map (Figure 39), a 'gravity high' can be identified in the central part of the country, between 7 and 8 degrees latitude and -1 and 0 degrees longitude (P.G. Ditmar, personal communication, January 6, 2017). This positive anomaly indicates an area of higher density than the surroundings. This could for example be an igneous intrusion at depth, surrounded by sediments of lower density (P.G. Ditmar, personal communication, January 6, 2017) as Kesse (1978) reports the occurrence of such intrusives in the Voltaian Basin. It can also simply be a basement high. Figure 39 shows the Premuase 1 well located at this 'gravity high'. Data from this well could provide important information on the origin of the gravity anomaly and a temperature log, if present, could show a high(er) thermal gradient in the case of an intrusion at depth. A similar 'gravity high' can be seen at the location of the Keta Basin, but it is not clear if this positive anomaly is due to the metamorphic nature of the rocks present in that area, or due to the intrusion present at depth in the basin.

Furthermore, the Premuase 1 well is also located on a magnetic anomaly (Figure 18, Top-left). Conclusions derived from this well data can be used for the interpretation of the other magnetic anomalies illustrated in Figure 18.

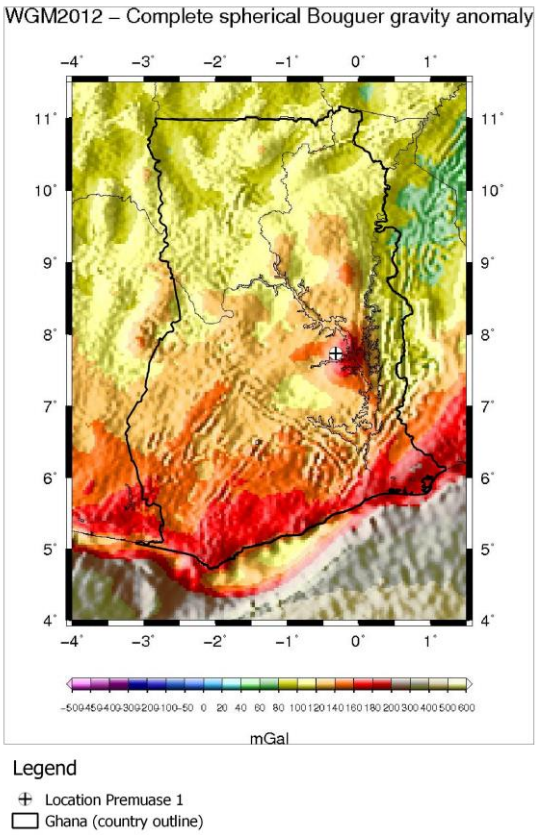

Figure 39: Bouguer gravity anomaly map showing location of Premuase 1 well. The well is located on a positive (high) anomaly. Created with QGis, 2016.

10.3.2 Saba

As stated above, the area of the 'horseshoe-shaped' sector collapse structure on the southwest part of Saba appears to be an excellent structural feature facilitating geothermal resources and it is recommended that all future exploration should focus on this area.

List of References

1. "Accra: Annual Weather Averages." *Weather Averages for Accra, Ghana*. N.p., n.d. Web. 14 Nov. 2016. Retrieved from http://www.holiday-weather.com/accra/averages

2. Affaton, P., Rahaman, M. A., Trompette, R., & Sougy, J. (1991). The Dahomeyide Orogen: Tectonothermal Evolution and Relationships with the Volta Basin. *The West African Orogens and Circum-Atlantic Correlatives,* 107-122. doi:10.1007/978-3-642-84153-8_6

3. Atta, S. (n.d.). The Mining Sector Support Programme: Airborne Geophysics over Voltaian, Keta Basin and other selected areas [PDF]. Ghana Geological Survey: Geophysics Division.

4. Beck, A.E., & Mustonen, E. (1972). Preliminary Heat Flow Data from Ghana. *Nature Physical Science, 235*(61), 172-174. doi: 10.1038/physci235172a0

5. Beutin, P., & LaPlaige, P. (2006, March 15-17). *Geothermal Development in the Caribbean - Bouillante Plant Presentation*. Reading presented at Eastern Caribbean Geothermal Energy Project in Dominica, Roseau. Retrieved November 22, 2016, from http://www.oas.org/dsd/reia/Documents/geocaraibes/bouillante_presentation.pdf

6. "The International Gravimetric Bureau". In: IAG Geodesist's Handbook, 2012 - Journal of Geodesy, V 86, N 10, Oct. 2012, Springer

7. Bonvalot, S., Balmino, G., Briais, A., Kuhn, M., Peyrefitte, A., Vales, N., Biancale, R., Gabalda, G., Moreaux, G., Reinquin, F., Sarrailh, M. World Gravity Map, 1:50000000 map, Eds. : BGI-CGMW-CNES-IRD, Paris, **2012**. © CGMW-BGI-CNES-IRD

8. Bourdon, E., Bouchot, V., Gadalia, A., & Sanjuan, B. (2011, March 25). *Geology and geothermal activity of the Bouillante Volcanic Chain* [Field excursion guide]. Guadeloupe, Bouillante.

9. Bouysse, P. (1984). The Lesser Antilles Island Arc: Structure and Geodynamic Evolution. *Initial Reports of the Deep Sea Drilling Project, 78A,* 83-103. doi:10.2973/dsdp.proc.78a.107.1984

10. Bouysse, P., & Westercamp, D. (1990). Subduction of Atlantic aseismic ridges and Late Cenozoic evolution of the Lesser Antilles island arc. *Tectonophysics,175*(4), 349-380. doi:10.1016/0040-1951(90)90180-g

11. Brigaud, F., Lucazeau, F., Ly, S., & Sauvage, J. F. (1985, September). Heat flow from the West African Shield. *Geophys. Res. Lett. Geophysical Research Letters, 12*(9), 549-552. doi:10.1029/gl012i009p00549

12. *Chapter 26. Terrestrial Heat Flow*. (n.d.). Retrieved October 11, 2016, from http://authors.library.caltech.edu/25038/271/Chapter%2026.%20Terrestrial%20heat%20flow.pdf

13. Church, R. E., & Allison, K. R. (n.d.). The Petroleum Potential of the Saba Bank Area, Netherlands Antilles.

14. Defant, M., Sherman, S., Maury, R., Bellon, H., Boer, J. D., Davidson, J., & Kepezhinskas, P. (2001). The geology, petrology, and petrogenesis of Saba Island, Lesser Antilles. *Journal of Volcanology and Geothermal Research,107*(1-3), 87-111. doi:10.1016/s0377-0273(00)00268-7

15. Dhansay, T., Wit, M. D., & Patt, A. (2014). An evaluation for harnessing low-enthalpy geothermal energy in the Limpopo Province, South Africa. *South African Journal of Science,110*(3/4), 1-10. doi:10.1590/sajs.2014/20130282
16. Dickson, M. H., & Fanelli, M. (2003). *Geothermal energy: utilization and technology*. Paris, FR: United Nations Educational, Scientific and Cultural Organization (UNESCO).

17. Electricity Generation | National Energy Authority of Iceland. (n.d.). Retrieved February 09, 2017, from http://www.nea.is/geothermal/electricity-generation/

18. Gehringer, M., & Loksha, V. (2012). *ESMAP Geothermal Handbook: Planning and Financing Power Generation* (Rep.). Washington DC: The World Bank.

19. geothermal energy. (n.d.). *The American Heritage©New Dictionary of Cultural Literacy, Third Edition.* Retrieved January 9, 2017 from Dictionary.com website http://www.dictionary.com/browse/geothermal-energy

20. Gharaibeh, A. J. (2008). Heat source study and geothermal reservoir assessment for the Zarqa Ma'in - Dab'a area, Central Jordan (Publication No. 17). Reykjavik: Geothermal Training Programme.

21. Harcouët, V., Guillou-Frottier, L., Bonneville, A., & Feybesse, J. L. (2005). Pre-mineralization thermal evolution of the Palaeoproterozoic gold-rich Ashanti belt, Ghana. *Geological Society, London, Special Publications, 248*(1), 103-118. <hal-00522360> doi:10.1144/gsl.sp.2005.248.01.05

22. Harvey, C., & GeothermEx, Inc. (2013). *Geothermal Exploration Best Practices: a guide to resource data collection, analysis, and presentation for geothermal projects* (Publication). Bochum, Germany: IGA Service GmbH.

23. Huttrer, G. W. (1998). *Final Report Regarding Prefeasibility Studies of the Potential for Geothermal Development, on Saba, N.A.* (Rep. No. K97-178019). Frisco, CO: Geothermal Management Company, Inc. Report produced for Lochheed Martin Idaho Technologies Company

24. Hymans, J. E. (n.d.). Geothermal Energy in Central America. Retrieved February 09, 2017, from http://revista.drclas.harvard.edu/book/geothermal-energy-central-america

25. Jaud, P., & Lamethe, D. (1985). The bouillante geothermal power-plant, guadeloupe. *Geothermics,14*(2-3), 197-205. doi:10.1016/0375-6505(85)90061-6

26. Kesse, G. O. (1978). *The search for petroleum (oil) in Ghana* (Rep. No. 78/1). Accra: Ghana Geological Survey.

27. LaFleur, J., & Hoag, R. (2010). *Geothermal Exploration on Nevis: A Caribbean Success Story* (Vol. 34, Publication). GRC Transactions.

28. Lesquer, A., & Vasseur, G. (1992, March 20). Heat-flow constraints on the West African lithosphere structure. *Geophys. Res. Lett. Geophysical Research Letters, 19*(6), 561-564. doi:10.1029/92gl00263

29. Lucazeau, F., Lesquer, A., & Vasseur, G. (1991). Trends of Heat Flow Density from West Africa. *Exploration of the Deep Continental Crust Terrestrial Heat Flow and the Lithosphere Structure,* 417-425. doi:10.1007/978-3-642-75582-8_20

30. Matek, B. (2016, March). *2016 Annual U.S. & Global Geothermal Power Production Report* (Rep.). Retrieved January 20, 2017, from Geothermal Energy Association website: http://geo-energy.org/reports/2016/2016%20Annual%20US%20Global%20Geothermal%20Power%20Production.pdf

31. Mendrinos, D., Karytsas, C., & Georgilakis, P. S. (2008). Assessment of geothermal resources for power generation. *Journal of optoelectronics and advanced materials,10*(5), 1262-1267.
32. Mensah, V. (2015). *Geological and structural interpretation of South-East Voltaian Basin, Ghana, using airborne gravity and magnetic datasets*. (Master's thesis, Kwame Nkrumah University of Science and Technology, Ghana). Retrieved from http://hdl.handle.net/123456789/8794

33. Milligan, G., Wood, G., Younger, P., Feliks, M., McCay, A., Gilliespie, M., Steen, P., McBeth, N., Townsend, D., Townsend, P., Stephenson, R. (2016). *Hill of Banchory Geothermal Energy Project Feasibility Study* (Rep.). LCITP. Report prepared for the Scottish Government by the Hill of Banchory Geothermal Energy Consortium

34. QGIS. (n.d.). Retrieved September 5, 2016, from http://www.qgis.org/ version 2.16

35. resource. (n.d.). *Dictionary.com Unabridged.* Retrieved January 10, 2017 from Dictionary.com website http://www.dictionary.com/browse/resource

36. Richter, A. (n.d.). Newest list of the top 10 countries in geothermal power. Retrieved February 09, 2017, from http://www.thinkgeoenergy.com/newest-list-of-the-top-10-countries-in-geothermal-power/

37. Roobol, M. J., & Smith, A. L. (2004). *Volcanology of Saba and St. Eustatius, Northern Lesser Antilles*. Amsterdam: Koninklijke Nederlandse akademie van Wetenschappen.

38. Schlüter, T. (2006). *Geological Atlas of Africa* (pp. 110-113). New York: Springer.

39. Sedimentary Basins. (n.d.). Retrieved January 17, 2017, from http://www.petrocom.gov.gh/sedimentary-basins.html

40. Smithson, S. B. (1971). Densities Of Metamorphic Rocks [Abstract]. *Geophysics,36*(4), 690-694. doi:10.1190/1.1440205

41. Tairou, M. S., Affaton, P., Anum, S., & Fleury, T. J. (2012, May 25). Pan-African Paleostresses and Reactivation of the Eburnean Basement Complex in Southeast Ghana (West Africa). *Journal of Geological Research, 2012*, 1-15. doi:10.1155/2012/938927

42. Tester, J.W., Anderson B.J., Batchelor A.S., Blackwell, D.D., Dipippo R., Drake E.M. (eds.) (2006). *The future of geothermal energy impact of Enhanced Geothermal Systems on the united States in the 21st century.* Prepared by the Massachusetts Institute of technology, under Idaho National Laboratory subcontract No. 6300019 for the U.S. Department of energy, Assistant Secretary for Energy Efficiency and Renewable energy, Office of geothermal Technologies. 358 p. (ISBN-10: 0486477711, ISBN-13: 978-0486477718).

43. The Resource | National Energy Authority of Iceland. (n.d.). Retrieved February 10, 2017, from http://www.nea.is/geothermal/the-resource/

44. Traineau, H., Lasne, E., & Sanjuan, B. (2015, April 19-25). Main Results of a Long-Term Monitoring of the Bouillante Geothermal Reservoir During Its Exploitation. In *World Geothermal Congress 2015*. Retrieved November 25, 2016, from https://pangea.stanford.edu/ERE/db/WGC/papers/WGC/2015/24024.pdf

45. Wright, J.B., Hastings, D.A., Jones, W.B., & Williams, H.R. (1985). *Geology and mineral resources of West Africa*. London: George Allen & Unwin, Ltd.

46. Yendaw, J.A. (2005). *Geology of Ghana* [Lecture Notes]. Retrieved from https://www.academia.edu/10359116/Geology_of_Ghana

Appendix A

Temperatures at depth [°C]	Low case	Base case	High case	Best case
Metavolcanics (Western Province)				
1 km	37	40	46	54
2 km	47	54	65	81
3 km	57	67	84	109
4 km	67	81	103	136
Metasediments (Western Province)				
1 km	36	40	48	57
2 km	46	54	69	87
3 km	56	68	90	117
4 km	66	82	111	147
Tarkwaian				
1 km	36	39	43	51
2 km	46	52	60	75
3 km	56	65	77	99
4 km	66	78	94	123
Voltaian Basin (Central Province)				
1 km	37	42	52	62
2 km	47	57	77	97
3 km	57	72	102	132
4 km	67	87	128	168
Dahomeyide orogenic belt (Eastern Province)				
1 km	39	45	56	65
2 km	51	63	85	103
3 km	63	81	114	141
4 km	75	100	143	179

Table 12: Subsurface temperature at depth estimations resulting from the calculated geothermal gradient presented according to geological province and scenario.

Appendix B

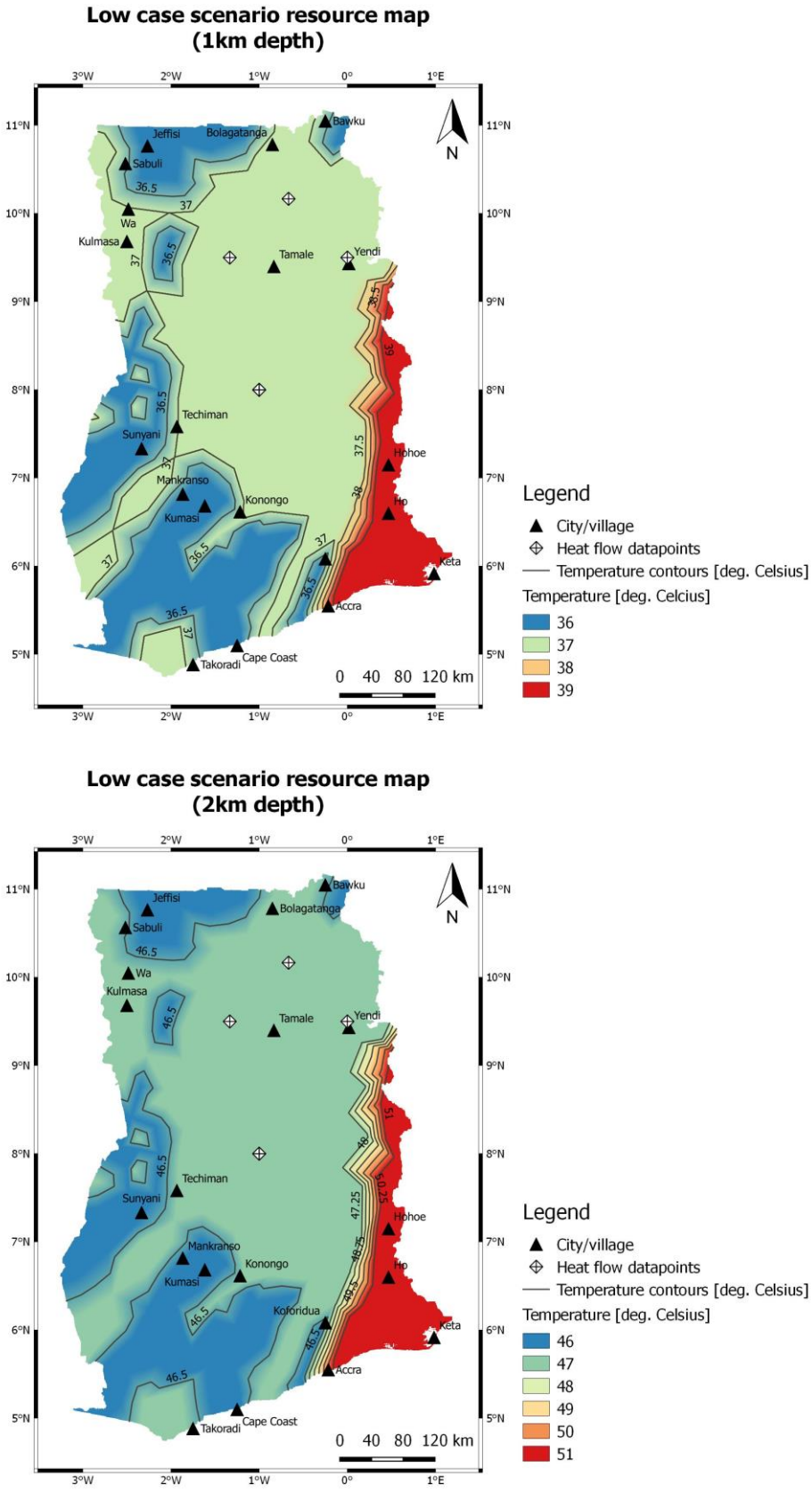

Figure 40: Subsurface temperature distribution for the low case scenario at a depth of 1km (top) and 2km (bottom). Created with QGis, 2016.

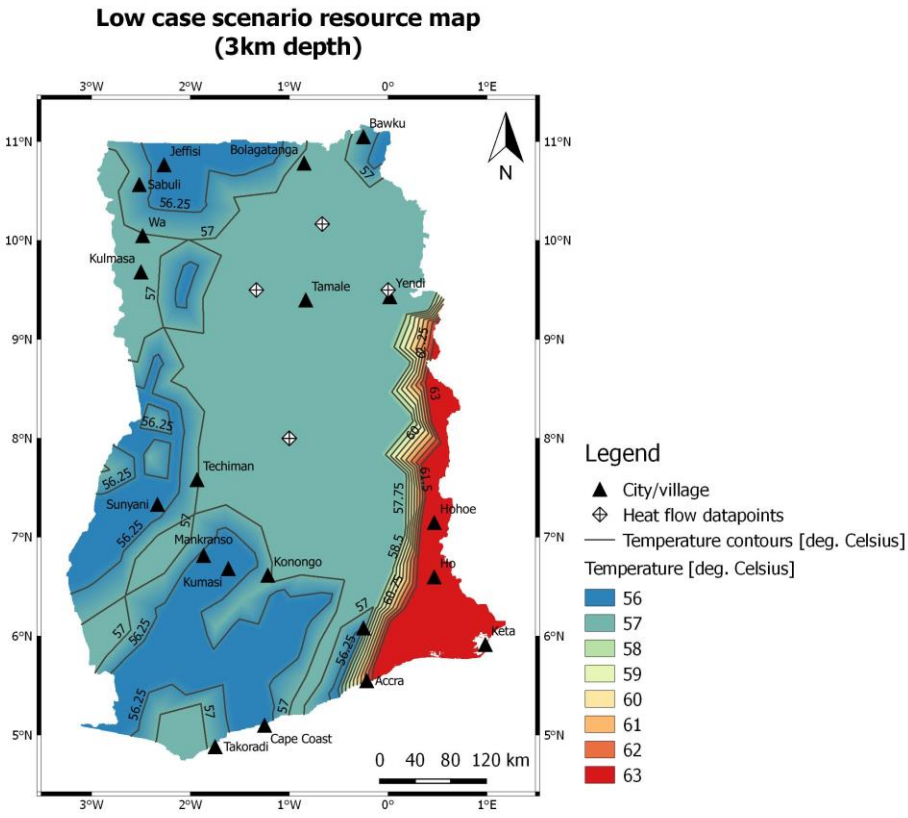

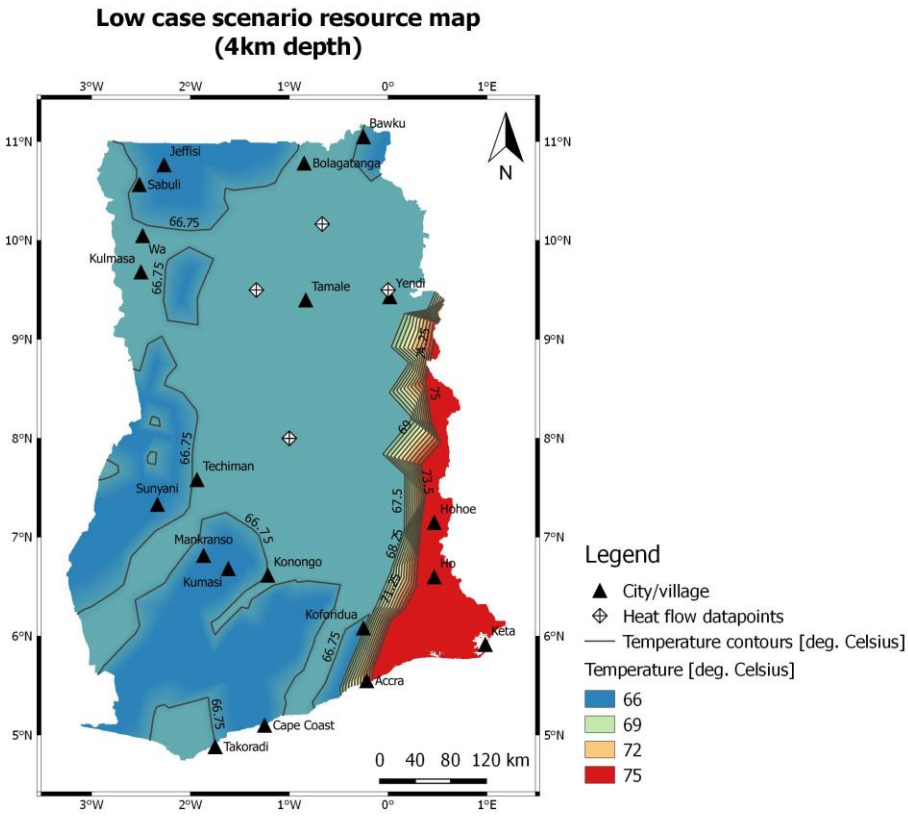

Figure 41: Subsurface temperature distribution for the low case scenario at a depth of 3km (top) and 4km (bottom). Created with QGis, 2016.

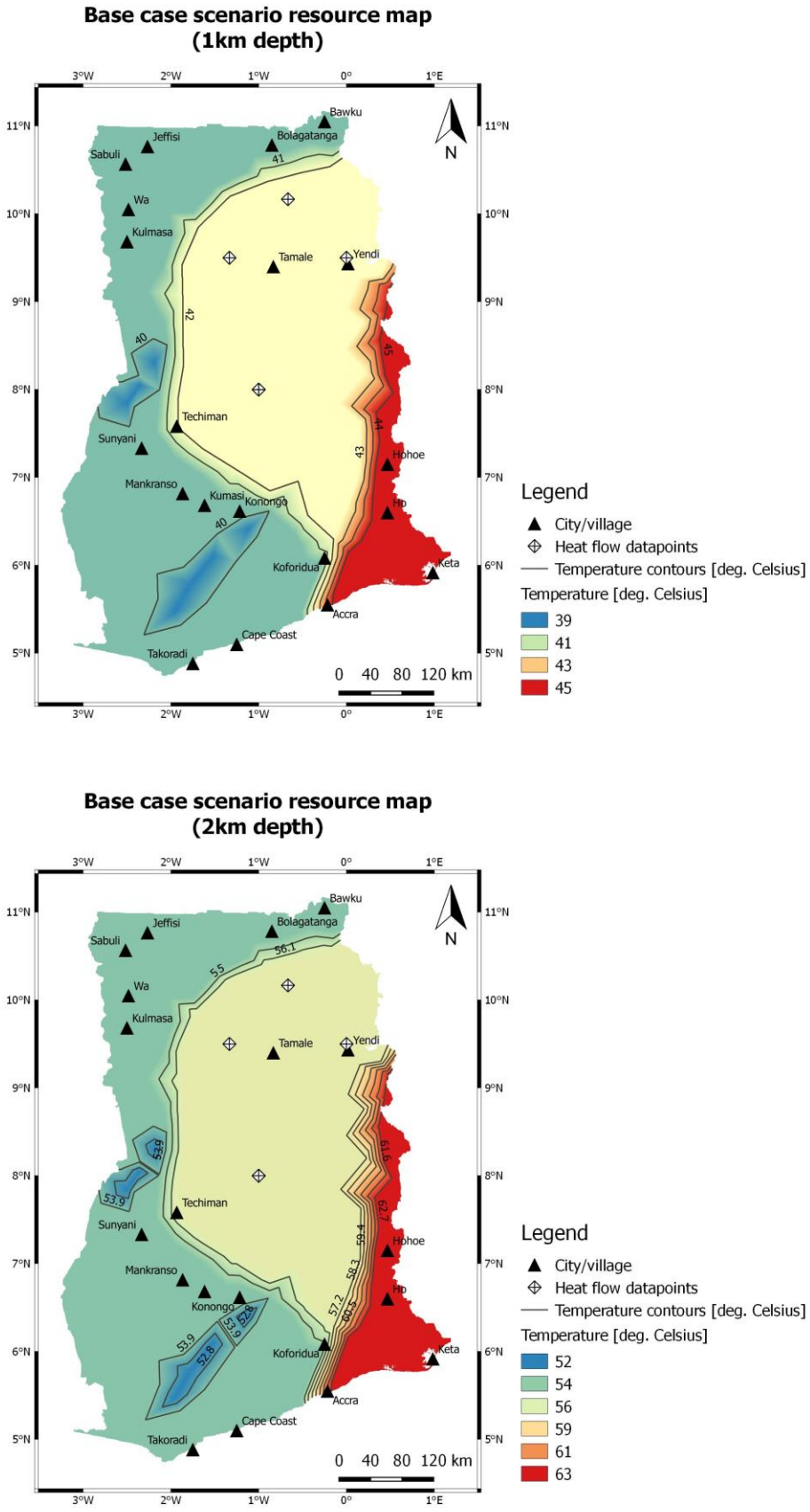

Figure 42: Subsurface temperature distribution for the base case scenario at a depth of 1km (top) and 2km (bottom). Created with QGis, 2016.

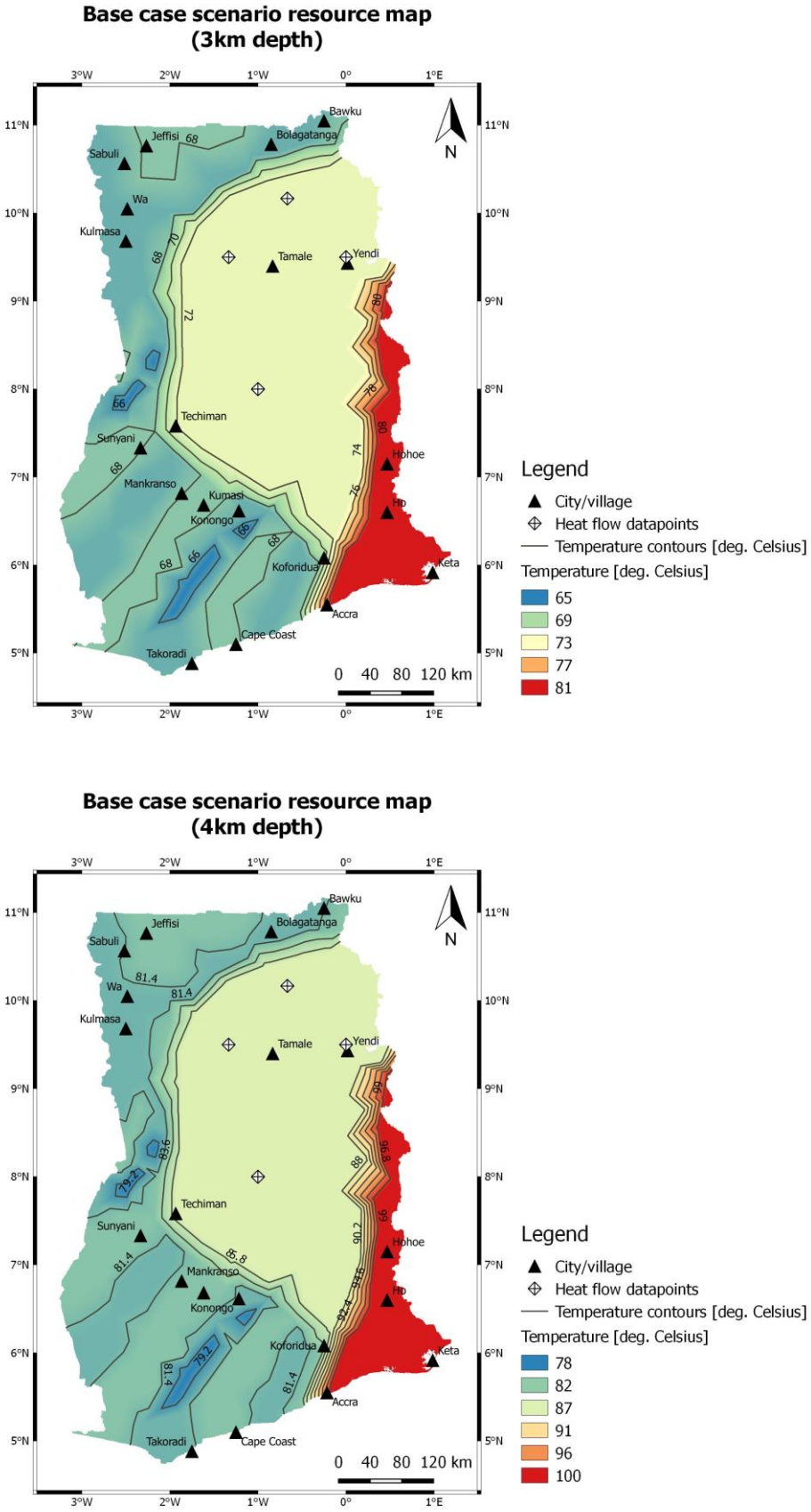

Figure 43: Subsurface temperature distribution for the base case scenario at a depth of 3km (top) and 4km (bottom). Created with QGis, 2016.

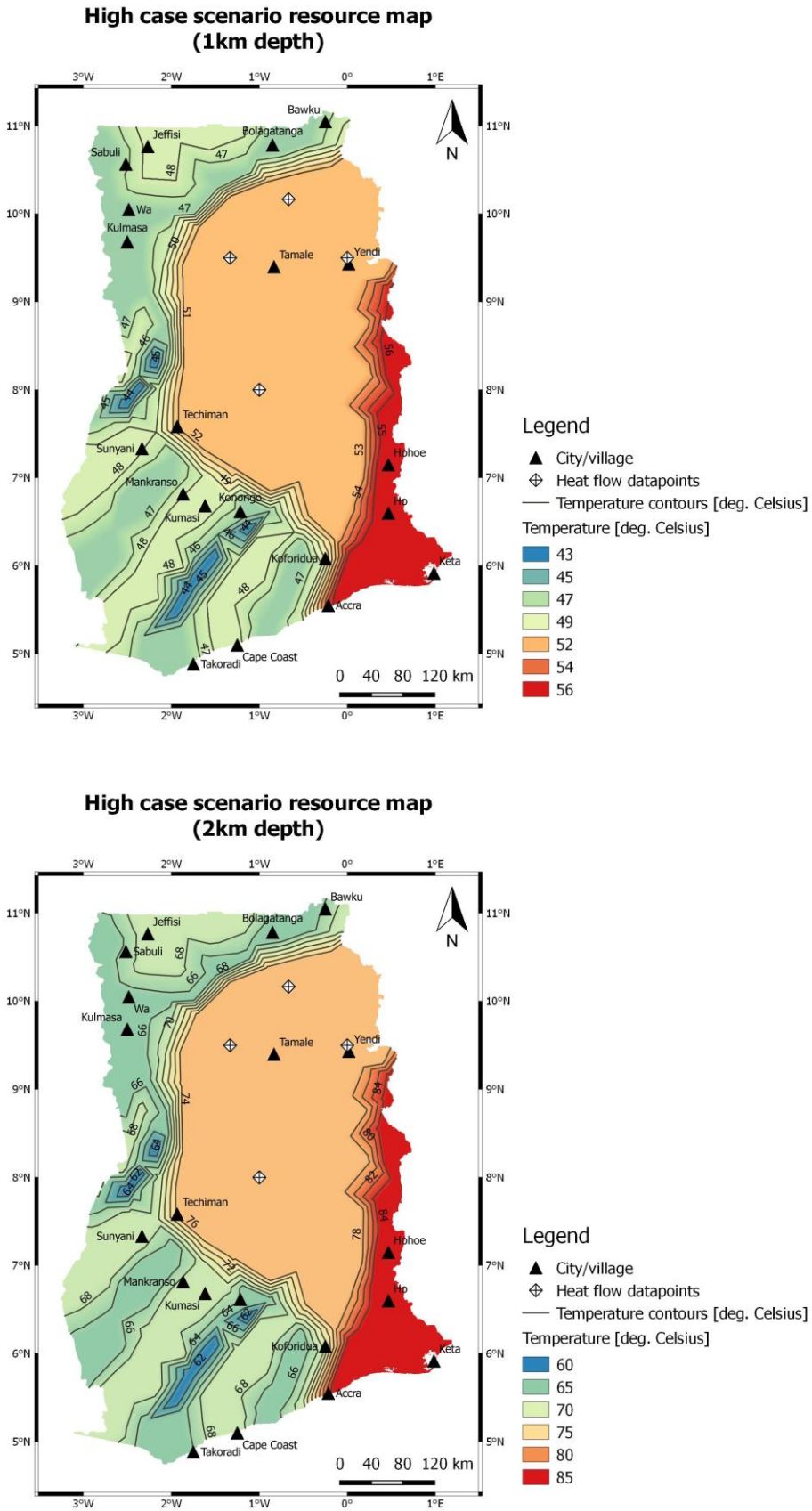

Figure 44: Subsurface temperature distribution for the high case scenario at a depth of 1km (top) and 2km (bottom). Created with QGis, 2016.

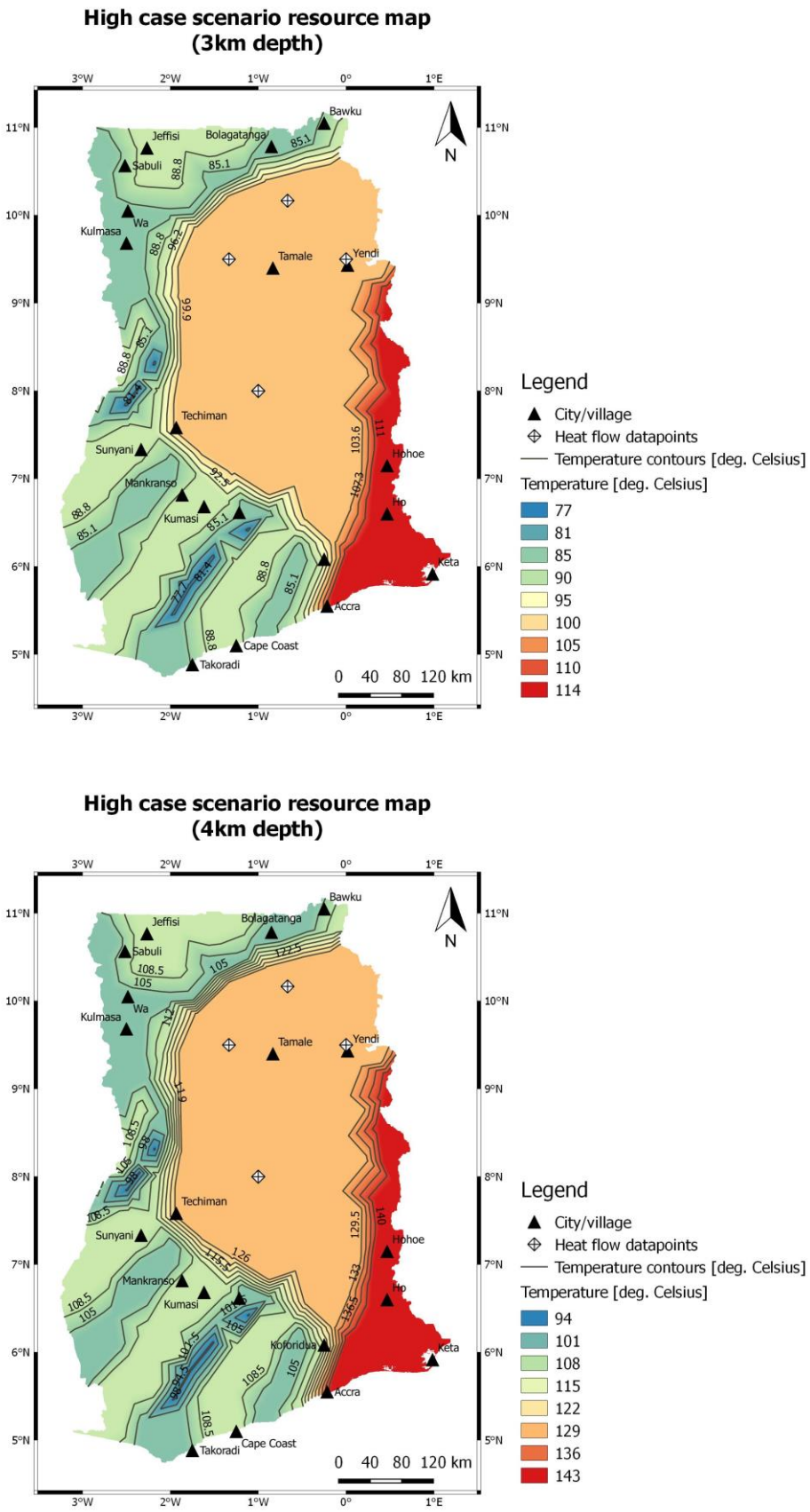

Figure 45: Subsurface temperature distribution for the high case scenario at a depth of 3km (top) and 4km (bottom). Created with QGis, 2016.

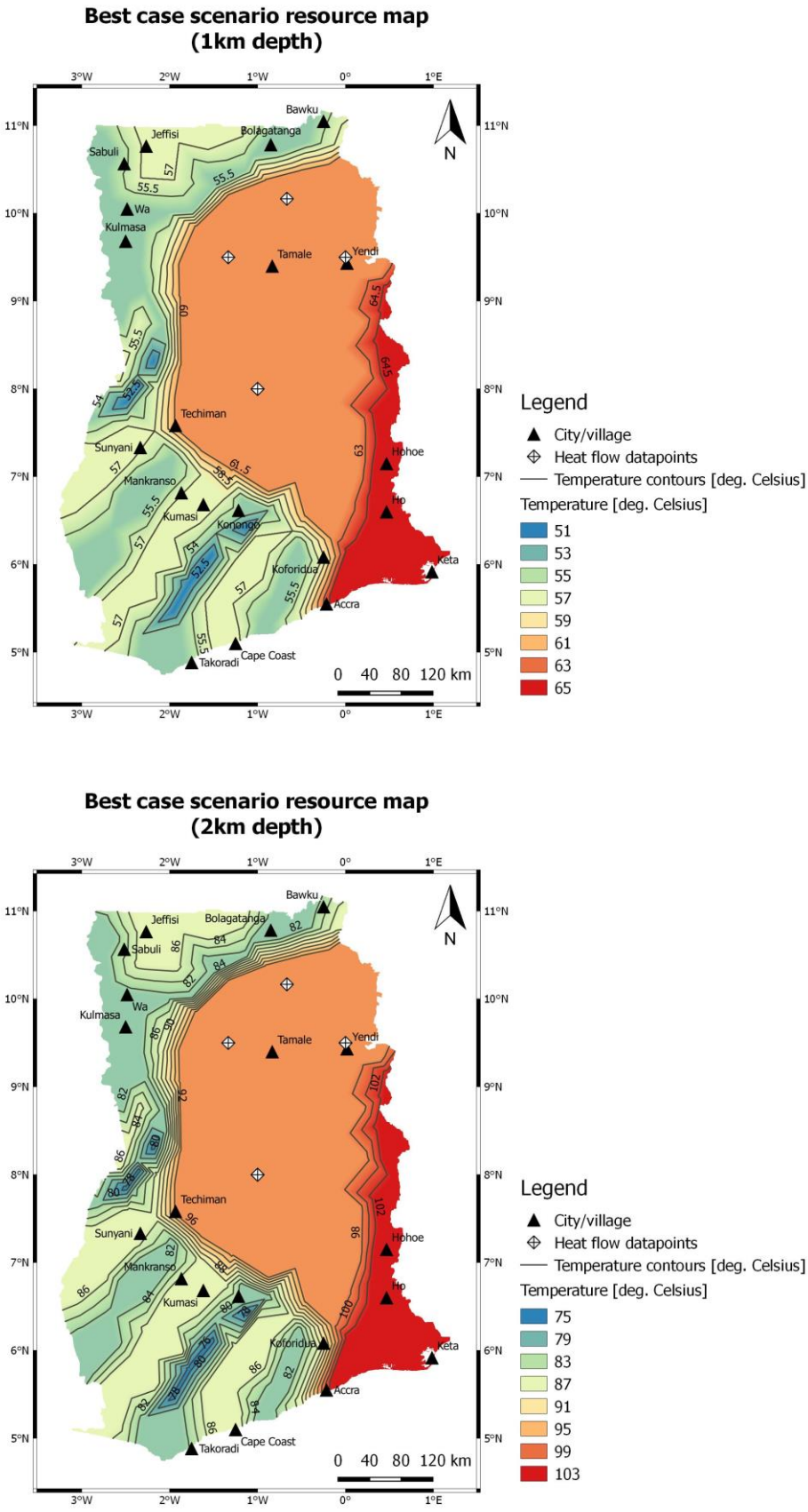

Figure 46: Subsurface temperature distribution for the best case scenario at a depth of 1km (top) and 2km (bottom). Created with QGis, 2016.

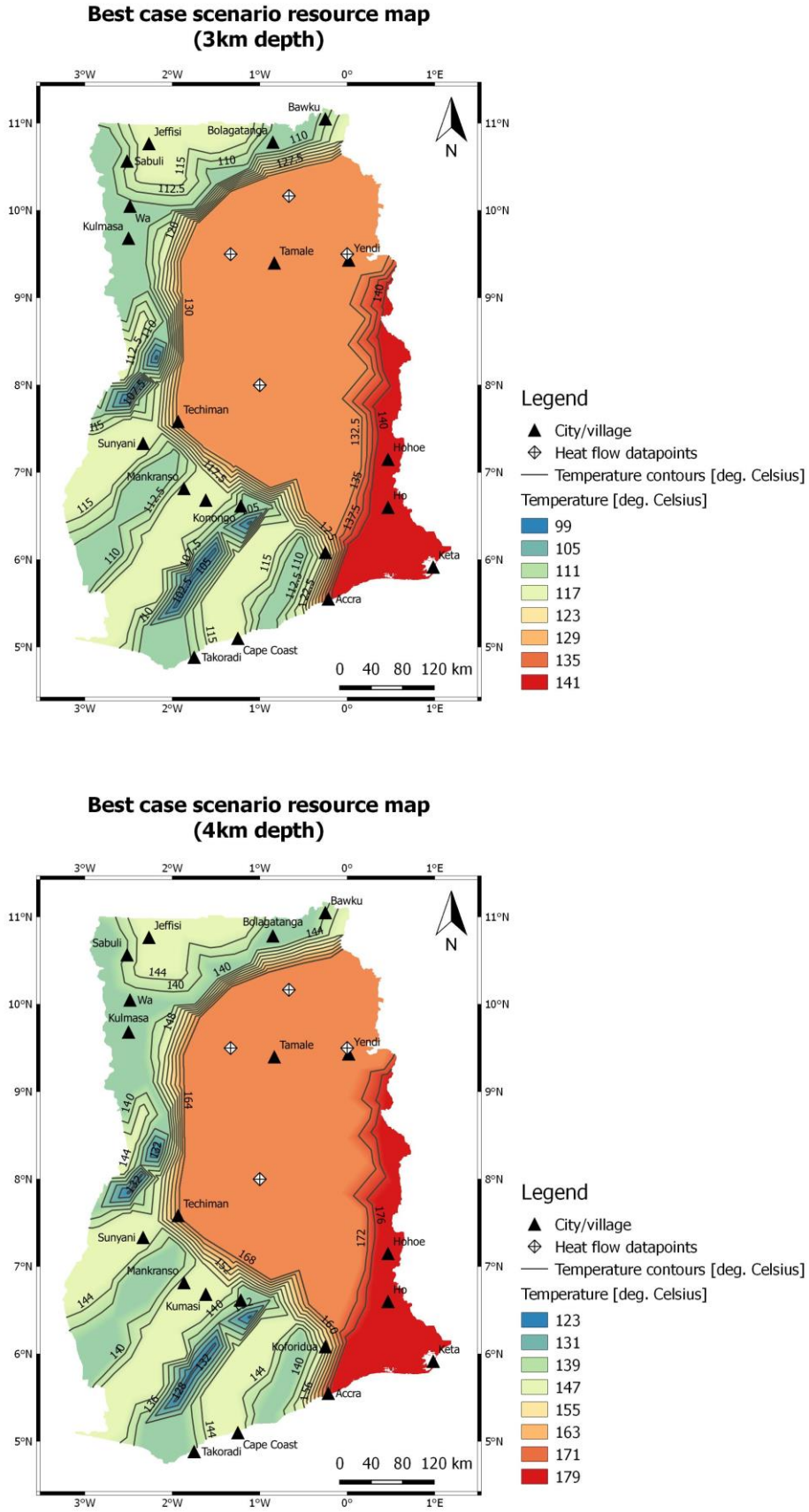

Figure 47: Subsurface temperature distribution for the best case scenario at a depth of 3km (top) and 4km (bottom). Created with QGis, 2016.

Appendix C

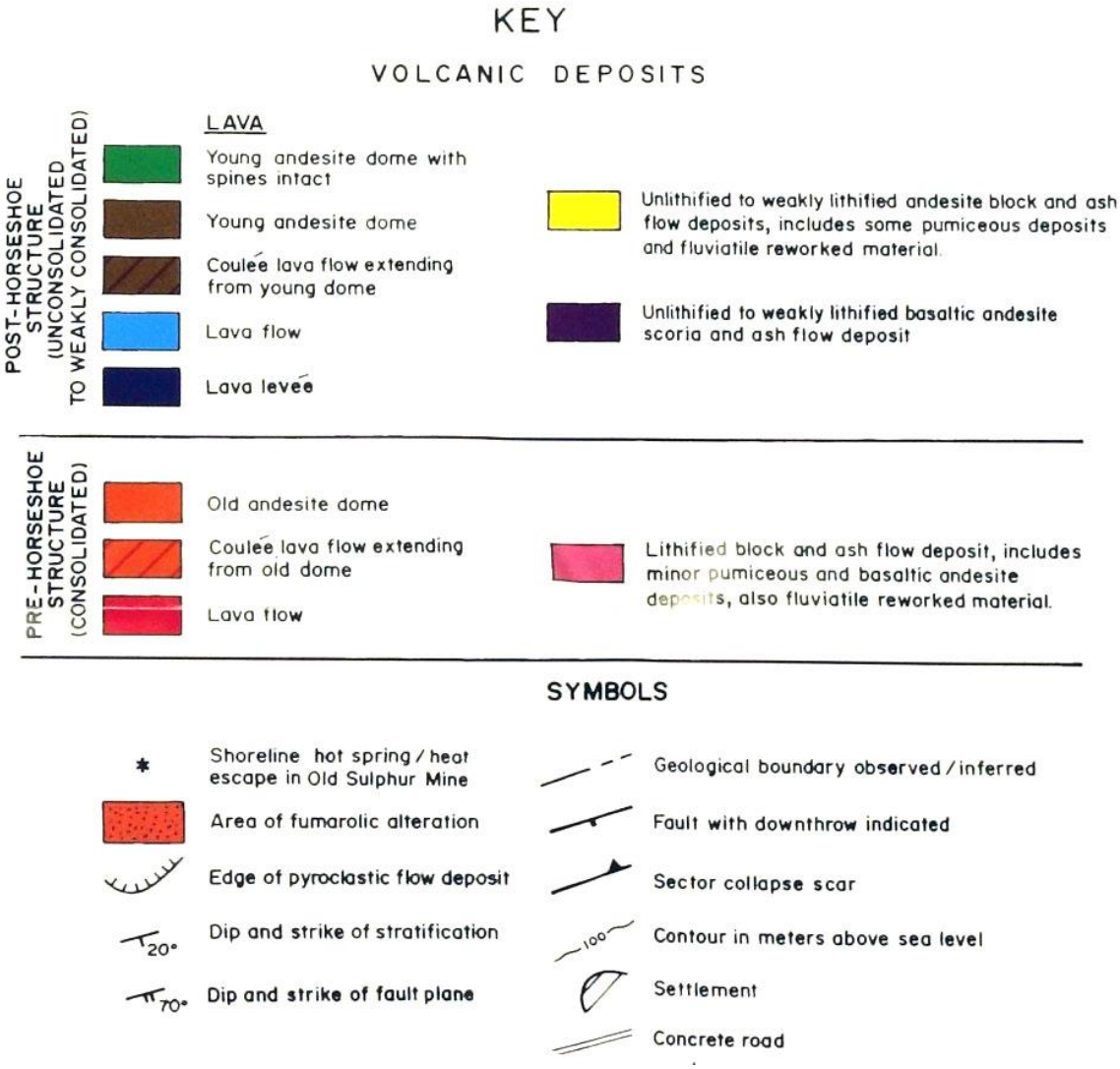

Figure 48: Enlarged legend/key for figure 27; Geological map of Saba. From Roobol & Smith, 2004.

Appendix D

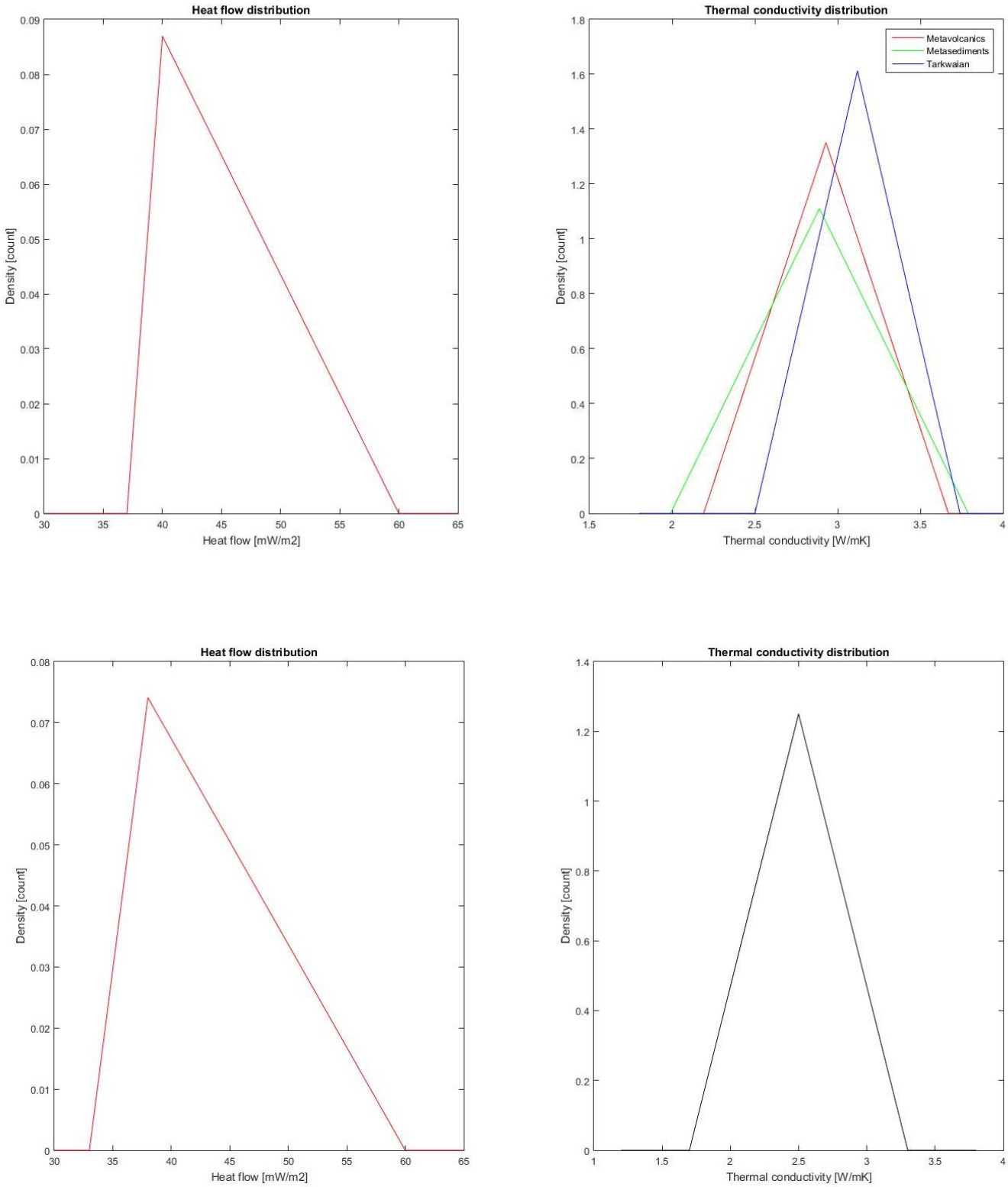

Figure 49: Input distributions of heat flow and thermal conductivity values for the Western Province (top) and the Central Province (bottom). Created with MatlabR2015a.

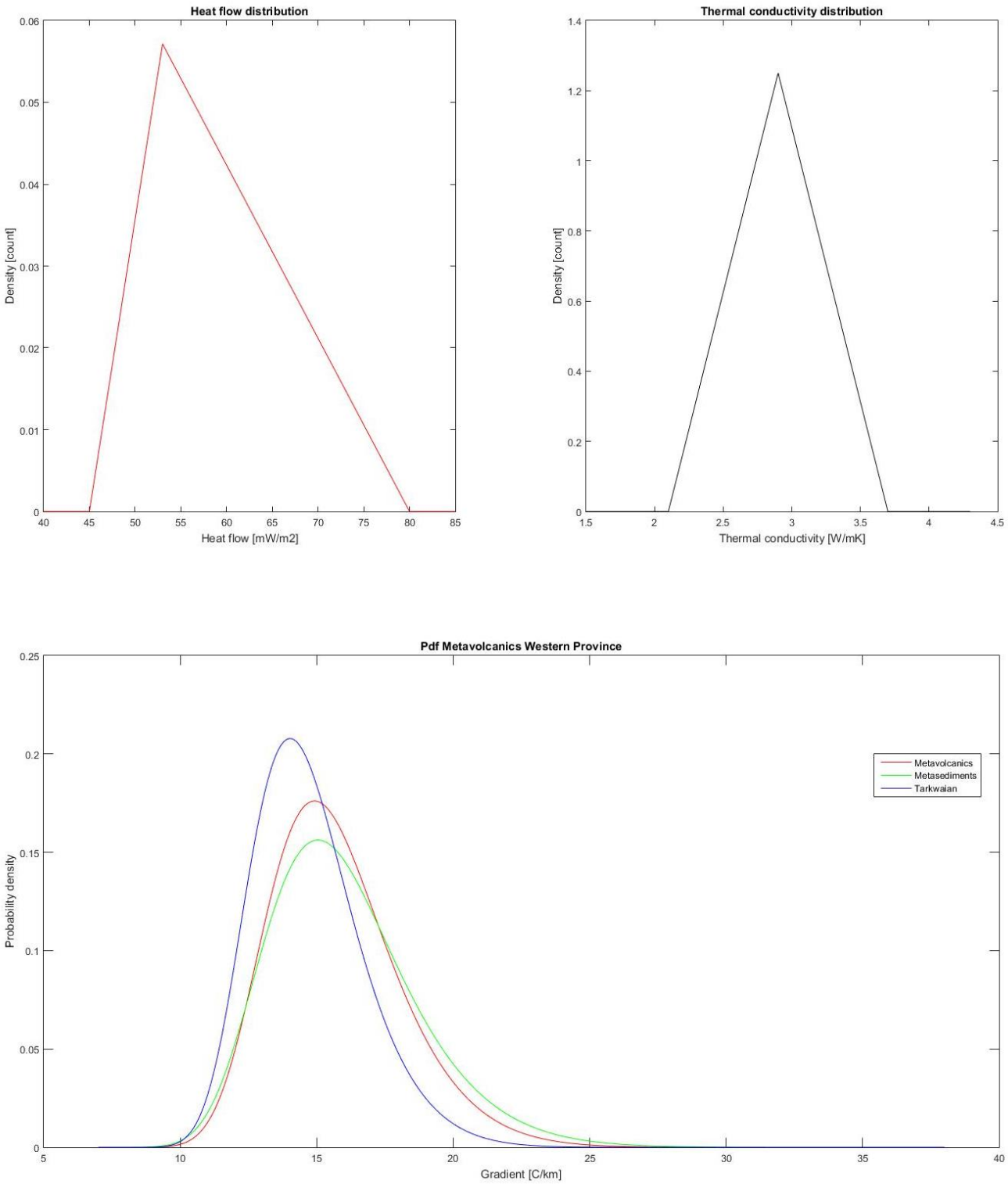

Figure 50: (Top) Input distributions of heat flow and thermal conductivity values for the Eastern Province. (Bottom) Probability density function for geothermal gradients in the Western Province. Created with MatlabR2015a.

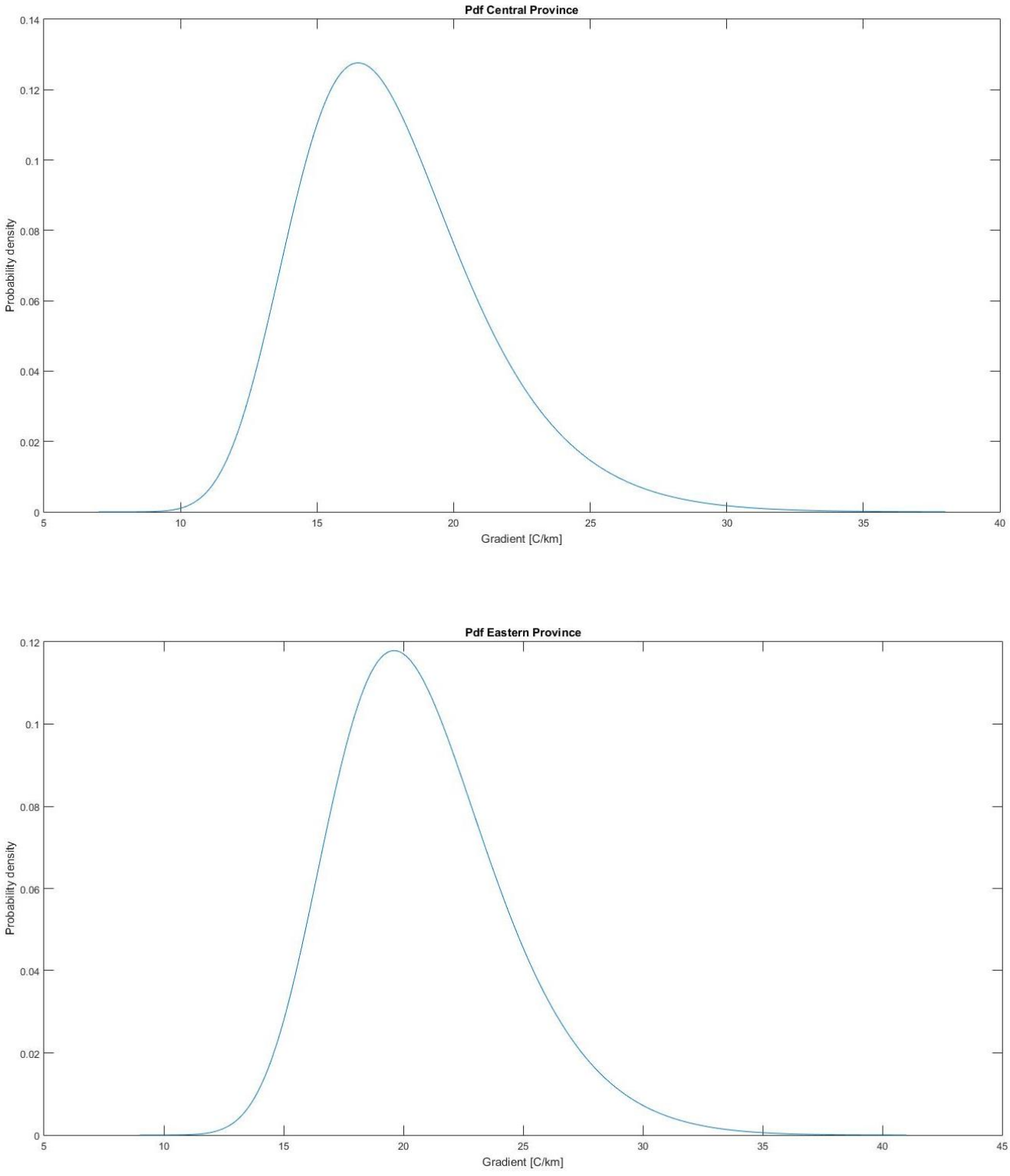

Figure 51: Probability density function for the geothermal gradient in the Central Province (top) and in the Eastern Province (bottom). Created with MatlabR2015a.

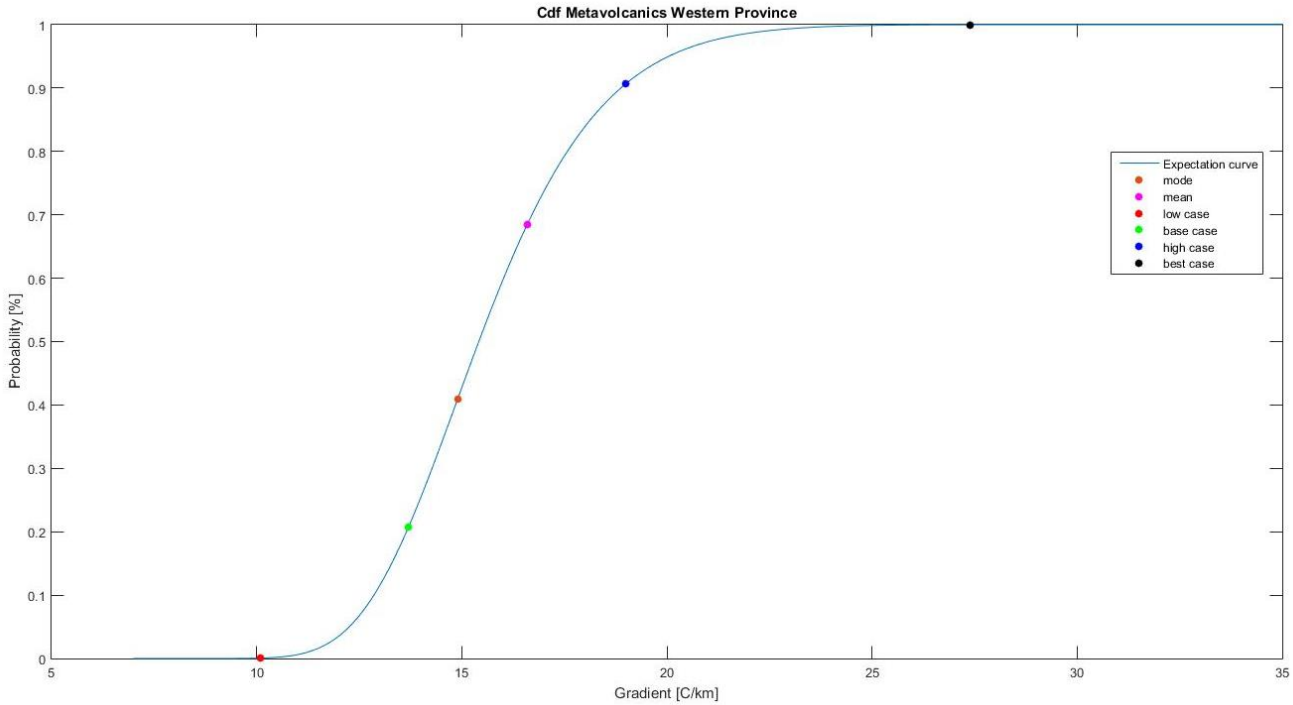

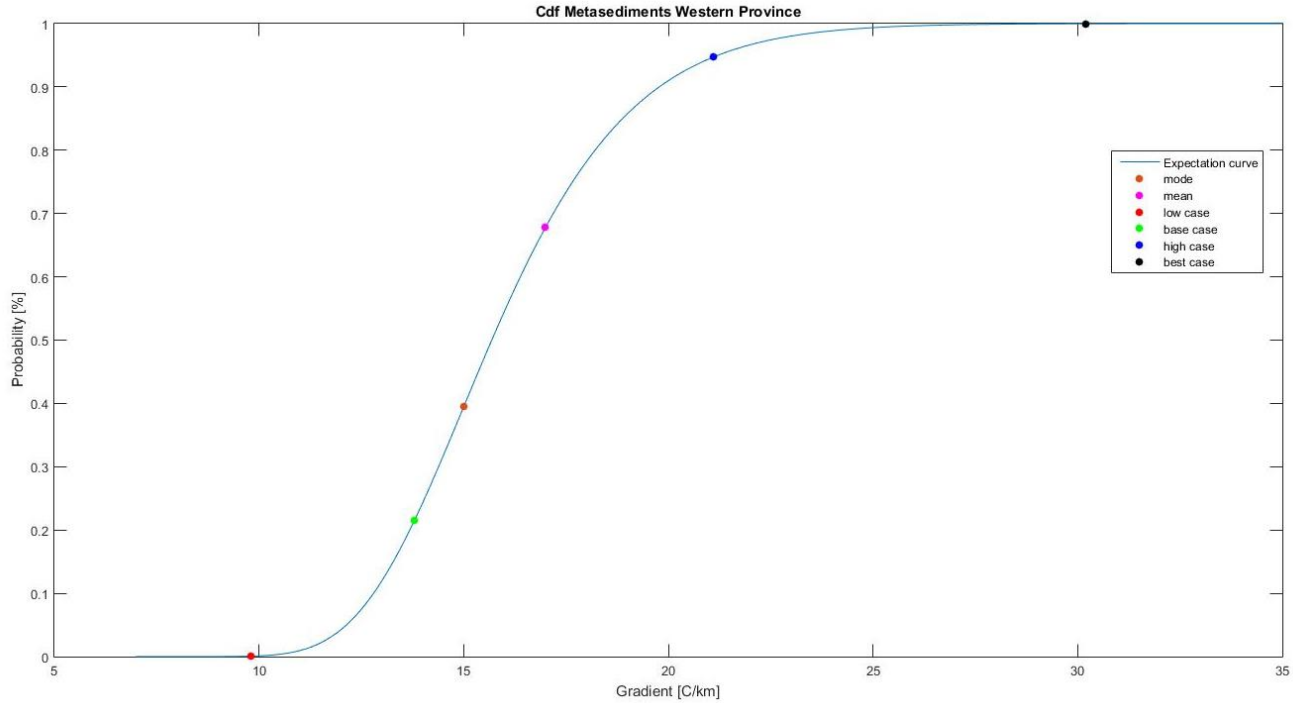

Figure 52: Cumulative probability density function for the geothermal gradient of the Metavolcanics (top) and the Metasediments (bottom) in the Western Province. Deterministic gradients according to the different scenarios are plotted. Created with Matlab R2015a.

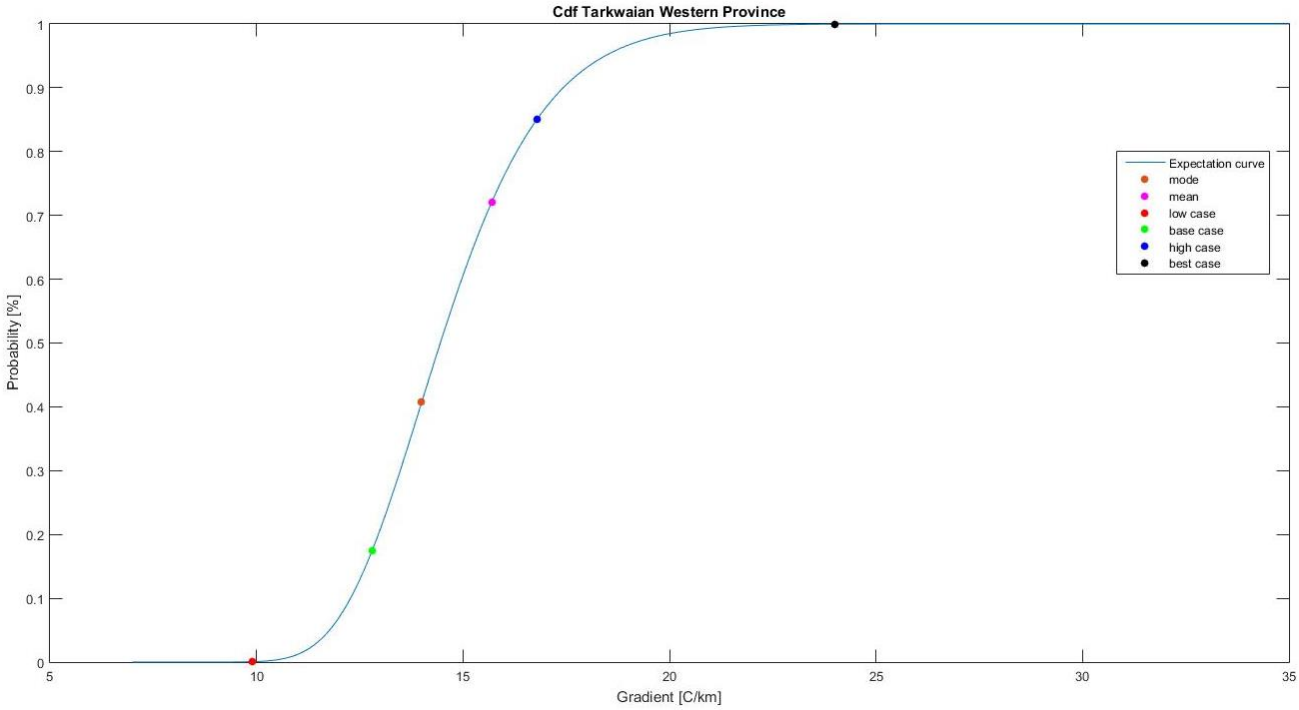

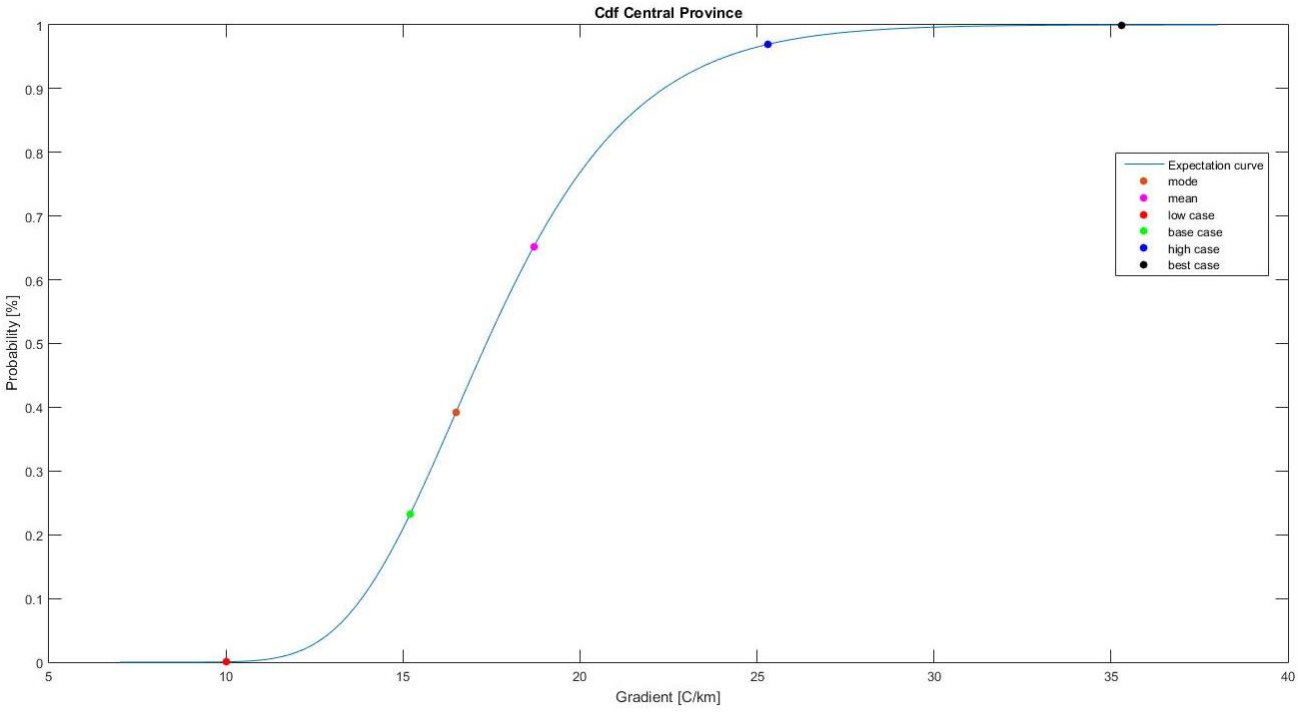

Figure 53: Cumulative probability density function for the geothermal gradient of the Tarkwaian in the Western Province (top) and the geothermal gradient in the Central Province (bottom). Deterministic gradients according to the different scenarios are plotted. Created with Matlab R2015a.

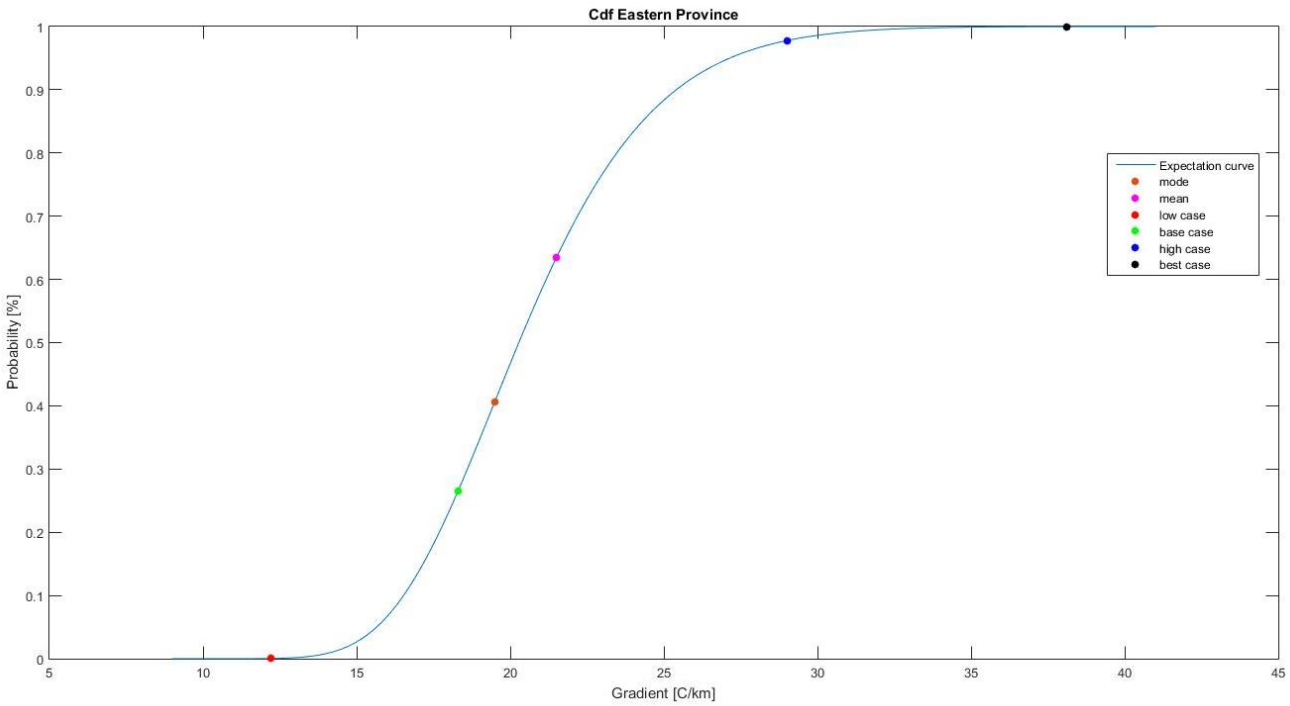

Figure 54: Cumulative probability density function for the geothermal gradient in the Eastern Province. Deterministic gradients according to the different scenarios are plotted. Created with Matlab R2015a.